SUBFAILURE DAMAGE MECHANICS

IN CEREBROVASCULAR INJURY

by

Jacob W. Sullivan

A thesis submitted to the faculty of
The University of Utah
in partial fulfillment of the requirements for the degree of

Master of Science

Department of Mechanical Engineering

The University of Utah

August 2013

The University of Utah Graduate School

STATEMENT OF THESIS APPROVAL

The thesis of **Jacob W. Sullivan**

has been approved by the following supervisory committee members:

Ken Monson	, Chair	**3/15/13** Date Approved
K. Larry DeVries	, Member	**3/15/13** Date Approved
Brittany Coats	, Member	**3/15/13** Date Approved

and by **Timothy A. Ameel** , Chair of

the Department of **Mechanical Engineering**

and by Donna M. White, Interim Dean of The Graduate School.

ABSTRACT

The ability of a cerebral vessel to deliver blood to the brain may become impaired through disease or trauma. Even in the absence of obvious structural disruption, the mechanical properties of a vessel may be changed as a result of trauma. A more complete characterization of the mechanical properties of blood vessels will allow for better prevention and treatment of traumatic brain injury (TBI). Accordingly, two types of mechanical tests were performed in vitro on sections of ovine middle cerebral artery (MCA).

The influence of subfailure damage on mechanical properties has been explored in soft tissues such as ligaments but remains unexplored in cerebral blood vessels. Eighteen vessels from eight different ewes were tested to determine the occurrence of subfailure injury. Injury was defined as a stretch level that produces an unrecoverable change in the passive mechanical response. Vessels were preconditioned around in vivo loads and then subjected to a baseline response test consisting of an axial stretch from the buckled state to in vivo length while pressurized at 13 kPa (100 mmHg). Each specimen was then subjected to a different level of axial overstretch (above the in vivo length but below ultimate strain) while similarly pressurized, simulating loading conditions potentially associated with TBI. Following injury, baseline response tests were repeated at various times to investigate any time-dependent recovery of vessel response.

A linear relationship was found between the level of axial overstretch and the percent change in maximum baseline force and stiffness. For each increase of .1 in overstretch, the maximum baseline force and stiffness were reduced about 16 and 14%, respectively. This postinjury laxity matches similar findings on ligaments. It was also found that there was no significant recovery after up to 6.5 hours in the maximum baseline force and stiffness. This indicates that within the range studied, any level of axial overstretch will permanently change the passive mechanical properties of a vessel.

Eighteen vessels were also subjected to biaxial tests to characterize the mechanical properties of uninjured ewe MCA. Tests were coordinated with concurrent lamb MCA testing so that experiments would offer a valid comparison between lamb and ewe. The mechanical properties of vessels may be further related to individual vessel wall constituents through microscopy imaging.

TABLE OF CONTENTS

ABSTRACT iii

LIST OF TABLES vii

LIST OF FIGURES viii

ACKNOWLEDGMENTS x

CHAPTER

1. INTRODUCTION 1

Objectives 1
Background 3
Summary 11

2. METHODS 13

Vessel Origin and Preparation 13
Setup 17
Test Protocols 18
Data Processing 23

3. RESULTS 28

Overview 28
Preconditioning 30
Subfailure Injury 33
Incremental Stretch 47
Biaxial Tests 49
Failure Analysis 50

4. DISCUSSION 53

5. CONCLUSION 59

APPENDIX..... 61

REFERENCES 100

LIST OF TABLES

Table

1: Method for finding the in vivo length 19

2: MCA properties (n=20) 28

3: Percent change of baseline parameters 31

4: Number of specimens grouped by 33

5: Correlation results between parameters (independent variables bolded) 42

6: Single Factor ANOVA results for F_{max} 46

7: Single Factor ANOVA results for E_{max} 46

8: Axial displacements from the image 47

9: Parameters of failure data 51

10: Effect of subfailure testing on failure properties 52

LIST OF FIGURES

Figure

1: Layers of a blood vessel modified version 5

2: Strain response of different materials under a constant load[27] 7

3: Plastic deformation of elastic materials[28] 7

4: The Mullins Effect in rubber preconditioning[33] 9

5: Cyclical loading of a human cerebral vessel[40] with potential..... 12

6: Example of MCA location..... 14

7: Example of a dissected vessel (mm)..... 15

8: Two needles attached to fluid path blocks with drop down 16

9: Fixing the vessel to the needles 16

10: Vessel bath..... 17

11: Testing Setup 19

12: A sample force-pressure curve used to..... 21

13: Example of measurements taken in Vision..... 24

14: Snapshots of a vessel during a baseline test 25

15: Fit of model to data..... 29

16: Raw force versus filtered force..... 30

17: Effect of additional preconditioning..... 31

18: Difference in mechanical response on a single vessel..... 32

19: Subfailure injury test subjected to an overstretch 34

20: Effect of overstretch on percent of baseline force 36

21: Effect of overstretch on percent of baseline stiffness 36

22: Effect of overstretch on percent of baseline A 38

23: Effect of overstretch on percent of baseline B 38

24: Effect of overstretch on percent of baseline C 39

25: Effect of cross-sectional area on percent of baseline force 39

26: Effect of cross-sectional area on percent of baseline stiffness 40

27: Effect of in vivo stretch on percent baseline force 41

28: Effect of cross-sectional area on percent baseline stiffness 41

29: Recovery after an overstretch of 1.19 42

30: Recovery after an overstretch of 1.26 43

31: Recovery after an overstretch of 1.36 43

32: Recovery after an overstretch of 1.45 45

33: Recovery after an overstretch of 1.54 45

34: Image analysis of matching the greater curvature to the 47

35: Axial stress-stretch curve for incremental test #1 48

36: Axial stress-stretch curve for incremental test #2 49

37: Vessel failure properties after various subfailure tests 51

ACKNOWLEDGMENTS

Many thanks are given to my adviser, Ken Monson, for his guidance. Thank you to fellow students David Bell, Kevin Nye, and Stewart Yeoh. These individuals assisted in the methodology of data collection and analysis. Also, thank you to MJ Dahl and the research lab of Dr. Kurt Albertine for their willingness to contribute both time and resources to this research project. Finally, special thanks are given to Rebecca Sullivan for her never-ending support and to friends and family for their encouragement.

CHAPTER 1

INTRODUCTION

Objectives

The proper function of blood vessels is vital to the delivery of blood throughout the body. The elasticity of large arteries is essential in maintaining a proper ratio between systolic and diastolic pressures in the body. These arteries passively dilate and contract according to cardiac rhythm and convert pulsatile flow into a more continuous flow with consistent pulse pressures.[1] The smaller arteries offer active muscular resistance that maintains the average blood pressure in the body. The ability of a vessel to transport blood effectively may diminish through disease or trauma.

There has been much research done in the last thirty years to assess the impact of impaired vascular function. Blood vessel function may become disrupted by diseases such as diabetes,[2] hypertension,[3-5] and atherosclerosis.[6] A vessel may also be damaged through internal trauma such as angioplasty[7] or external trauma such as traumatic brain injury (TBI).[8-10] The focus of this study relates to vessel impairment through overstretch, a loading condition believed to be common in TBI. In this study, overstretch was defined as stretching above the in vivo length and below the ultimate strain.

Cerebral vascular impairment leads to stroke and is a common outcome of TBI. Each year in the United States, 52,000 deaths occur from over 1.7 million cases of TBI.[11]

The number of deaths from stroke each year is over 140,000.[12] The total combined annual cost of both TBI and stroke has been estimated between 60[11] and 65.5[13] billion dollars.

Studies have indicated that cerebral blood flow is altered after head injury.[14-16] Cerebral vessel mechanics play a key role in maintaining the flow of blood throughout the brain. A further understanding of cerebral vascular mechanics including subfailure injury will help to identify threshold limits of such injury and may lead to new methods of injury mitigation. Subfailure describes stretch levels beneath the point of failure by rupture. Injury was defined as a stretch level that produces an unrecoverable change in the passive mechanical response.

The main objective of this study is to characterize the mechanical effects of subfailure injury in the middle cerebral artery (MCA). After preconditioning in order to return vessels to the in vivo configuration and to create repeatable results, testing will include axial overstretch in order to simulate vessel damage that may occur during TBI. A secondary objective is to coordinate the comparison of adult and pediatric MCA mechanical properties. These objectives will be accomplished by addressing the following questions:

- How does axial overstretch affect the mechanical response of the MCA?
- Does a passive elastic limit exist for the MCA where the vessel will not be able to recover from overstretch?
- How will data be compared between the adult and pediatric MCA?

Background

Cerebrovascular Function

An understanding of the function and morphology of cerebral vessels is beneficial to this study. The human brain accounts for approximately 2% of total body weight, yet 20% of cardiac output is directed to the brain.[17] Cerebral vessels play an important role in controlling the flow and pressure of blood in the brain and throughout the body. The resistance of cerebral vasculature was found to be 45-50% of total vascular resistance in rats.[18]

Cerebral blood vessels actively autoregulate the flow of blood by dilating and contracting in order to maintain a constant flow pressure over a large pressure range (60 - 160mmHg).[9] Autoregulation is partly driven by sensor cells along the lumen of the vessel called endothelial cells. Through these endothelial cells, the vessel will be told to dilate or contract.

In addition to autoregulation in cerebral vessels, the brain also has a redundant system in place to allow blood flow through alternate pathways to reach the same destination. A key element in this system is the Circle of Willis which is located at the base of the brain and acts as a central hub for all blood entering the brain. Both the redundant system and autoregulation contribute to maintaining a constant flow of blood to the brain, preventing stroke.

Active and Passive Response

Blood vessels are an active tissue which undergo constant remodeling in response to the hemodynamic, metabolic, pathologic,[5] or traumatic changes imposed upon it.

Martinez-Lemus et al. suggest that this "remodeling continuum" may be driven to retain "tensional homeostasis" in resistance vessels.[19] Research in the field of vascular remodeling has been well established.[19-22] An example of vessel remodeling is the process of adding "fascicles of smooth muscle cells" in the vascular wall of sheep as they age.[23]

Additionally, blood vessels have passive mechanical properties defined by the individual constituents inside the vessel wall, mainly collagen and elastin. The combination of both active response and passive mechanical properties enables vessels to distribute blood effectively throughout the body. Any change in the blood vessels' active or passive response would impact the delivery of blood throughout the body.

The vessel wall is made up of three layers known as the tunica intima, the tunica media, and the tunica externa or adventitia, as shown in Figure 1. The inner layer called the tunica intima is comprised of endothelial cells that line the lumen of the vessel which guide the active response of the vessel. These cells do not generally contribute to the vessel's mechanical response unless they become hardened through the process of atherosclerosis.[24] Endothelial cells are attached to a basement membrane composed of extracellular matrix (ECM). The internal elastic lamina, composed of elastin, separates the intima from the media.

The tunica media is the most important layer that contributes to the passive mechanical response of the vessel under normal physiological conditions.[25] This is mainly due to the presence of elastin and collagen. The main constituents, as well as smooth muscle cells, are interconnected.

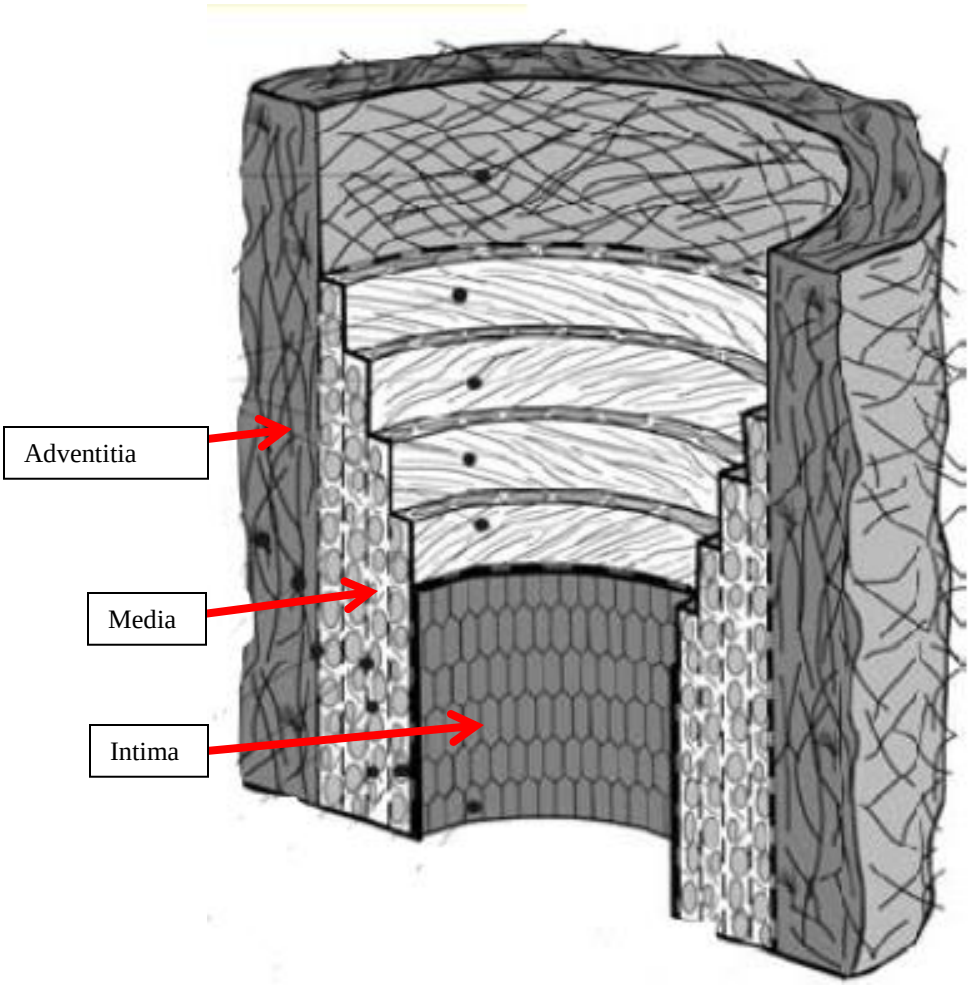

Figure 1: Layers of a blood vessel modified version from Holzapfel[24]

As opposed to the other two layers, the media stands out as being "coherently organized."[26] The collagen fibers are circumferentially oriented in a helical pattern with a small pitch like a fine thread screw. This configuration allows vessels to effectively resist loads both circumferentially and axially. Cerebral vessels have significantly less elastin present in the media compared to larger arteries proximal to the heart. The external elastic lamina separating the media from the externa and the tunica externa itself is virtually nonexistent in cerebral vessels.[24]

Elasticity and Viscoelasticity

An understanding of how blood vessels relate to common materials will help to understand their unique properties. Elastic materials internally resist applied forces. This internal resistance allows the material to recover to the original state when the force is removed. The relationship between stress and strain in linear elastic materials is described by Hooke's Law in equation 1. Hooke's Law does not adequately describe blood vessel behavior due to their nonlinear stress strain curves.

$$\sigma = E\varepsilon \qquad (1)$$

where E is the material property of Young's Modulus, σ is the stress, and ε is the strain. The response of an elastic material under a constant load is shown in Figure 2. In this case, the strain responds instantly and remains constant. When the stress is removed, the strain recovers immediately. A material that is stretched beyond its elastic limit enters the plastic region and is permanently changed, as shown in Figure 2 and Figure 3. Stored elastic energy within the material is absorbed when the material deforms plastically causing the material to return to a different state when the stress is removed.

Blood vessels are classified as viscoelastic materials suggesting a dual nature exhibiting both viscous and elastic properties. Zhang et al. suggests that blood vessels have viscoelastic properties in order to reduce stresses and strains in the vessel wall. This study concluded that these properties may be beneficial for the fatigue life of blood vessels.[29]

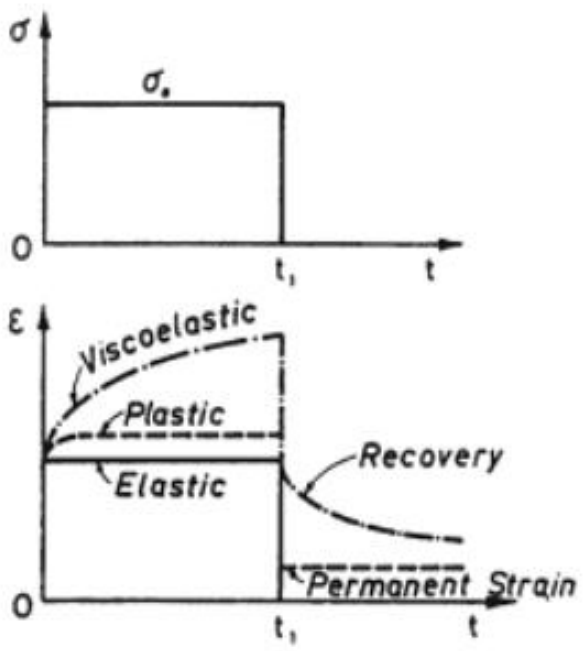

Figure 2: Strain response of different materials under a constant load[27]

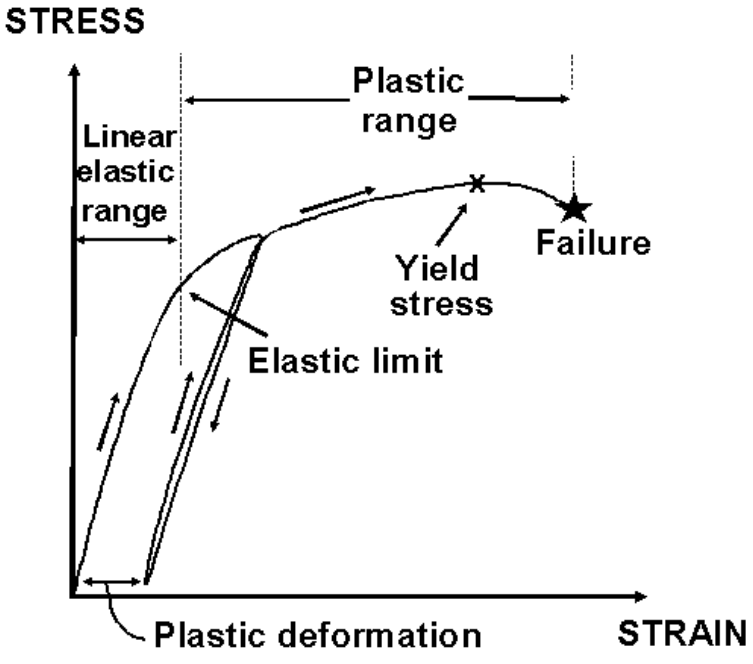

Figure 3: Plastic deformation of elastic materials[28]

Generally, for all viscoelastic materials under a constant load (see Figure 2), the strain response is not immediate and the material deforms as a function of time, also known as viscoelastic creep. When the stress is removed, the material partially recovers immediately and recovers the rest as a function of time. For many models, the elastic nature of a viscoelastic material is modeled as a spring using Hooke's law as a governing equation. The viscous nature is modeled as a dashpot with Newton's Law of Viscosity as a governing equation. According to Newton's Law of viscosity for Newtonian fluids, stress is related to the constant η, or viscosity, multiplied by the rate of change of strain shown in equation 2. Generally, stress is therefore a function of strain rate in viscoelastic materials; however, in blood vessels, the dependence is not as clear. Some researchers have found significant dependence,[30] while others have not.[31-32]

$$\sigma = \eta \frac{\partial \varepsilon}{\partial t} \qquad (2)$$

The spring and dashpot may be configured in a variety of ways to create models with different characteristics. The most basic of these are the Maxwell model and the Kelvin-Voigt model. Independent of the model chosen, all viscoelastic materials exhibit certain behaviors due to their dual nature.

Hysteresis is one such behavior. Hysteresis represents energy dissipation during loading. The loss of energy causes the unloading curve to be shifted to the right from the loading curve. When a viscoelastic material such as rubber is subjected to cyclical axial loading to a fixed strain, as shown in Figure 4, the maximum stress occurs during the first cycle. The greatest difference in maximum stress is between the first and second cycle.

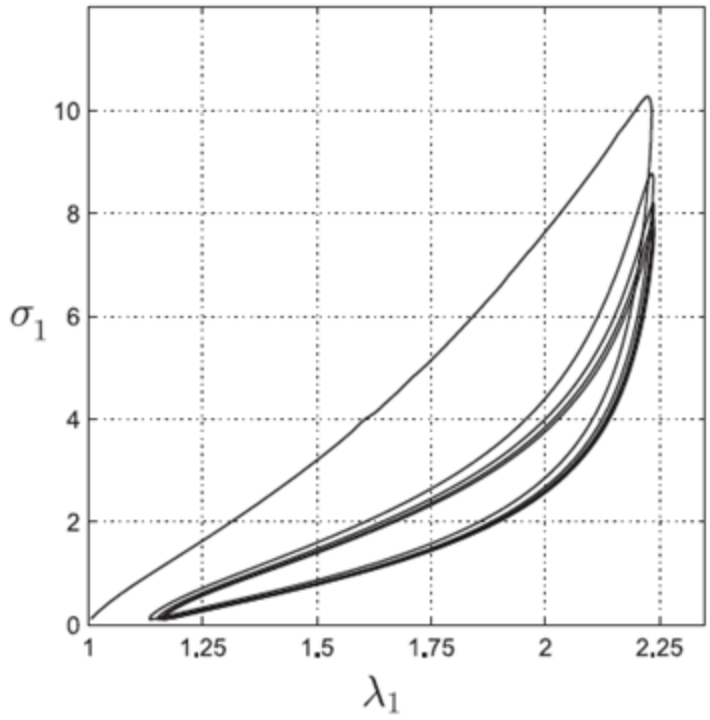

Figure 4: The Mullins Effect in rubber preconditioning[33]

For rubber, it was suggested that this difference becomes negligible after 4-5 cycles.[33] This is consistent with data from the author's lab and with findings reported by other researchers for blood vessels. After a vessel has been cyclically preconditioned, the response of the vessel becomes consistent and hysteresis is minimized.

Another characteristic of viscoelastic materials is stress relaxation. This occurs when a constant strain is imposed on the material. It will begin to relax so that the stress decreases over time. A vessel may be preconditioned through cyclic loading or stress relaxation. In theory, after a vessel has been preconditioned, the effect of stress relaxation will be minimized.

Subfailure Injury

After discussing cerebrovascular function and properties, it is also important to note vessel behavior in respect to axial loading. The axial stress-strain curve for vessels is nonlinear.[34] In this curve, the initial region of increasing slope is referred to as the toe region. This is followed by a somewhat constant slope. The change in slope is due mainly to the network of elastin and collagen fibers and their orientations which cause uneven loading between fibers and layers. Roach and Burton proposed that the initial slope of each curve is a "reliable index of the state of elastin…and the final slope can be used as an index of the state of the collagenous fibers."[35] Any changes in these indices may be indicative of subfailure injury; however, the relationship between vascular mechanical response and subfailure injury is not clear because little research has been done on this topic.

The study of subfailure mechanics has been a topic of interest in ligaments. An example is the work done by Panjabi et al.[36] in which 10 pairs of rabbit ACL were tested. Randomly, one ACL from each pair was subjected to control testing to evaluate the effectiveness of preconditioning and then stretched to failure. The other ACL was preconditioned with the force response recorded and then subjected to 80% of failure overstretch. After subfailure injury, the same preconditioning test was repeated and recorded to compare against the pre-injury response. The control testing found that the method of preconditioning was effective in producing consistent mechanical response. Furthermore, the results showed that the subfailure axial stretch caused greater ligament laxity and decreased the relaxation force by 50%.

This result was further confirmed by a study done by Provenzano et al.[37] in which subfailure overstretch tests were conducted on the MCL of rats. The use of confocal microscopy was used to show the microstructural changes in the ligament as a result of various subfailure strains ranging from 0 to 75%. It was hypothesized that the joint laxity was caused by torn or plastically deformed fibers or by a biochemical degradation of the extracellular matrix, or the ECM.

For blood vessels, the characterization of failure properties of blood vessels has been a topic of research;[8, 32, 38-39] however, subfailure injury has been largely unexplored. Preliminary data from the author's lab[40] show the effects of cyclical loading at incremental strains for human cerebral arteries. In a testing scenario similar to Donovan et al.,[41] a vessel was cycled 10 times to each displacement setting until failure. Little recovery time was allowed between cycles. The first stretch in each cycle is shown in Figure 5. The grey line connects the maximum loads for each displacement level. A change in the slope of this grey line occurs near a displacement of 8 mm possibly indicating the presence of subfailure damage occurring in a blood vessel.

Summary

To maintain this complex functionality, blood vessels have complex properties. They are nonhomogenous, viscoelastic and anisotropic materials.[42] Additionally, they exhibit a nonlinear stress-strain curve.[34] The proper function of blood vessels is vital to the effective delivery of blood throughout the body. Understanding the subfailure damage mechanics of blood vessels is an important step in further characterizing the thresholds of damage and effect of injury in blood vessels.

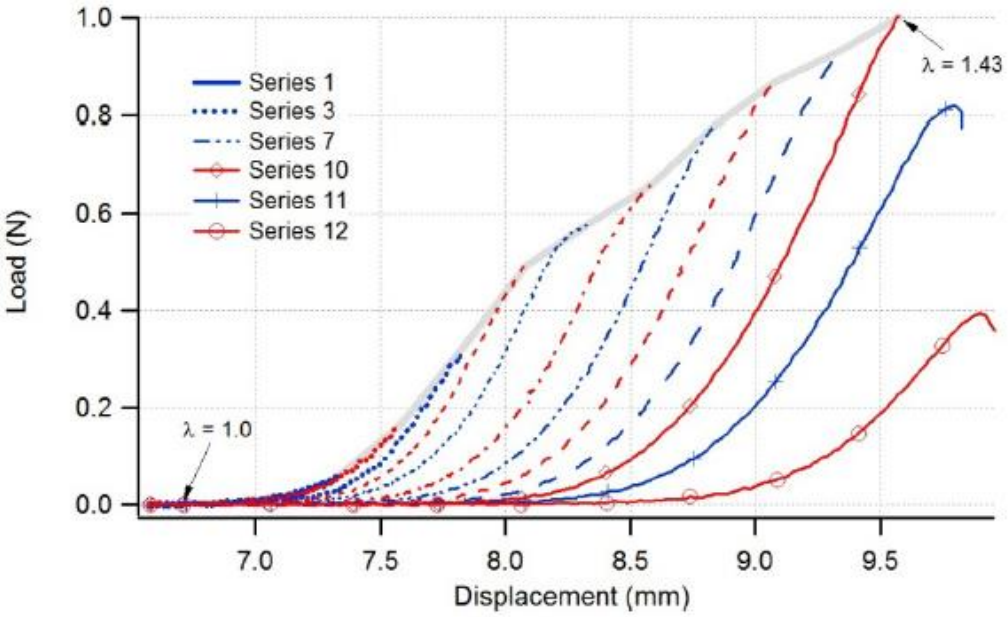

Figure 5: Cyclical loading of a human cerebral vessel[40] with potential subfailure damage occurring near 8 mm of displacement

CHAPTER 2

METHODS

Vessel Origin and Preparation

Sections of the middle cerebral artery (MCA) were dissected and tested from eleven pregnant Colombia-Ramboullet ewes. Ewe brains were donated by the Kurt H. Albertine lab at the University of Utah. All procedures met requirements of the American Association for Laboratory Animal Science and IACUC at the University of Utah. Each ewe was between three and seven years old and weighed between 90 to 120 kg. The ewes were given 6 mg of dexamethasone, ketamine, and isoflurane after scheduled parturition through C-section. Each delivery occurred between 130 to 140 days of gestation. In order to ensure a passive response, the ewe brain was stored in calcium free Hank's Buffered Saline Solution (HBSS; KCl .40, KH_2PO_4 .06, NaCl 8.00, Na_2HPO .0477, D-Glucose 1.00, $NaHCO_3$ .35; concentrations in g/L for 1X solution) at 34°F. All specimens were tested within 48 hours of death which is an accepted limit of vessel degradation of passive properties.[39]

Sections of the MCA were resected along with the surrounding brain tissue, as shown in Figure 6. After removing a section, the brain was promptly returned to refrigeration at 34°F. The vessel was kept in a calcium-free HBSS bath during preparation. The arachnoid was removed from over the top of the vessel under a

Figure 6: Example of MCA location

dissecting microscope using a pair of surgical scissors and micro-forceps. One side of the vessel was gently lifted as the branches connecting the vessel to the brain tissue were severed. Particular care was given to avoid stretching of the vessel. Sections ranging between 3 and 7 mm were used depending on the extent of branching and curvature in the vessel, as shown in Figure 7. Segments with constant outside diameter were preferred. For cross-sectional area, a thin slice was cut from the end of the vessel and photographed under the microscope. Typical imaging resolution was .0024 mm/pixel.

In order to allow internal pressure, the micro-branches lining the length of the artery were then ligated using single fibrils of unwound 6-0 silk suture. The testing apparatus is similar to that noted by Monson et al.[38] Briefly, two 21-22 gauge needles

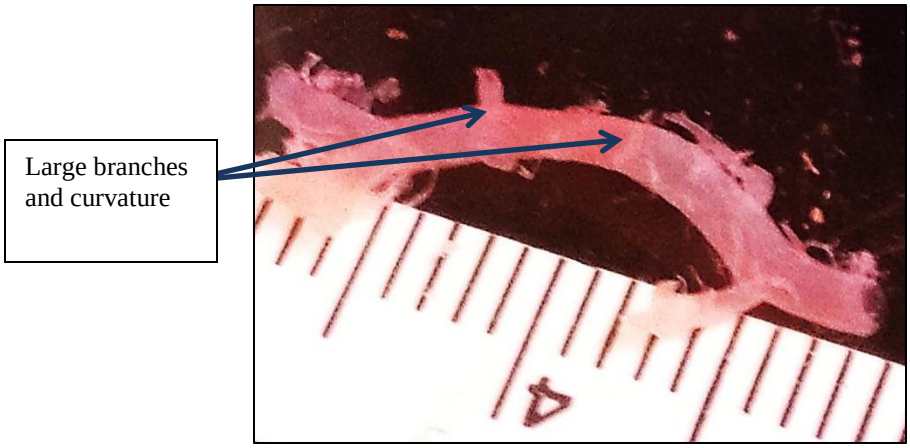

Figure 7: Example of a dissected vessel (mm)

with machined grooves near the tips were attached to two acrylic blocks with a drilled out fluid path. This path allowed for flow and pressure to be measured inside the blood vessel using two in line pressure sensors. During preparation, these blocks were held rigid by an adjustable support arm, as shown in Figure 8. The vessel was then cannulated onto the needles and ligated at the machined groove using 6-0 silk suture under a microscope while still inside the calcium-free HBSS bath.

Once the vessel was ligated on the needles, the saline solution bath was removed and the vessel was wicked dry using a chem wipe. Cyanoacrylate glue (All Purpose Instant Krazy Glue) was applied under microscope to the ends of the vessels, as shown in Figure 9. The suture provided a buffer to keep the glue from running onto the vessel. Saline was applied to the vessel using a syringe while the ends dried. The glue and suture combination fixed the vessel to the needles and prevented vessel sliding during the test. After the glue was dry, a small cuvette was brought down over the vessel and snapped into place, sealing the chamber. The bath was filled with calcium-free room-temperature[38] HBSS, as shown in Figure 10.

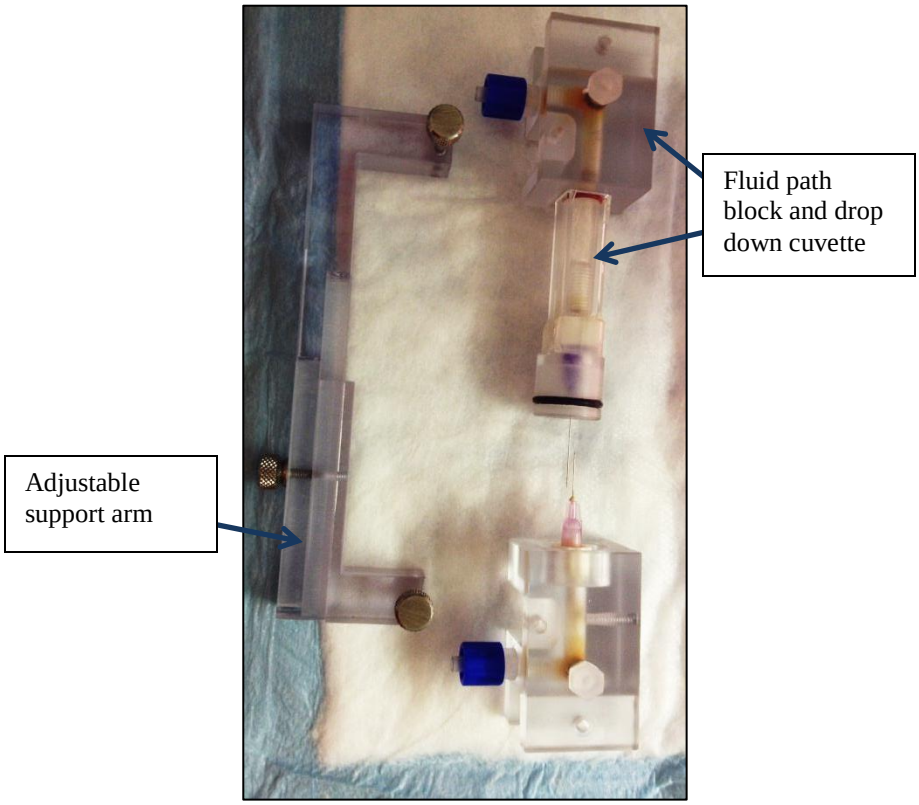

Figure 8: Two needles attached to fluid path blocks with drop down vessel bath cuvette and adjustable support arm

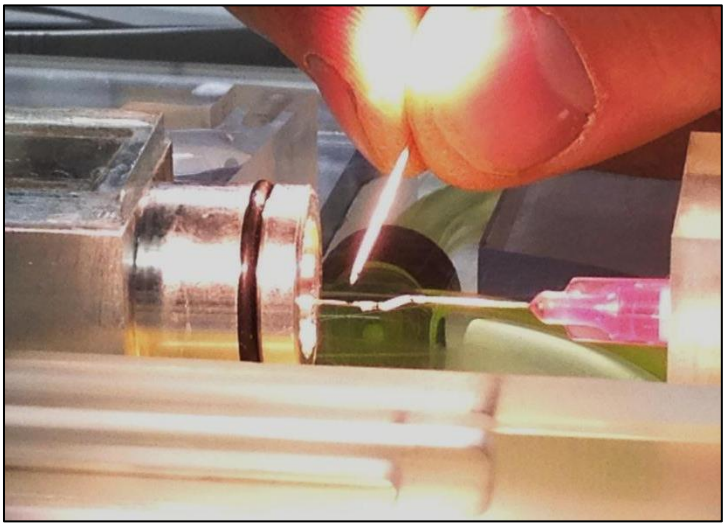

Figure 9: Fixing the vessel to the needles

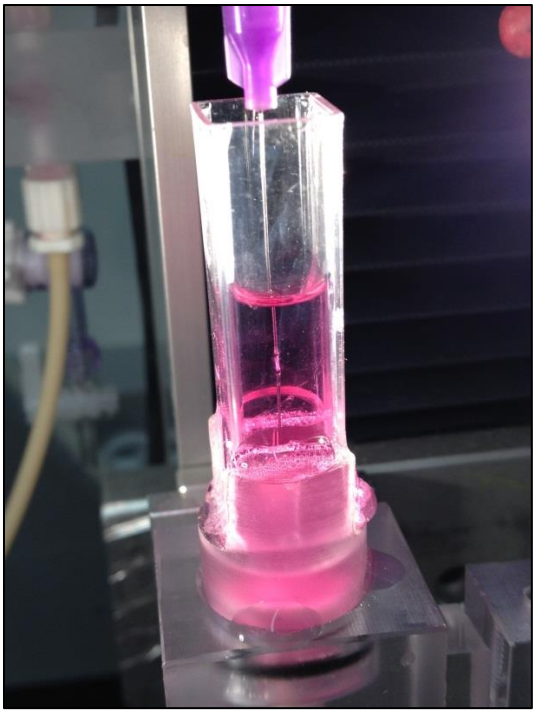

Figure 10: Vessel bath

Setup

The mechanical testing setup is similar to work done by Monson et al.[38] and has been used previously in the author's lab by Bell et al.[8] with the only difference being that a 1000 gram capacity load cell (Model 31 Low, Honeywell, Golden Valley, MN) was used. The system was designed to either use a voice coil (MGV52-25-1.0, Akribis, Singapore) or a custom Daedal linear stage (Parker Automation, Cleveland, OH) for longitudinal displacement of the vessel. The voice coil was used for the first two tests but subsequently had a malfunction. The Daedal stage was then used for all successive tests. Both setups led to identical loading conditions during experiments. The testing setup is shown in Figure 11. For circumferential displacement, the vessel was attached to a luminal pressure control system driven by a linear actuator (D-AO.25-AB-HT17075-4-P,

Ultra Motion, Cutchogue, NY). Pressure sensors (26PCDFM6G, Honeywell, Golden Valley, MN) were placed proximally and distally to the vessel. The average between these two sensors provided the set point for controlling pressure with Labview (National Instruments). Additionally, the vessel was connected to the load cell previously mentioned which was connected to an X-Y stage (MS-125-XY, Newport, Irvine, CA) to allow for needle alignment. Images were collected through a digital video camera (PL-A641, Pixelink, Ottawa, Canada) equipped with a zoom lens (VZM 450i, Edmund Optics, Barrington, NJ) with typical imaging resolution .011 mm/pixel.

Test Protocols

Preliminary

It is common practice when testing in vitro to precondition blood vessels. When a vessel is cut in the body, it retracts showing its natural state of tension. Burton suggests that this is a maintenance tension to hold the hydrostatic pressure of the blood without any continuous expenditure of energy.[43] The removal of tension during resection may cause structural changes in the vessel, especially as the vessel relaxes in its new, unloaded state. The first objective of preconditioning is returning the vessel as close as possible to its original configuration. The second is to cyclically load the vessel to minimize the effect of hysteresis and be able to produce a repeatable response.

This has become an universally applied technique for identifying the in vivo length. Similar to work done by Monson et al.[38] and Bell et al.,[8] the vessel was first tested in a buckled state and the axial strain was incrementally increased after each round of preconditioning until the criteria in Table 1 were met. For preconditioning, each round

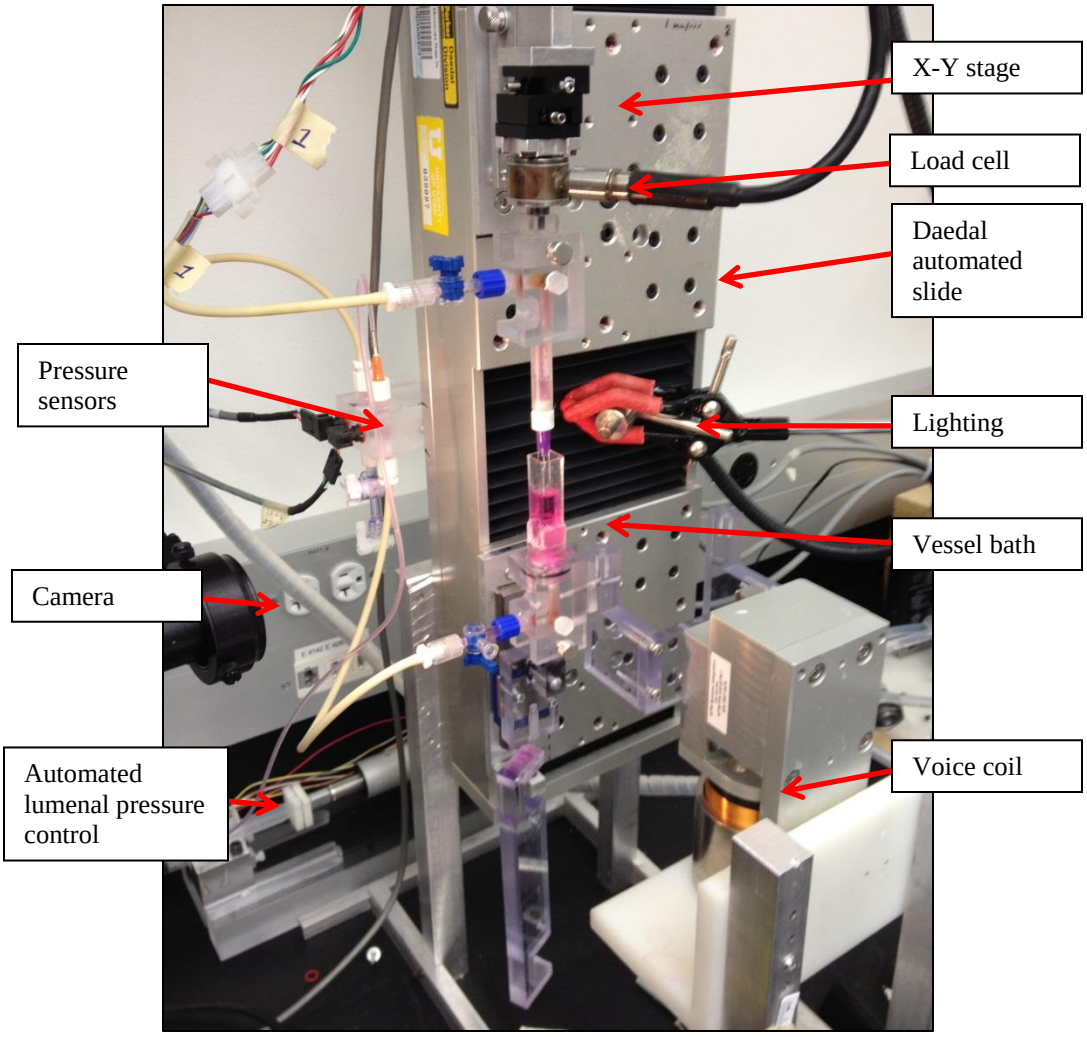

Figure 11: Testing setup

Table 1: Method for finding the in vivo length

Force Response	Steps taken
Axial force decreased as pressure increased at constant axial strain	The axial strain was increased and another round of preconditioning was conducted.
Axial force was constant as pressure increased at constant axial strain	The vessel may be at the in vivo length. The axial strain was slightly increased and another round of preconditioning was run to verify.
Axial force increased as pressure increased at a constant axial strain	The vessel is loaded beyond the in vivo length.

included five cycles of oscillating internal pressures between physiologically relevant pressures of 6.7 kPa and 20 kPa while being held at a constant axial strain before the axial force response was measured. Each vessel's preconditioning process typically included five to seven rounds until the in vivo length was identified. A plot of the Force-Pressure curve generated through preconditioning, shown in Figure 12, demonstrates the force response as pressure is increased at a constant strain

After the vessel was preconditioned and the in vivo length was identified, a zero load test was run to find the reference configuration. This involved opening the pressure to atmosphere while stretching the vessel between a buckled state and the in vivo length. The zero load length was identified as the strain at which the force began to increase. This was used as a reference strain to normalize all stretch data.

A preconditioned vessel is assumed to be in a steady state configuration with a repeatable response. In order to evaluate the efficiency of the preconditioning, a baseline axial force response was measured after completing the preconditioning rounds. The baseline was then repeated after performing additional tests within the window of preconditioning and any change in response was noted.

Subfailure Injury Test Protocol

Similar to work done by Panjabi et al. on ligaments,[36] the purpose of this protocol was to determine the effect of subfailure injury by comparing pre- and postinjury mechanical behaviors in the same vessel. A baseline response was established by holding physiological pressure, or 13.3 kPa, in the vessel and stretching it from a buckled state to slightly above the in vivo length. This simulates the mechanical response of the vessel

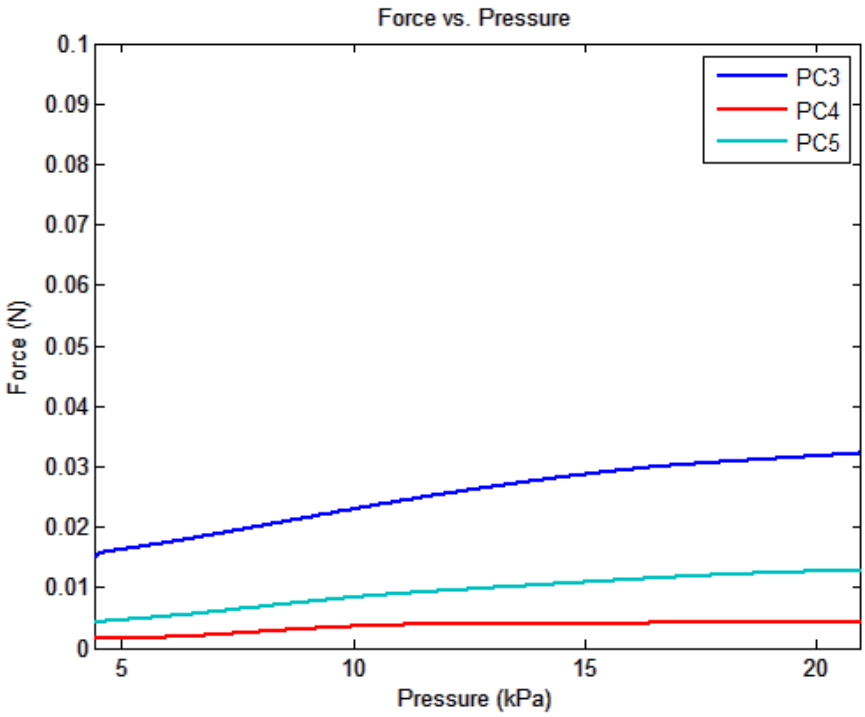

Figure 12: A sample force-pressure curve used to identify the in vivo length at constant force with increasing pressure, the axial strain during Cycle 4 was chosen as the in vivo length

around in vivo loading conditions. The resulting axial force-stretch curve is referred to as the pre-injury baseline. To ensure preconditioning, the baseline was repeated four times before images were captured. After establishing the pre-injury baseline, each specimen was quasi-statically stretched axially beyond the in vivo length. The amount of overstretch was varied to gain insight on how the amount of overstretch impacts vessel properties. Based on previous work showing rate independence on cerebral vessels,[31-32] a quasi-static loading rate of .1 mm/sec was chosen for this overstretch. Immediately following overstretch, a postinjury baseline test was performed using the same parameters as the preinjury baseline. Additional postinjury baselines were performed at

different time increments to investigate the role of time in any viscoelastic recovery. The exploration over time of possible passive recovery has not been explored before to the author's knowledge. These data provided insight into how the MCA passively responds after various levels of overstretch.

Incremental Test Protocol

Limited data from the author's lab[40] show evidence of changes in the properties of blood vessels as a result of loading above in vivo values but below failure. As previously noted, in Figure 5, there is a change in the slope of the line that connects the maximum force at circa 8 mm of displacement suggesting subfailure injury. These experiments were done on unpressurized sections of human cerebral vessel walls. The purpose of this test method was to recreate the incremental stretch plot in Figure 5 using specimens from the current study for comparison. Accordingly, upon reaching preconditioned stabilization, the internal pressure was removed. The vessel was cyclically stretched axially, ten times to each strain increment, at increasing strains starting at buckled until failure. Each strain increment was run immediately following the preceding cycle to minimize any recovery effects. The force response of the first cycle at each strain was recorded. These data provide a qualitative comparison between previous data from the author's lab and the current study.

Biaxial Comparison Test Protocol

The purpose of this test method was to collect data for comparison to lamb MCA and evaluation of the change in mechanical properties with age. Lamb vessel studies are

being conducted in parallel by another student and are outside the scope of this project. The biaxial test followed the outline used by Monson et al.[38] and Bell et al.[8] Briefly, three inflation tests were performed at constant strain with oscillating pressures followed by three axial tests performed at constant pressure with changing strain. No time was allowed between cycles. The three quasi-static inflation tests were performed by oscillating pressures from 0-20 kPa at constant axial strain of 1.0, 1.05 and 1.1 multiplied by the experimentally determined in vivo length (this preconditioning was done experimentally and the zero load length was not found until postprocessing). The three quasi-static axial stretch tests were accomplished by cycling the strain between the zero load length and 1.1 times the in vivo length at constant pressure of 6, 13.3, 20 kPa. For each of the six tests, the vessel was cycled to the prescribed setting four times before data were recorded to further ensure proper preconditioning. It should be noted that vessels subjected to this test method received higher levels of preconditioning than the other two protocols. After the in vivo length was identified, the vessel was preconditioned to a larger range (1.1 times the in vivo length) in order to allow for a repeatable response in the biaxial tests.

Data Processing

Data were collected through a DAQ system similar to work done by Monson et al.[38] and Bell et al.[8] (NI SCXI -1000, -1314, -1600, -1163, National Instruments, Austin, TX) and processed in a custom Labview program. The data were recorded at 100 Hz. The load cell noise was smoothed using a low pass SAE J211 filter (SAE, 1995). The corner frequency used in this filter was .6 Hz. Images of the vessel were recorded at 3 Hz. These

were synced to the data using linear interpolation. Measurements were taken from the images using imaging software (Vision Assistant, National Instruments, Austin, TX), as shown in Figure 13. The data processing was done in Matlab (Matlab R2007a Student, Mathworks, Natick, MA) and Excel (Microsoft Office 2010, Redmond, WA).

It is necessary to identify and define parameters used in the data analysis. Stretch was defined as $\lambda_z = l/L$ where l is the current length of the vessel and L is the zero load length. Similarly, the in vivo stretch was defined by $\lambda_{iv} = l_{iv}/L$. The assignment of force or stress varied slightly between test protocols.

The incremental protocol and failure data were processed using axial stress defined by the 1st Piola Kirchhoff stress of $\sigma = F_{zz}/A_c$. F_{zz} is the axial force measured by the load cell. A_c is the cross-sectional area of the vessel measured, using thin slice images, in Vision Assistant. Vessels were assumed to have constant cross-sectional area.

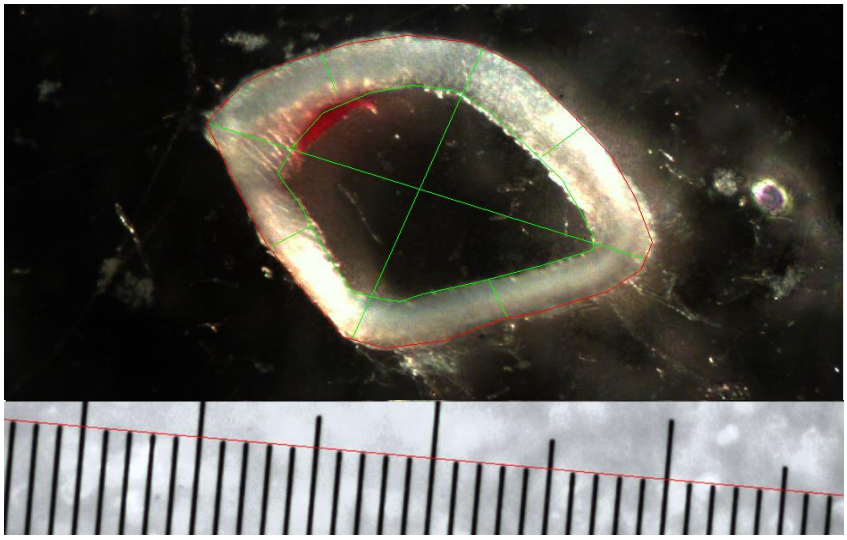

Figure 13: Example of measurements taken in Vision Assistant, custom ruler measure in .076 mm increments, cross-sectional image captured under microscope

For the subfailure injury protocol, it was found that pressurized vessels either became buckled or had natural curvature creating nonuniform stresses. Figure 14 shows a vessel during a baseline test initially in a buckled or in a curved state and then becoming axially aligned during the test. The presence of buckling, natural curvature, or the combination of both introduces nonuniform stresses making it difficult to predict stress distributions and thus complicating the use of stress as a parameter for this protocol. This causes the side of the vessel with greater curvature to be in tension and the opposite in compression. The nonuniform distribution of stress complicates the analysis. To simplify the analysis, percent change in force was used to compare pre- and postinjury baselines. The percent change is identified in equation 3.

$$\%_{change} = \frac{new - old}{old}(100) \tag{3}$$

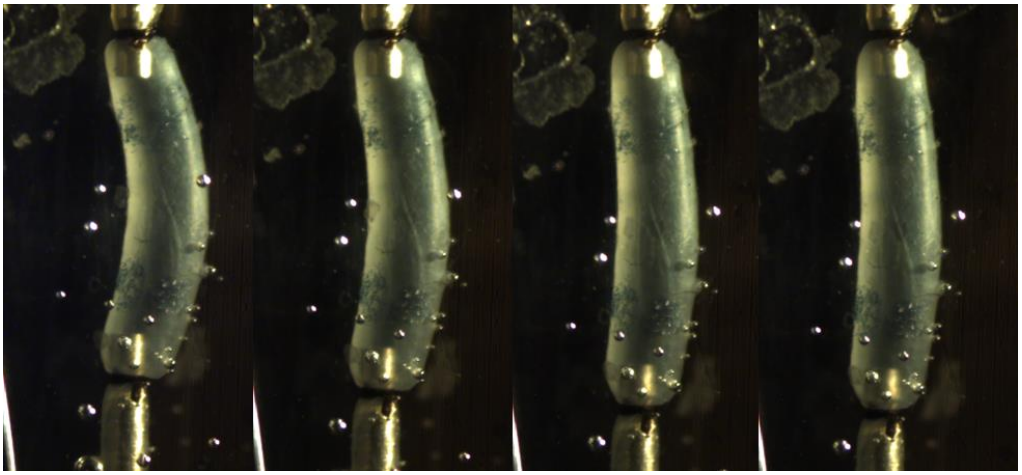

Figure 14: Snapshots of a vessel during a baseline test
initially buckled and becoming unbuckled

In order to characterize the effects associated with subfailure damage, the pre- and postinjury baselines needed to be parameterized. Equation 4 was suggested by Fung[46] and used by Monson et al.[32] to characterize the toe region of blood vessels.

$$P_{zz} = \frac{B}{A}\left(e^{A(\lambda_z - 1)} - 1\right) \qquad (4)$$

The axial stress, P_{zz}, is defined as an exponential function of λ_z with modeling constants of A and B. The unitless constant A describes the degree of curvature while B, with units of MPa, describes the slope of the curve at λ_z=1. According to this equation, the stress of the vessel at the zero load length is zero or $P_{zz}(\lambda_z=1)= 0$. This equation modeled the uniaxial work done by Fung and Monson well. As noted, the presence of nonuniform stress required a change in the model. It was determined to use axial force, $F_{zz,}$ instead of axial stress, P_{zz}.

Luminal pressure was included in some of the present experiments in order to match physiological conditions of 13.3 kPa. Pressure was not included in the uniaxial tests of Monson. This difference required that the constant C be added to equation 4 in order to account for the luminal pressure of the vessel which induced a non-zero force reading at the zero load length. Equation 5 uses F_{zz} instead of P_{zz} and adds an offset constant to account for axial force induced by luminal pressure. The maximum in vivo stiffness, E_{iv}, was defined as the derivative of equation 5 evaluated at $\lambda_z=\lambda_{iv}$ as shown in equation 6.

$$F_{zz} = \frac{B}{A}\left(e^{A(\lambda_z - 1)} - 1\right) + C \tag{5}$$

$$\frac{\partial F_{zz}}{\partial \lambda}_{\max} = B\left(e^{A(\lambda_{\max} - 1)}\right) \tag{6}$$

The model was fit to the data using an interface developed by Geoffrey M. Boynton[47] for the fminsearch function in Matlab. The fit of the model was optimized by minimizing the sum of the squares error as noted in equation 7. All Matlab code is located in the Appendix.

$$SSE = \frac{(X_{model} - X_{data})^2}{SE_{mean}{}^2} \tag{7}$$

Descriptive statistics were obtained to describe vessels and testing parameters in the format of mean±SD (sample size). Additional statistics were performed using the Data Analysis Toolpack in Microsoft Excel (Microsoft Office 2010, Redmond, WA). These tests included two-tailed t-tests and analysis of variance (ANOVA). Results were considered statistically significant when $p < 0.05$ ($\alpha = 0.05$).

CHAPTER 3

RESULTS

Overview

Twenty-six out of thirty-nine vessel tests were successful. The thirteen failed vessel tests were caused from either human error during vessel preparation, suture failure on the microbranches leading to a loss in luminal pressure, or software control failure using the Labview interface. Of the twenty-six successful tests, six were set aside to be processed simultaneously with the lamb biaxial tests in order to reduce data processing inconsistencies. MCA property statistics are recorded in Table 2; see Appendix for complete table. The in vivo stretch, $\lambda_{iv,}$ and the reference length, L, were identified during postprocessing in Matlab. The vessel cross-sectional area, CS, the outer diameter, OD, and wall thickness, t, were found by averaging measurements in Vision Assistant.

Table 2: MCA properties (n=20)

	λ_{iv}	L (mm)	CS (mm^2)	OD (mm)	t (mm)
Mean	1.083	4.546	.459	1.081	.152
SD	.030	.774	.123	.157	.023
Max	1.132	6.879	.705	1.365	.201
Min	1.035	3.535	.275	.836	.121

It was found that the model in equation 5 fit the toe region of the baseline curves very well with a sum of the squares error of .0000343±.00005 (n=20). The baseline test in Figure 15 is an example of a fitted baseline curve. The parameters from the model were used to compare changes in baseline curves. It should be noted that the maximum force in many of the traces such as the one in Figure 15 begins to level off at the end of the baseline. This is believed to be caused by end effects due to the low pass filter used to smooth out the force signal as shown in Figure 16.

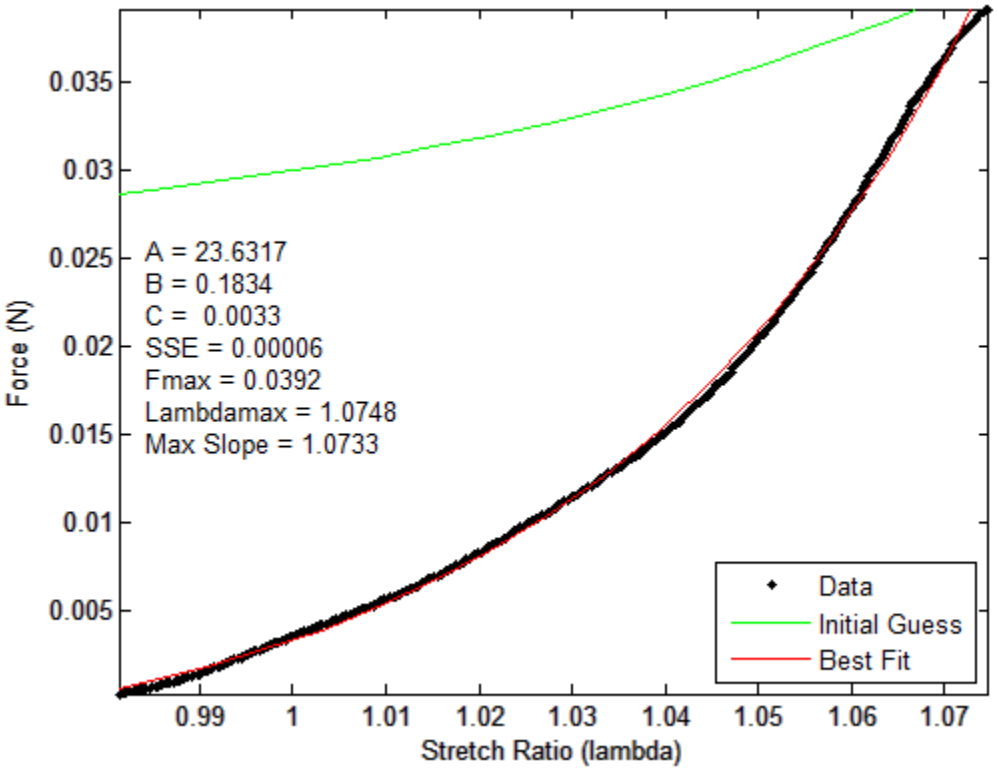

Figure 15: Fit of model to data

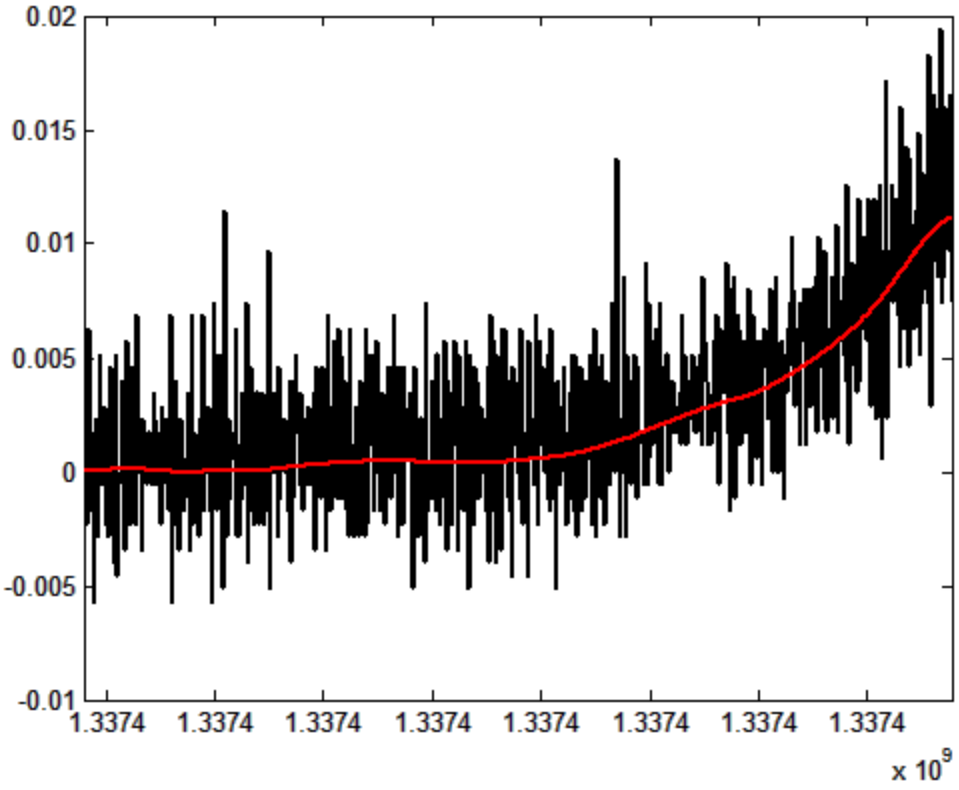

Figure 16: Raw force versus filtered force

Preconditioning

In order to show that hysteresis had been minimized in the current preconditioning method, a baseline response test was run on two vessels immediately after preconditioning. The vessels were then subjected to additional preconditioning through stress relaxation. Each vessel was held at in vivo conditions for 12 minutes after which another baseline test was repeated. Figure 17 shows the before and after mechanical response in one of the specimens. As shown in Table 3, the maximum force and maximum stiffness remained fairly constant with a mean change of -2.01±5.09% (n=2) and -4.49±9.05% (n=2), respectively.

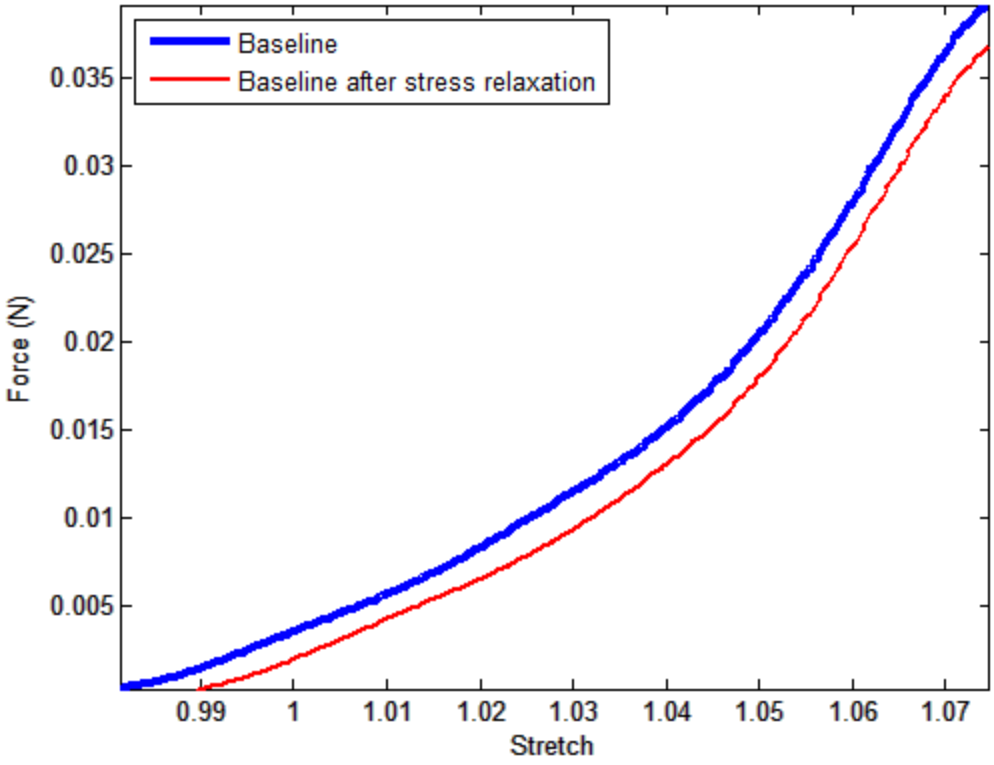

Figure 17: Effect of additional preconditioning

Table 3: Percent change of baseline parameters after additional tests

	Stress relaxation (n=2)	Biaxial tests (n=6)
A	-3.31 ± 15.69%	-5.8 ± 15.46%
B	-17.66 ± 40.40%	2.52± 24.91%
C	-41.94 ± 3.57%*	2.52 ± 37.94%
E_{max}	-4.49 ± 9.05%	-14.22 ± 16.81%
F_{max}	-2.01± 5.09%	-10.24± 8.57%*

* Significant change in baseline response ($p<0.05$)

The effectiveness of the current preconditioning method was further characterized by repeating the same procedure for six vessels before and after a set of biaxial tests. These tests were conducted within the preconditioned window and theoretically should not affect the baseline response. Figure 18 shows an example of the change in the force-strain response. As shown in Table 3, the maximum force and maximum stiffness decreased 10.24±8.57% (n=6) and 14.22±16.81% (n=6), respectively, as a result of the six biaxial tests. The maximum force was confirmed statistically different from the pre-biaxial test baseline (p=.033). The drop in force is expected because preconditioning can only minimize hysteresis not eliminate it.

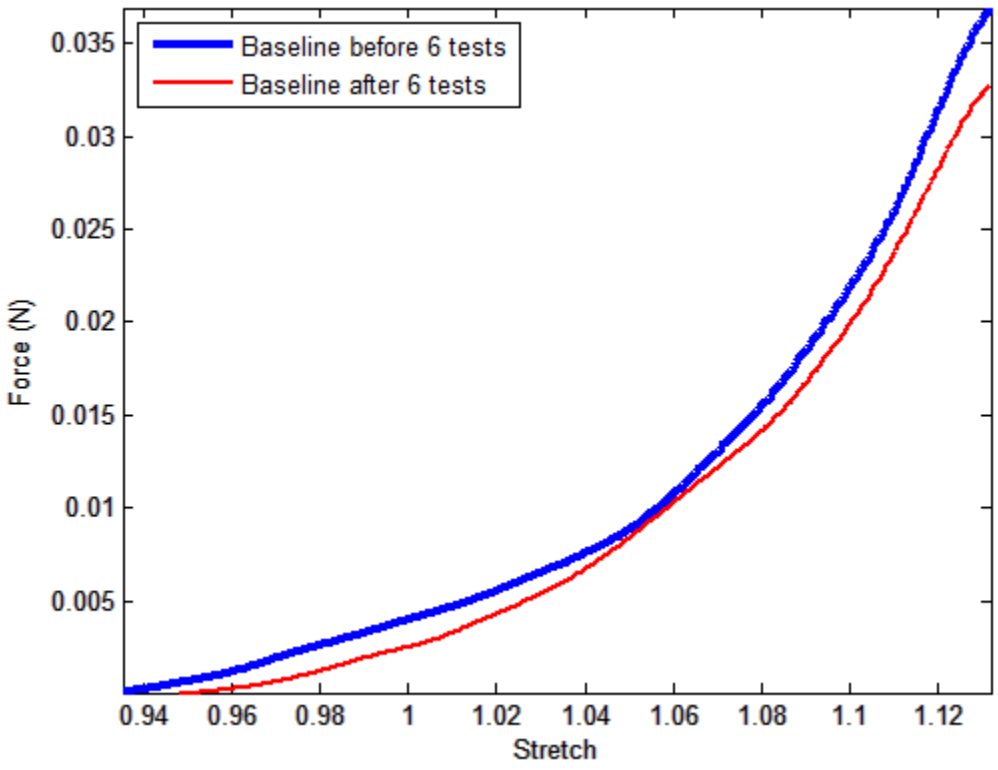

Figure 18: Difference in mechanical response on a single vessel after six biaxial tests

Subfailure Injury

Eighteen vessels from eight different ewes were tested for subfailure injury by comparing the pre-injury mechanical baseline response to repeated postinjury baselines over time. These tests were grouped into five levels of injury. While symmetry between these groups was desired, the level of overstretch could not be fully accounted for until postprocessing of the data. Table 4 shows the amount of vessels tested at each level of overstretch. The smallest overstretch was 1.1, slightly higher than λ_{iv} which was found to be 1.083±.03 (n=20).

The average length of time over which baselines were repeated after overstretch was 115 minutes. The longest time after overstretch that a baseline was repeated was 390 minutes. The length of recovery time varied as it was unknown how much time a vessel needed for recovery. Upon completion of the baselines, four vessels were stretched to failure and six vessels were fixed in 4% paraformaldehyde for 2 to 12 hours for structural imaging on the confocal microscope. The actual imaging was considered to be beyond the scope of this project.

In tests at in vivo conditions and below, the magnitude of the axial force reading was quite small. The average maximum axial force in the pre-injury baseline was found to be .033±.007 N (n=20). Small variations were noticed in the axial force responses

Table 4: Number of specimens grouped by level of overstretch (with zero load reference)

	1.1	1.2	1.3	1.4	1.5
Number of specimens	3	3	2	6	4

between baseline tests even though the force was zeroed out before each baseline to account for drift over time in the load cell. This was achieved by bringing the vessel to a buckled position, reducing the luminal pressure to atmospheric levels, and then zeroing the axial force signal in Labview. Even so, Figure 19 shows small variations in the beginning of the axial force response for different baselines. The variations made it difficult to evaluate any viscoelastic recovery as a function of time.

In order to quantify the noise in the data, seven random baseline tests were chosen. The force response was examined at a point in the test where the vessel buckled at zero strain with a luminal pressure of 13.3 kPa. On average, 100 data points were taken

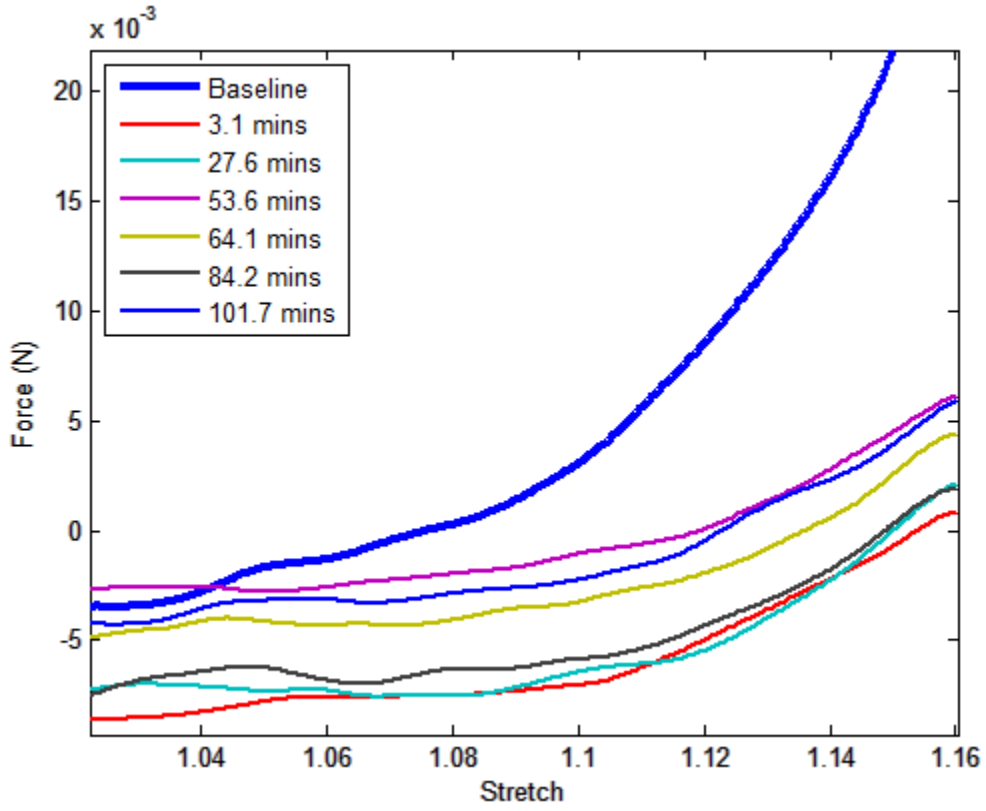

Figure 19: Subfailure injury test subjected to an overstretch of 1.36 with variations in the baselines

from each test and the maximum and minimum forces were noted. The average range of force measured by the load cell was found to be .0014±.0008N (n=7). While these data provide a sense of the variation in the data immediately before the baseline test, it is believed that this is due to load cell noise which has a nonlinearity limit of .01 N.

A state of equality between baselines was needed to evaluate the effects of overstretch on the pre- and postinjury baselines. Accordingly, the data were adjusted during postprocessing by finding the average axial force immediately before the start of the baseline test and deducting it from the axial force reading during the baseline. After applying this postprocessing method to the data, all axial force readings begin at the same starting point making it easier to analyze recovery over time. It should be noted that by doing so, the axial force values were no longer negative in the buckled configuration, but this was consistently applied to all data to allow comparison. Negative axial force is a consequence of non-zero internal pressure when there is no axial stress in the vessel wall, as required by equilibrium.

Upon creating a state of equality between the baseline responses, the pre-injury response was compared to the response immediately after overstretch. A complete list of pre- and postinjury parameters is located in the Appendix. The percent change in the parameters of A, B, C, F_{max}, and E_{max} were noted. The clearest changes after injury are seen in Figure 20 and Figure 21 which show a linear relationship between the level of overstretch and the in vivo force and stiffness, respectively. The in vivo force is decreased about 16% for each .1 of additional overstretch. The stiffness is reduced by about 14% for each .1 increase in overstretch. While statistical analysis of these values

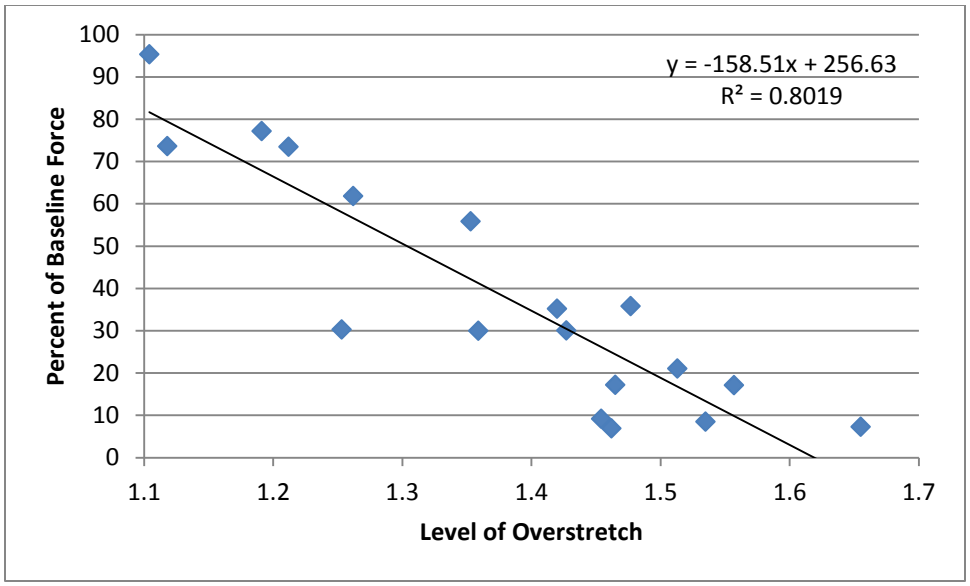

Figure 20: Effect of overstretch on percent of baseline force

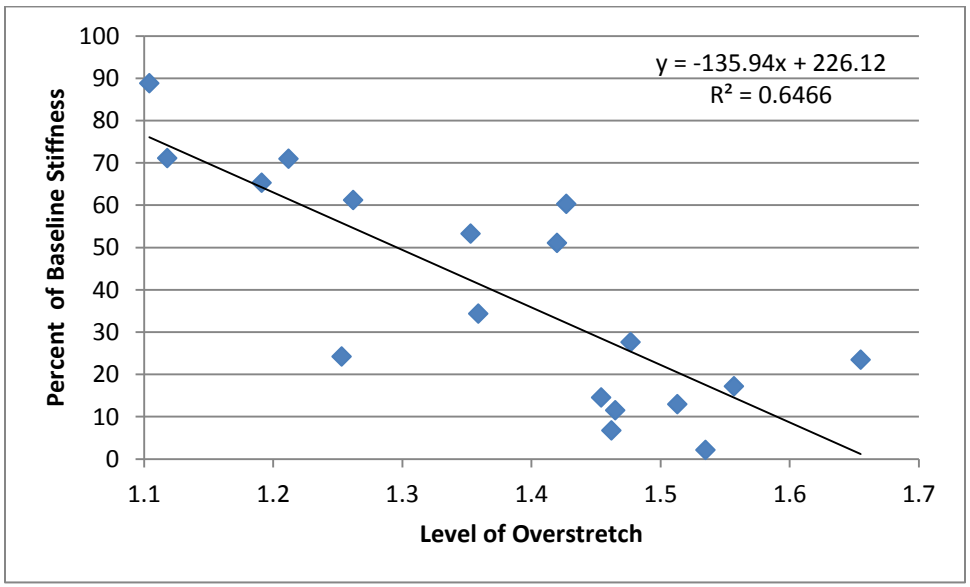

Figure 21: Effect of overstretch on percent of baseline stiffness

was found to be inconclusive, the results are expected to become significant with additional samples.

The effect of overstretch on percent change in A, or the degree of curvature in the toe region, is shown in Figure 22. These data seem to be constant at low levels of stretch and become noisy at high levels of overstretch. The percent change of B, or the slope of the curve at λ_z=1, decreases as the level of overstretch increases, as shown in Figure 23. This is believed to be caused by an elongation in the toe region during overstretch. The percent change in C, or the offset due to pressure in the vessel, in regards to overstretch is shown in Figure 24 where no clear trend is seen.

Furthermore, the relationships between these parameters and the cross-sectional area and the in vivo length were explored in order to characterize any additional influences that might be affecting the data. Postinjury response was found to not be influenced by the size of the vessel. Figure 25 shows the percent change of force related to the cross-sectional area of the vessel where no clear trend is established. Figure 26 shows the percent change in stiffness versus the cross-sectional area where again no trend is clear. The other parameters were tested but produced similar results.

Additionally, the percent change in the parameters from pre- and immediate postinjury response was compared with the in vivo length. It was found that the differences in the in vivo length between vessels did not affect vessel response postinjury. Figure 27 and Figure 28 show that the percent of baseline force and stiffness, respectively, held no clear trend with in vivo lengths. The other parameters were tested but no clear trends were identified.

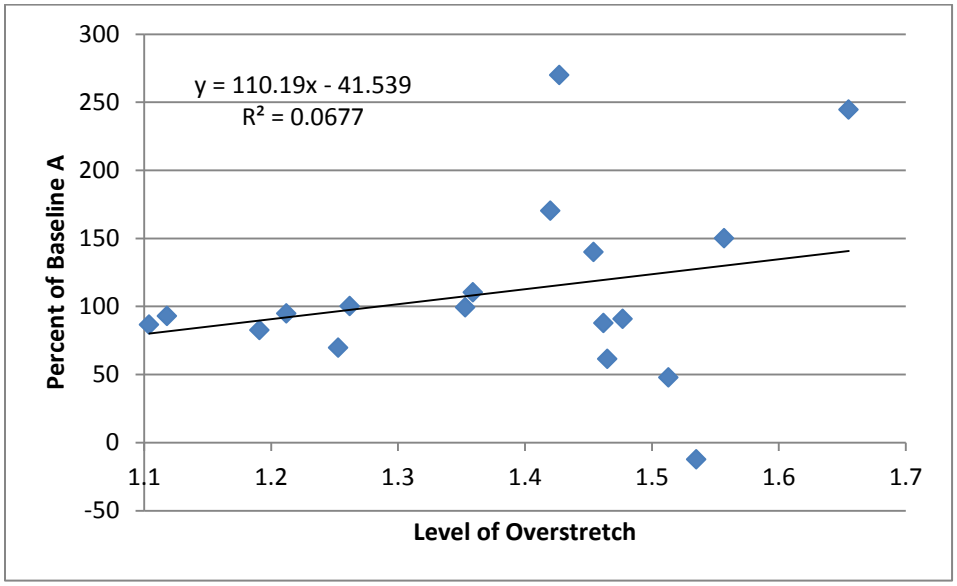

Figure 22: Effect of overstretch on percent of baseline A

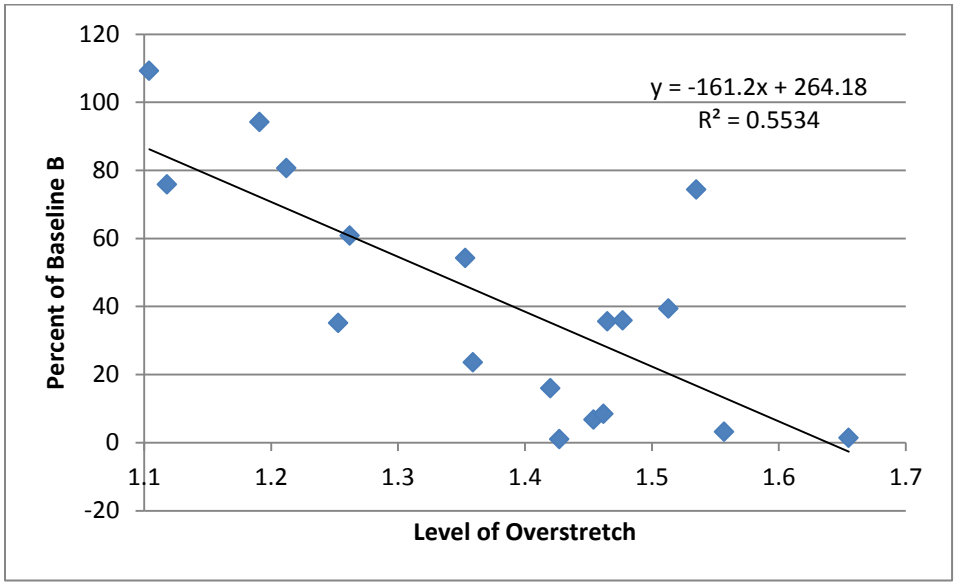

Figure 23: Effect of overstretch on percent of baseline B

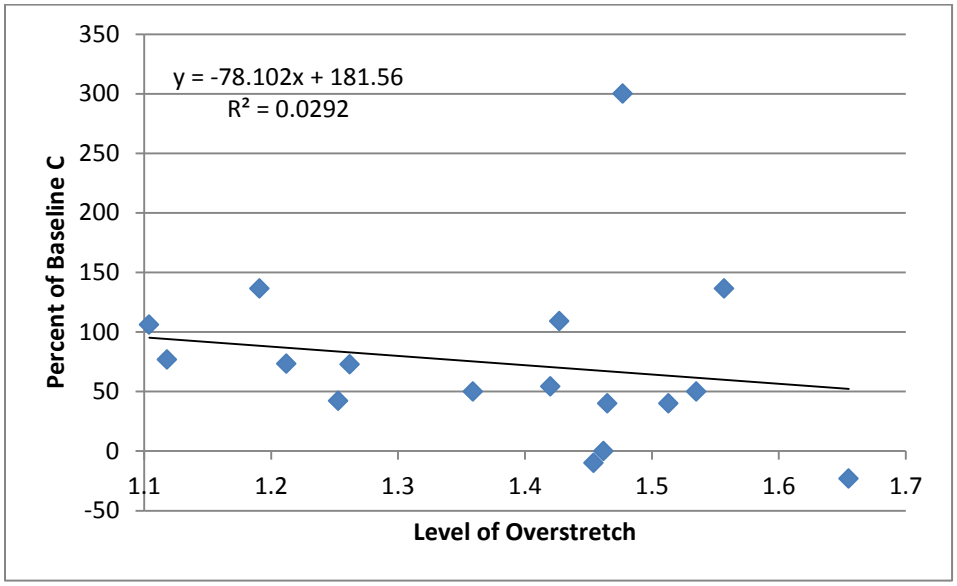

Figure 24: Effect of overstretch on percent of baseline C

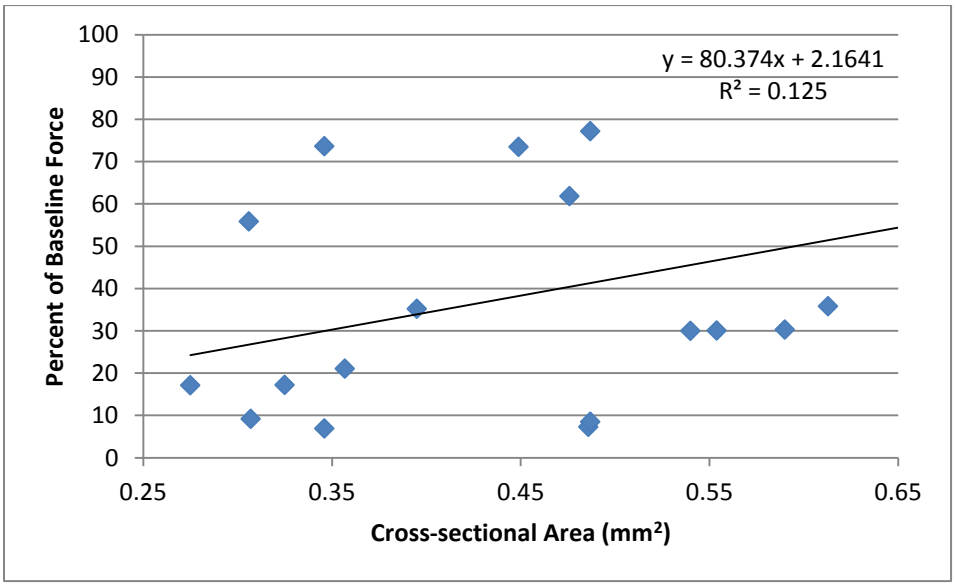

Figure 25: Effect of cross-sectional area on percent of baseline force

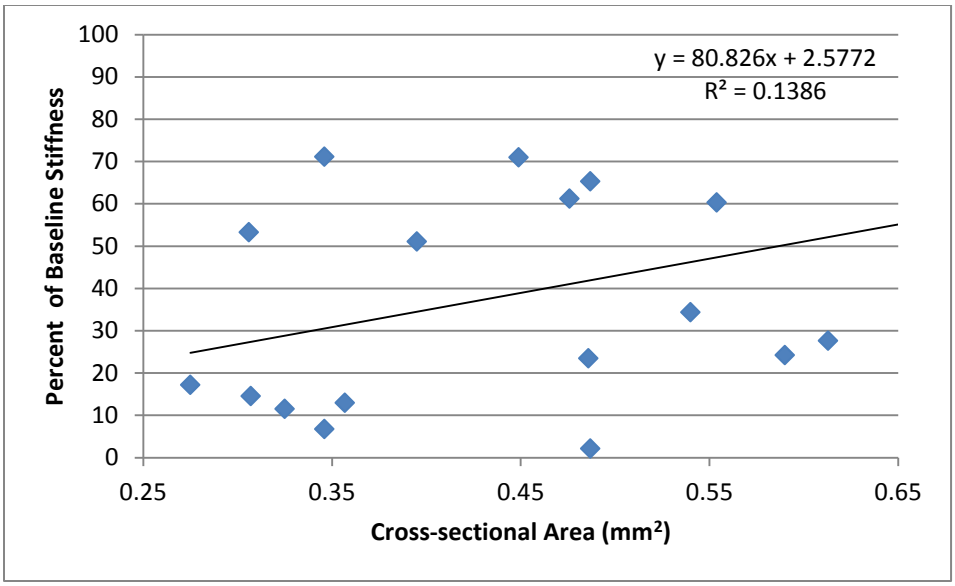

Figure 26: Effect of cross-sectional area on percent of baseline stiffness

In order to better understand the relationships between these parameters and overstretch, size, and natural configuration, a correlation tool was used in Excel's data analysis toolpack. The coefficient of correlation has a range of -1 (perfect inverse relationship) and 1 (perfect relationship). Zero represents no relationship. Coefficients found between these points show a certain level of strength in that direction. The results are found in Table 5. These correlations confirm the trends already presented with the addition of a strong correlation between F_{max} and E_{max}, as expected.

Next, the postinjury responses over time were compared and analyzed in order to identify any recovery after overstretch. Figure 29 shows a recovery plot for a single vessel before and after an overstretch of 1.19 with the axial forces from each baseline at a state of equality. The "Baseline" curve in each plot refers to the pre-injury baseline. After overstretch, the same baseline test was repeated at varying time increments as noted. Figure 30 shows a recovery plot after an overstretch of 1.26. Figure 31 shows a recovery

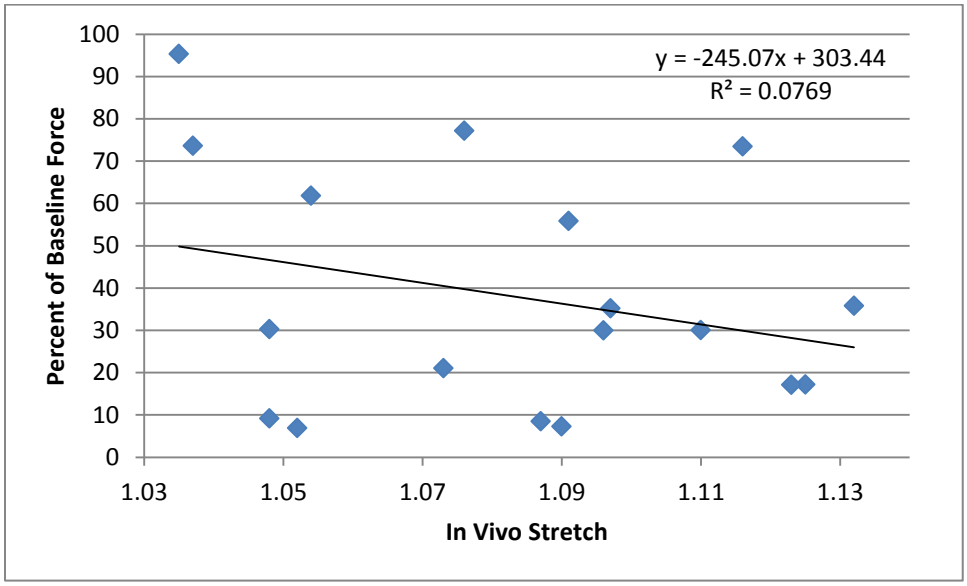

Figure 27: Effect of in vivo stretch on percent baseline force

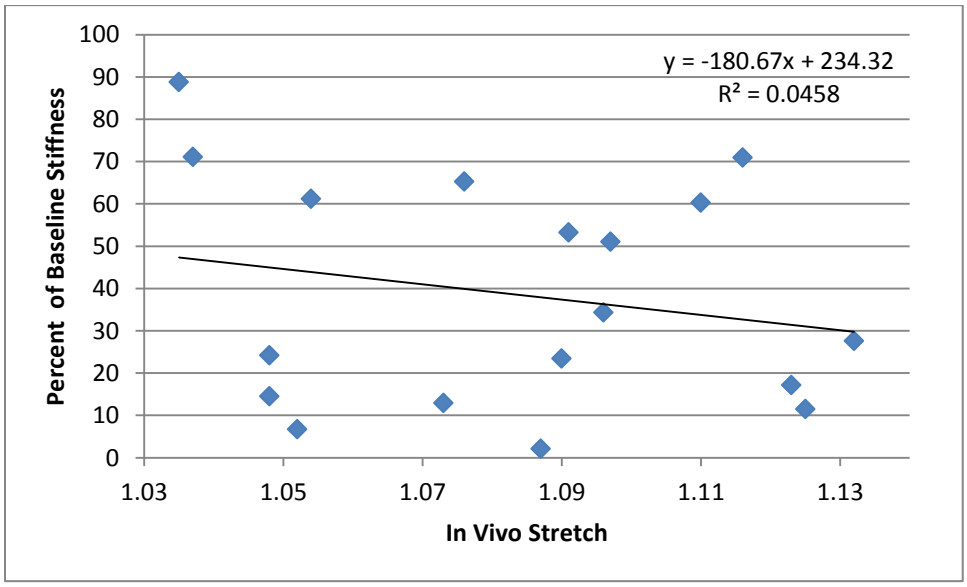

Figure 28: Effect of in vivo stretch on percent baseline stiffness

Table 5: Correlation results between parameters (independent variables bolded)

	A	B	C	F_{max}	E_{max}	Overstretch	λ_{iv}	CS
A	1.000							
B	-0.596	1.000						
C	-0.061	0.163	1.000					
Fmax	-0.144	0.810	0.265	1.000				
Emax	0.204	0.595	0.217	0.925	1.000			
Overstretch	**0.260**	**-0.744***	**-0.092**	**-0.895***	**-0.804***	**1.000**		
λiv	**0.216**	**-0.315**	**0.194**	**-0.277**	**-0.214**	**0.495**	**1.000**	
CS	**0.028**	**0.336**	**-0.154**	**0.354**	**0.372**	**-0.329**	**-0.092**	**1.000**

*Note: Values were found to be statistically significant ($p<.05$)

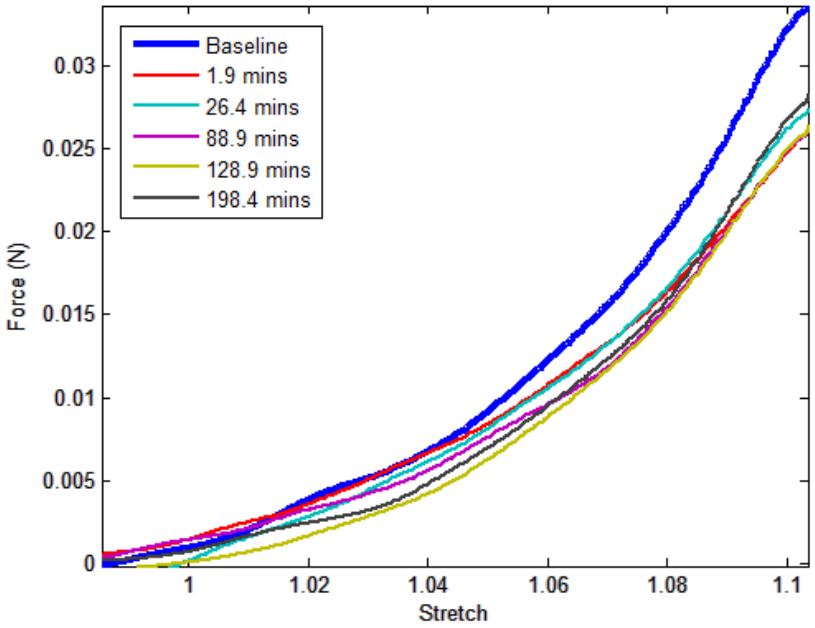

Figure 29: Recovery after an overstretch of 1.19

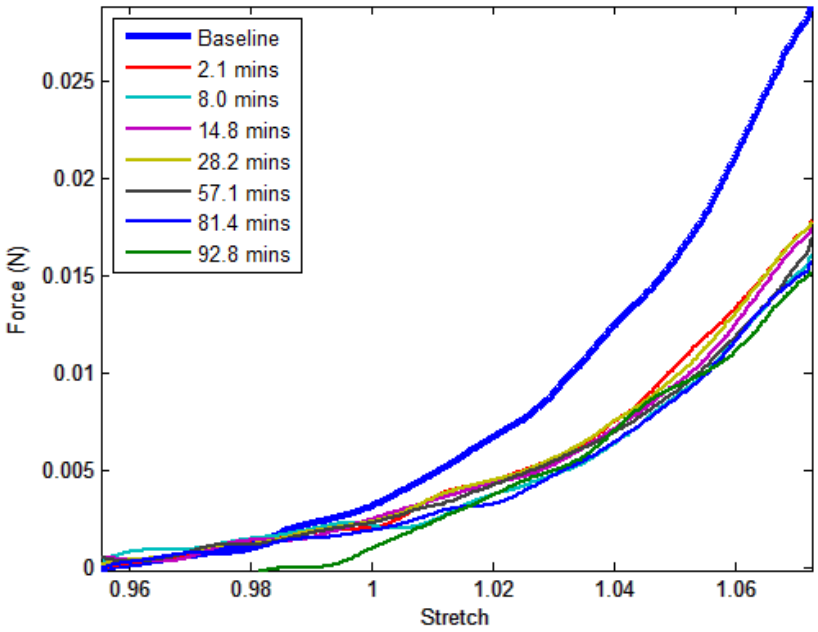

Figure 30: Recovery after an overstretch of 1.26

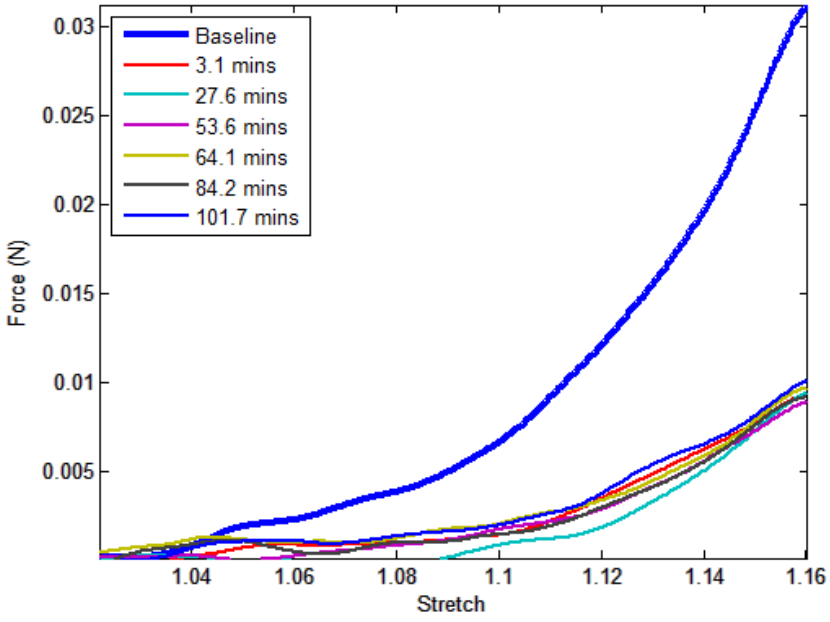

Figure 31: Recovery after an overstretch of 1.36

plot after an overstretch of 1.36. Figure 32 shows a recovery plot after an overstretch of 1.45. Figure 33 shows a recovery plot after 1.54. These data, as well as additional data in the Appendix, suggest that there is no passive recovery over time after overstretch.

The recovery plots were analyzed statistically using a single factor ANOVA. The pre- and postbasline traces of all specimens were parameterized using equation 5 for each test. Each specimen test was assigned to a category based on the length of overstretch. The modeling parameters of A, B, and C did not seem to show any patterns and were set aside for this analysis. Three postinjury baselines were selected from the following categories: shortly (typically 3 minutes) after overstretch, midway (typically 30 minutes) after overstretch, and long (typically 90 minutes) after overstretch. The percent change in maximum force and maximum stiffness were noted from these postinjury baselines.

The null hypothesis was set as the mean would be equal for all categories of time suggesting no recovery. It was found that for all levels of overstretch, the null hypothesis could not be rejected; all p-values were above .05. As such, the results are inconclusive; however, they are consistent with the means at various times being equal. The results are outlined in Table 6 for the maximum force and Table 7 for the maximum stiffness.

The possibility of noise in the force data required further analysis to assess the possibility of blood vessel recovery over time. Video footage from specimens stretched to λ=1.1 and λ=1.4 was analyzed in Vision Assistant. For each specimen, a reference image was determined in the pre-injury baseline test as the point where the vessel was no longer buckled. This was found by matching the closest video image with the point where pre-injury baseline force response became positive. A line was drawn over the image connecting the center of the needles. A perpendicular reference line was then drawn in

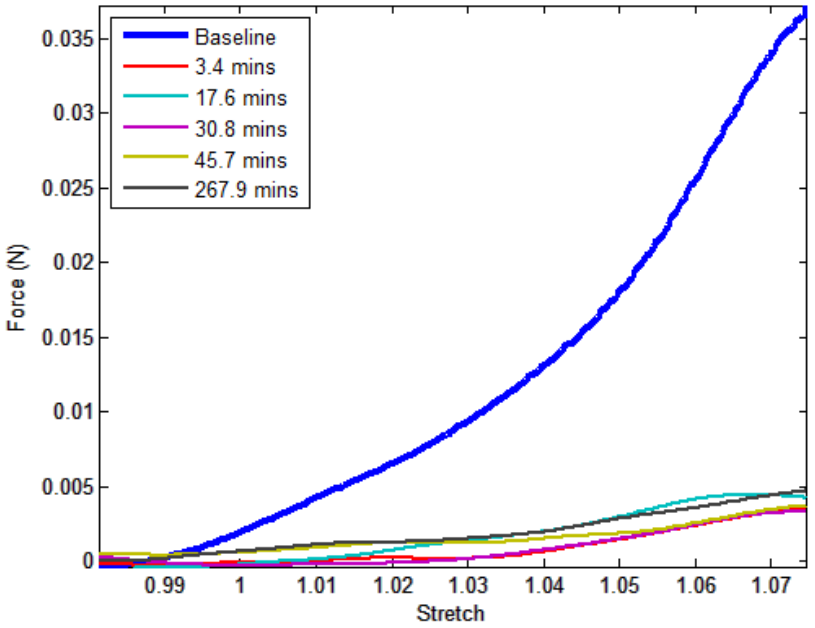

Figure 32: Recovery after an overstretch of 1.45

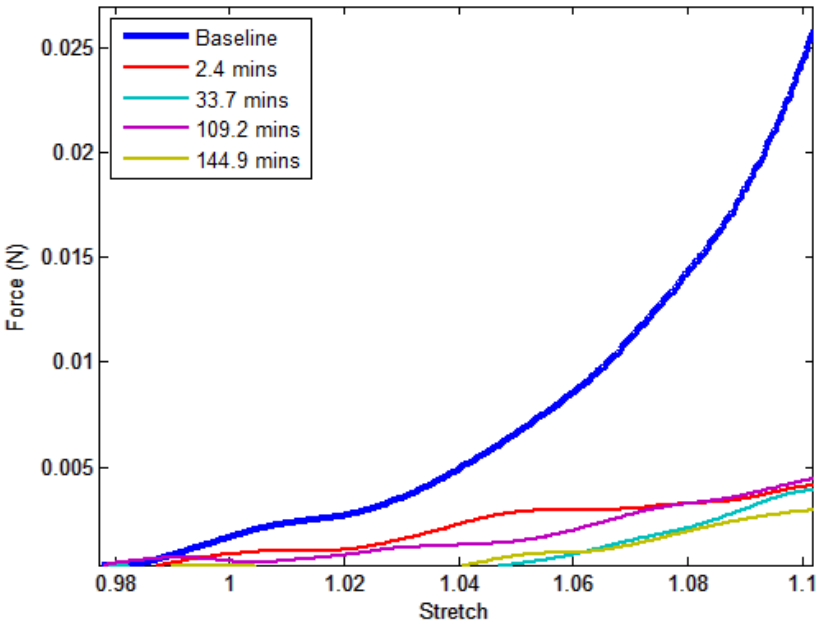

Figure 33: Recovery after an overstretch of 1.54

Table 6: Single Factor ANOVA results for F_{max}

λ	n	Average $\%_{change}$ F_{max} t=short	t=mid	t=long	p-value
1.1	3	-17.97	-14.51	-19.44	0.825
1.2	3	-44.81	-38.14	-45.37	.921
1.3	2	-57.1	-56.77	-62.5	.93
1.4	6	-77.64	-74.93	-73.12	.868
1.5	4	-86.52	-85.76	-86.53	.978

Table 7: Single Factor ANOVA results for E_{max}

λ	n	Average $\%_{change}$ E_{max} t=short	t=mid	t=long	p-value
1.1	3	-24.93	-19.2	-17.44	.666
1.2	3	-47.88	-44.5	-48.5	.977
1.3	2	-56.2	-58.5	-68.46	.581
1.4	6	-71.37	-77.57	-78.35	.76
1.5	4	-86.09	-84.29	-87.12	.872

the center of vessel to the outside of the greater curvature. The axial displacement value was noted at this reference image.

Three periods of time were again selected at shortly, midway, and long after overstretch. The image was then identified in each postinjury baseline where the greater curvature met the tip of the reference line. Figure 34 shows images from the analysis of one of the specimens. The corresponding axial displacement was noted for each image. This method is a measure of how much axial displacement it took for the vessel to return to where the original baseline was no longer buckled. Table 8 shows the results of this analysis. It should be noted that statistical analysis was not performed on these data because of the single sample size at the two levels of overstretch.

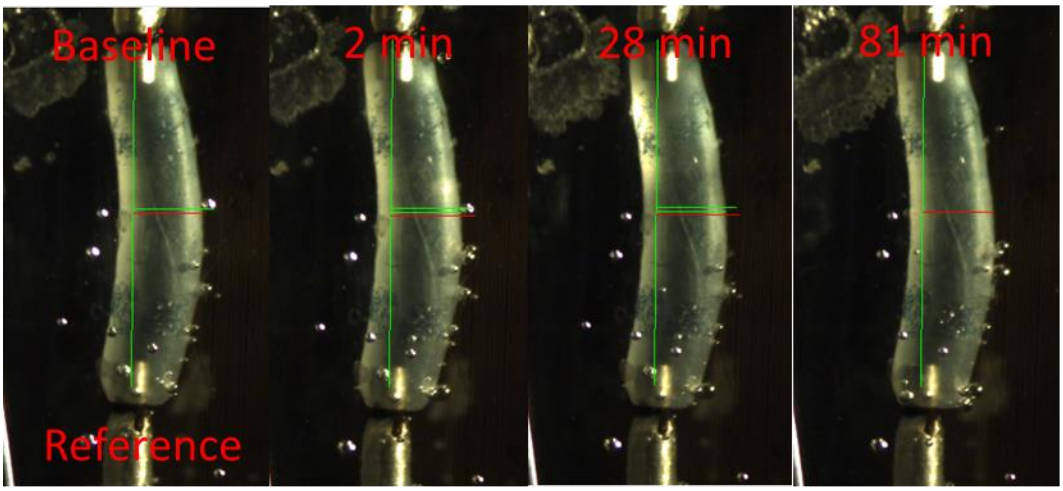

Figure 34: Image analysis of matching the greater curvature to the reference point at various time increments

Table 8: Axial displacements from the image analysis of recovery over time

	Axial Displacement (mm)			
λ	reference	t=short	t=mid	t=long
1.1	0.66	0.73	0.719	0.712
1.42	0.457	0.679	0.686	0.6845

Incremental Stretch

Two vessels were successfully tested for incremental stretch and are shown in Figure 35 and Figure 36. Both tests have been plotted using identical axes for better comparison. Incremental test #1 had an axial failure stress of 1.67 MPa and a failure stretch of 1.62. The gray line connects the maximum stress of each cycle. There appears to be a slight decrease in slope of the gray line around 1.3 stretch and a more noticeable increase in slope at 1.44 stretch suggesting a change in vessel response that may be

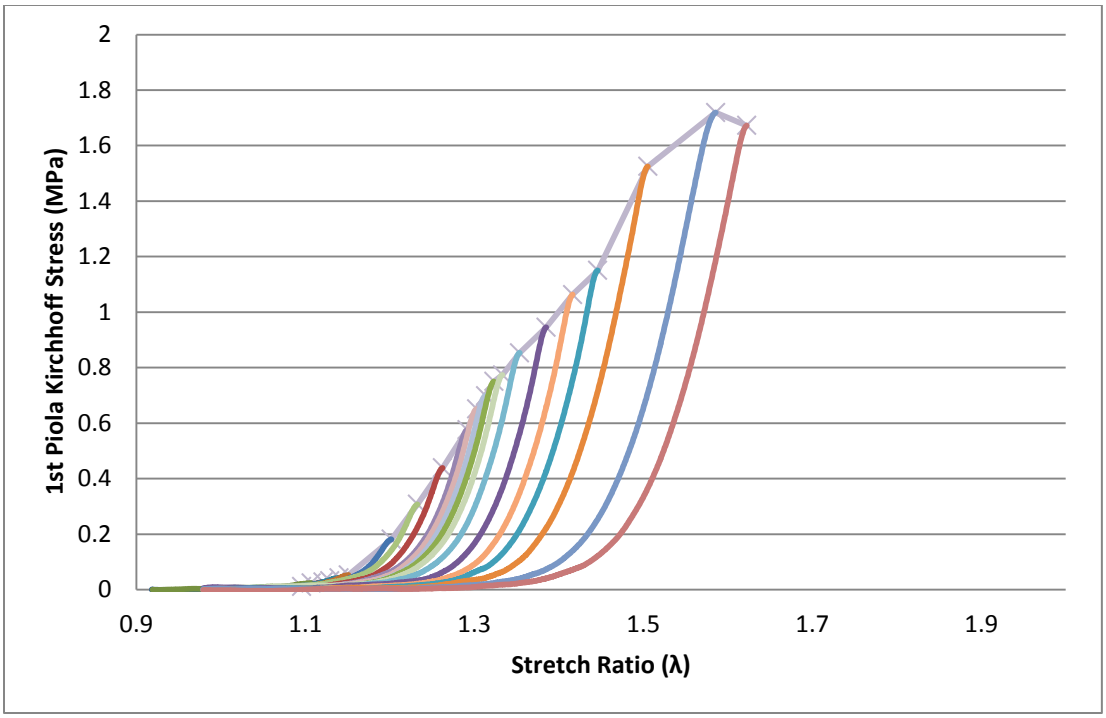

Figure 35: Axial stress-stretch curve for incremental test #1

related to subfailure damage at these points. The stress increases until its ultimate value at 1.71 MPa, after which it decreases and fails.

Incremental test # 2 has an ultimate and failure stress of 1.42 MPa and stretch of 1.99. The slope of the connected maximum stress (shown in gray) is fairly constant up until about a stretch of λ1.5 where it begins to decrease slightly. This slope increases dramatically at around a stretch of 1.6 until it becomes plateaued at a stretch of 1.77 until ultimate failure. The slope of the toe region remains constant up until around a stretch of 1.5 where it begins to decrease suggesting subfailure damage in the vessel.

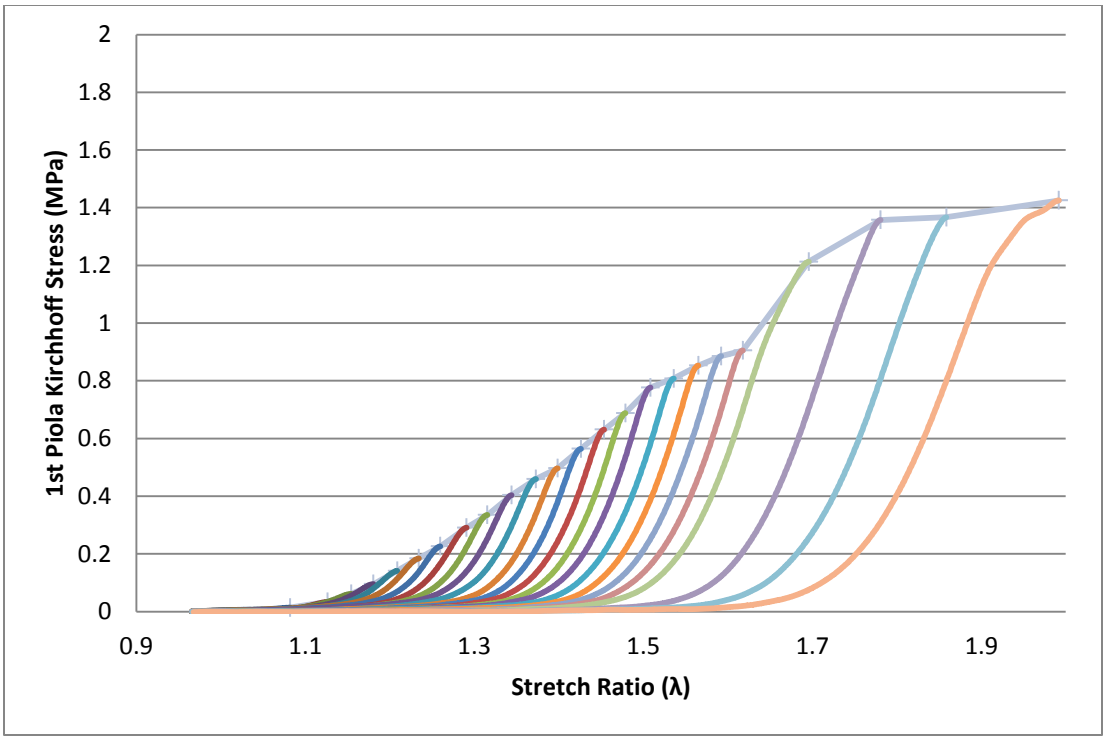

Figure 36: Axial stress-stretch curve for incremental test #2

Biaxial Tests

Eighteen vessels from nine different ewes were subjected to six biaxial tests. After completing the six tests, five specimens were stretched to failure, one specimen slipped off the needle during ultimate failure stretch, and twelve were subjected to additional subfailure injury testing. Tests were coordinated with concurrent lamb MCA testing so that experiments would offer a valid comparison between lamb and ewe. These data will be processed jointly with concurrent lamb MCA biaxial tests to minimize any processing error.

Failure Analysis

Five biaxial tests, four subfailure injury tests, and both incremental tests were stretched to failure. The stress-strain curves of these tests are shown in Figure 37. The point of maximum stress and maximum slope is indicated by a triangle and circle, respectively, on each trace. The toe region was fit to equation 4 because the vessels were not pressurized. Table 9 lists the important parameters for each trace.

In order to compare the effects of the different tests, the mean and standard deviation were found for each test type, as shown in Table 10. The overstretch tests resulted in the highest average maximum stress and maximum stiffness of 1.68±.28 MPa (n=4) and 1.65±.12 MPa (n=4), respectively. The incremental tests resulted in failure points with the largest stretch ratio of 1.90±.13 (n=2).

It should be noted that the sum of squares error or SSE values was higher than previous model results. Unlike previous baseline data reported where the entire trace was considered part of the toe region, the end of the toe region was chosen manually through observation in the failure plots. This may account for some of the error.

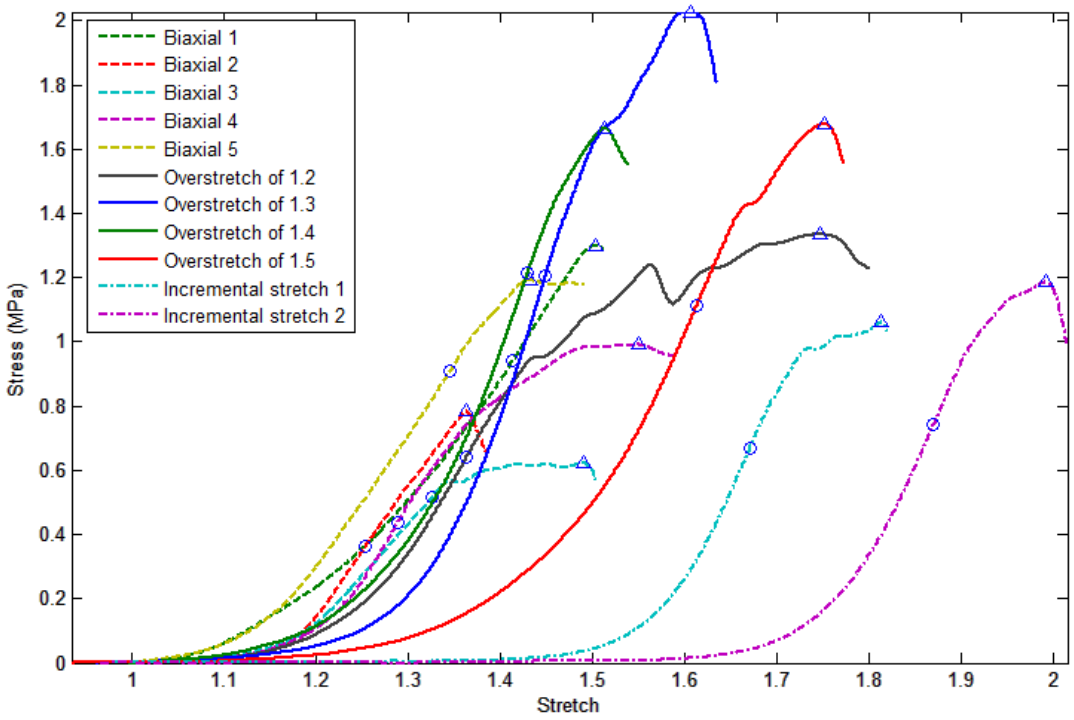

Figure 37: Vessel failure properties after various subfailure tests

Table 9: Parameters of failure data

Test	A	B	SSE	E_{max} (MPa)	σ_{max} (MPa)	λ_{max}
Biaxial 1	6.89	0.5247	0.1399	1.2989	1.5026	4.8154
Biaxial 2	23.37	0.0295	0.0518	0.7834	1.3638	4.4667
Biaxial 3	17.89	0.0618	0.001	0.6229	1.49	3.6027
Biaxial 4	1.035	0.0631	0.0095	0.9907	1.5498	5.047
Biaxial 5	16.8579	0.3027	0.0091	1.1922	1.4321	4.7257
Overstretch of 1.2	13.0879	0.095	0.032	1.334	1.7462	10.3331
Overstretch of 1.3	12.8464	0.0598	0.0735	2.0276	1.6061	19.1551
Overstretch of 1.4	12.8086	0.1811	0.0807	1.6656	1.5136	16.8249
Overstretch of 1.5	10.335	0.0671	0.1598	1.6797	1.7509	13.4774
Incremental 1	8.2545	0.0001	0.0179	1.0604	1.8128	13.2326
Incremental 2	17.54	0	0.0457	1.1864	1.9914	13.4827

Table 10: Effect of subfailure testing on failure properties

Test	A	B	SSE	σ_{max} (MPa)	λ_{max}	E_{max} (MPa)
Biaxial (n=5)	15.6±6.1	.2±.21	.042±.058	.98±.28	1.47±.07	4.53±.56
Overstretch (n=4)	11.1±2.2	.1±.06	.086±.053	1.68±.28	1.65±.12	14.9±3.86
Incremental (n=2)	16.2±1.9	.00005	.032±.02	1.12±.09	1.90±.13	13.4±.18

CHAPTER 4

DISCUSSION

The present study was focused on characterizing the passive subfailure properties of cerebral blood vessels. Tests were performed in vitro so that loading condtions could be better defined. The two major findings of the study were identifying a linear relationship between increasing degrees of overstretch and decreasing percent baseline force and stiffness values as well as showing that no significant recovery occurs after overstretch. It was also found that the present preconditioning methods were well suited to produce repeatability and minimize hysteresis. Incremental stretch tests on the MCA suggested the possibility that subfailure damage occurs between λ=1.3 and 1.6. The failure properties of the blood vessels were also changed as a function of the type of subfailure testing.

This study focused on axial subfailure damage in order to mimic the loading a vessel might experience during a traumatic brain injury. There is a connection between axial and circumferential injury. Previous studies have shown that axial stretch decreases the circumferential distensibility; however, increasing pressure has a lesser effect on axial behavior.[38, 48] Axial behavior was the focus of the current study; however, it might be interesting to characterize the effect of axial overstretch on circumferential properties.

It is interesting to note that much research has been dedicated to show the effect of pregnancy on blood vessels. While researchers agree that the uterine artery undergoes significant change during pregnancy,[49] the level of effect of pregnancy on systemic vasculature is a topic of research. It is generally accepted that pregnancy affects the ability of cerebral vessels to autoregulate blood flow in the brain.[50-51] The focus of the current study is not autoregulation but to characterize subfailure passive mechanical properties.

One study initially seems to indicate that pregnancy affects the passive mechanical properties. Work done by Jovanovic and Jovanovic[52] suggests that there is a hypotrophy of endothelial and smooth muscle cells in the carotid artery in pregnant guinea pigs. Eight to ten guinea pigs were tested from four different groups: nonpregnant, early pregnant, midpregnant, and late pregnant. The cross-sectional area of the carotid artery layers was measured using light and electron microscopy. The external diameter, wall thickness, and cross-sectional area of both the media and intima progressively decreased with pregnancy. The tunica externa remained constant. Electron microscopy showed that the size of the endothelial and smooth muscle cells decreased.

While the change in size and composition of blood vessel suggests that the mechanical properties would be different, another study looked directly at the mechanical response as a function of pregnancy. K.K. Greindling et al. found that the mechanical response of a sheep carotid artery is constant in nonpregnant and pregnant sheep. [53] Two main uterine aterties and both carotids were resected from seven nonpregnant and ten pregnant sheep. These arteries were then subjected to passive mechanical tests as well as active smooth muscle tests. The uterine artery of the near term pregnant sheep underwent

significant change in both the passive and active response. However, the carotid showed no apparent change in mechanical response between the pregnant and nonpregnant sheep. It was reasoned that mechanical properties remained stable during pregnancy because of the distance between the carotid and the uterine arteries. In the current experiment, it was assumed that the proximal nature of the MCA to the carotid would show similar results.

Vessel dissection and preparation of cerebral vessels is a tedious process. The average length of the specimens was 4.4±.77mm (n=20). Cerebral vessels have a large amount of tiny microbranches that must be sutured without tearing the vessel in order to hold pressure. The bulk of experiment time was spent preparing vessels.

All tests were conducted quasi-statically at a loading rate of .1 mm/sec. Even though the purpose of injury test was to simulate TBI, a quasi-static rate was chosen based on previous research on cerebral vessels. Also, the data collection equipment has a better response at lower rates. This allowed more precise control on levels of preconditioning and stretch. Chalupnik et al. in a study found no strain rate dependence in 28 human cerebral vessels between rates of .001 and 50 s^{-1}.[31] Furthermore, in a study conducted on 18 human cerebral arteries, Monson et al. found that strain rate independence between the ranges of .01 and 524 s^{-1}.[32]

In contrast to these results, it should be noted that Stemper et al. tested 62 specimens of porcine thoracic aorta within in ranges of loading rates from 1 to 500 mm/sec. It was found that increases in loading rate significantly increased the stress at initial subfailure and ultimate failure and significantly decreased the strain at initial subfailure and ultimate failure.[30] The difference in findings on the loading rate should be kept in mind.

The preconditioning method was found to be sufficient for repeatable results. The sample size was small for this reuslt. There was a a lot of variation in the data as a result. One parameter of note, the percent change in baseline maximum force, had a significant decrease after 6 biaxial tests were conducted within the supposed state preconditioned window. This result suggests that an extra cycle of preconditioning at the highest strain level in the biaxial test may optimize the preconditioning.

One key objective was to identify the effect of subfailure injury on mechanical properties. As expected, there was a reduction in the vessel's maximum force and stiffness after overstretch. This is believed to be caused by fibers in the vessel being extended during overstretch which results in less resistance during subsequent baseline testing. It was interesting to note that the relationship between percent of baseline force and stiffness is a linear function of the level of overstretch. This key finding gives an idea in how vessel properties are changing depending upon the level of injury. Furthermore, these results match the laxity found in ligaments that were overstretched to subfailure levels by Panjabi[36] and Provenzano.[37] The latter of which connected these findings to confocal microscopy images which is the next step for the current study.

The percent change of in vivo stiffness and force were also plotted against the cross-sectional area to see if a vessel's ability to retain its original stiffness was linked to the size of the vessel. A weak correlation was noted. These two properties were also plotted against the in vivo stretch length to see if vessels with a lower native stretch value were more likely to resist overstretch. A poor correlation was noted.

A second key objective was to identify any threshold of axial overstretch that would still allow a vessel to recover its in vivo mechanical response. Levels of

overstretch started slightly above the measured in vivo stretch ratio of λ=1.083±.03 (n=20). It should be noted that this value matches similar cerebral vessel in vivo stretch ratios of 1.15 to 1.17 in porcine basilar arteries[54] and 1.10 ±.03 in rat MCAs.[8] The maximum overstretch was 1.655. An unexpected result in this study was that no significant passive recovery occurred for all levels of overstretch. This was confirmed through analysis of the force readings and subsequent image analysis.

The response of the original configuration was permanently changed upon any level of overstretch. A subsequent search of evidence found that work done by Fung suggests that a "natural state"[55] of a blood vessel, or a configuration that the vessel remembers, does not exist. The results of the current study seem to confirm this statement. This suggests that the vessel is dependent on active remodeling for any vessel recovery of the original in vivo properties.

The incremental test protocol results revealed similar results as Monson et al.[40] It should be noted that the tests in the current study were conducted on cannulated vessels where as the tests by Monson et al. clamped the ends of the vessels. The same lengthening of the toe region was noted with increasing incremental axial stretch. According to Roach and Burton,[35] initial slope of the curve is an index for the state of elastin. The change in slope may be an indication of subfailure injury to the elastin. Figure 17 and Figure 18 suggest that the slope changes somewhere between 1.3 and 1.6. This change is even more noticeable at the point of maximum modulus in each trace. Further analysis using confocal microscopy imaging could better connect the changes in mechanical response to vessel wall structure.

It is interesting to note how the failure points changed depending on the type of subfailure testing. Vessels subjected to biaxial testing which kept the vessel with the preconditioned window failed at the lowest axial stress and axial stiffness. The single overstretch tests had the highest axial stress stiffness. This suggests that subfailure axial overstretch may reduce the percent baseline axial stiffness but it also makes the vessel less likely to fail than surrounding noninjured vessels. Vessels that experienced incrementally increasing strains had the highest axial failure stretch which is believed to be due to continuous preconditioning at incremental strains.

This study had certain limitations to the effectiveness of these results. The number of samples was limited due to availability of specimens and the difficulty of the vessel dissection and preparation. Data processing was also limited due to the buckled nature of a pressurized vessel below the in vivo limit. It is recommended that future experiments identify a postinjury zero-load length to use as a new reference point. This will allow for identifying the unbuckled state which means stress may be used instead of force to describe the vessel. Due to the nonuniform nature of stress and strain in the buckled configuration, the current study was limited to comparing force data. It should be noted that this comparison offers a good relative idea of the change in mechanical response of a single test but does not provide a good comparison between different tests.

CHAPTER 5

CONCLUSION

The current study explores the first known subfailure mechanical response on the cerebral blood vessels. The passive mechanical properties of the sheep MCA were tested in vitro under in vivo conditions. Several findings help to more fully characterize passive response to uniaxial overstretch:

- The percent baseline axial stiffness and force is a decreasing linear function of the level of overstretch.
- After axial overstretch, there is no passive recovery in the original configuration.
- Vessels that experience more subfailure preconditioning are less likely to fail than surrounding vessels with lower preconditining.

These results provide a better understanding of passive subfailure damage mechanics in sheep MCA. During the progression of this research, additional opportunities for future work have been identified as the following:

- The connection between mechanical response and the structure of the vessel wall may be established through processing the six fixed vessels at various levels of overstretch under the confocal microscope.

- A horizontal testing fixture with the same capability of the current testing setup would minimize the possiblity of vessel damage between vessel preparation and testing. This fixture should allow for imaging on the confocal microscope.
- Increasing the sample size would give statistical significance to the results.
- Finding the zero load length after overstretch would allow for better data comparison between specimens.

APPENDIX

Table 11: Vessel properties

Test	Starting Length (VC=0) (mm)	ZL Length (mm)	IVL/ZLL	CS (mm^2)	t (mm)	OD (mm)	OverStretch (Max/ZL)
4/6/2012	4.678	4.825	1.110	0.554	0.165	1.218	1.427
4/7/2012	6.573	6.879	1.054	0.476	0.163	1.121	1.262
5/11/2012_2	4.005	4.163	1.035	0.705	0.182	1.365	1.104
5/14/2012	4.149	4.227	1.048	0.307	0.134	0.836	1.454
5/15/2012	4.109	4.2685	1.125	0.325	0.137	0.886	1.465
5/15/2012_2	3.921	3.921	1.091	0.306	0.126	0.892	1.353
5/16/2012	4.262	4.377	1.116	0.449	0.156	1.025	1.212
5/18/2012	3.307	3.535	1.090	0.486	0.131	1.270	1.655
5/18/2012_2	5.392	5.4495	1.073	0.357	0.131	1.052	1.513
5/19/2012	4.116	4.3035	1.097	0.395	0.142	1.117	1.42
5/20/2012	3.262	3.761	1.123	0.275	0.132	0.848	1.557
5/26/2012	4.656	5.0425	1.096	0.540	0.168	1.204	1.359
5/26/2012_2	4.286	4.286	1.132	0.613	0.188	1.231	1.477
6/1/2012	3.872	3.9585	1.087	0.487	0.152	1.128	1.535
6/1/2012_2	4.512	4.5795	1.077	0.487	0.152	1.128	1.191
6/1/2012_3	4.517	4.739	1.037	0.346	0.121	0.889	1.118
6/2/2012	4.483	4.499	1.052	0.346	0.121	0.889	1.462
6/14/2012	5.544	5.544	1.049	0.590	0.171	1.158	1.253
5/12/2012	4.5	4.901	1.102	0.529	0.166	1.173	Incremental
5/26/2012_3	3.53	3.654	1.062	0.612	0.201	1.184	incremental

Table 12: Baseline parameters

Test	Filename	A	B	C	F_{max}	E_{max}	λ_{max}	Error
4/6/2012	'Baseline'	21.038	0.031	0.001	0.016	0.357	1.116	0.000
	'2 min'	56.794	0.000	0.001	0.005	0.216	1.115	0.000
	'12 min'	22.364	0.012	0.001	0.007	0.153	1.116	0.000
	'20 min'	26.775	0.007	0.000	0.006	0.158	1.116	0.000
	'35 min'	23.731	0.009	0.000	0.006	0.147	1.116	0.000
	'50 min'	22.003	0.012	0.001	0.007	0.155	1.116	0.000
	'73 min'	31.218	0.006	0.000	0.006	0.209	1.116	0.000
	'92 min'	12.948	0.022	0.000	0.005	0.097	1.116	0.000
4/7/2012	'Baseline'	24.423	0.129	0.003	0.029	0.762	1.073	0.000
	'2 min'	24.482	0.078	0.002	0.018	0.466	1.073	0.000
	'8 min'	28.934	0.057	0.002	0.016	0.468	1.073	0.000
	'15 min'	26.299	0.070	0.002	0.018	0.471	1.073	0.000
	'28 min'	25.417	0.074	0.002	0.018	0.471	1.073	0.000
	'57 min'	25.129	0.069	0.002	0.017	0.425	1.073	0.000
	'81 min'	26.439	0.064	0.002	0.016	0.437	1.073	0.000
	'93 min'	18.812	0.090	0.001	0.015	0.353	1.073	0.000
5/11/2012_2	'Baseline'	19.020	0.118	0.003	0.026	0.542	1.080	0.000
	'2 min'	16.461	0.129	0.004	0.024	0.481	1.080	0.000
	'9 min'	17.734	0.117	0.003	0.024	0.483	1.080	0.000
	'15 min'	20.027	0.099	0.004	0.024	0.490	1.080	0.000
5/14/2012	'Baseline'	23.632	0.183	0.003	0.039	1.073	1.075	0.000
	'Baseline after stress relaxation'	25.471	0.163	0.002	0.037	1.094	1.075	0.000
	3 min'	35.661	0.011	0.000	0.003	0.159	1.075	0.000
	18 min'	18.386	0.037	0.000	0.005	0.133	1.070	0.000
	31 min'	36.159	0.011	0.000	0.003	0.164	1.075	0.000
	46 min'	27.857	0.012	0.001	0.004	0.099	1.075	0.000
	268 min'	17.246	0.028	0.001	0.005	0.101	1.075	0.000
5/15/2012	'Baseline'	22.973	0.029	0.002	0.038	0.897	1.149	0.000
	'Baseline after stress relaxation'	19.665	0.043	0.001	0.039	0.799	1.149	0.000
	'3 min'	12.080	0.015	0.000	0.007	0.092	1.149	0.000
	'84 min'	13.155	0.014	0.001	0.007	0.101	1.149	0.000
	'91 min'	7.497	0.020	0.001	0.006	0.060	1.149	0.000

Table 13: Continued

Test	Filename	A	B	C	F_{max}	E_{max}	λ_{max}	Error
5/15/2012_2	'Baseline before 6 tests'	18.198	0.040	0.000	0.032	0.632	1.152	0.000
	'Baseline after 6 tests'	18.819	0.032	0.000	0.027	0.556	1.152	0.000
	'Baseline after stress relaxation'	18.824	0.037	0.000	0.031	0.638	1.152	0.000
	'2 min'	18.706	0.020	0.001	0.017	0.339	1.152	0.000
	'15 min'	16.822	0.025	0.001	0.018	0.314	1.152	0.000
	'347 min'	13.880	0.027	-0.001	0.012	0.219	1.152	0.000
	'360 min'	18.271	0.014	0.001	0.012	0.221	1.152	0.000
	'392 min'	12.119	0.030	0.001	0.013	0.185	1.152	0.000
5/16/2012	'Baseline before 6 tests'	21.136	0.041	0.001	0.030	0.674	1.132	0.000
	'Baseline after 6 tests'	18.467	0.054	0.002	0.031	0.613	1.132	0.000
	'3 min'	17.501	0.043	0.001	0.023	0.435	1.132	0.000
	'17 min'	16.884	0.052	0.002	0.027	0.480	1.132	0.000
	'32 min'	16.720	0.051	0.002	0.027	0.463	1.132	0.000
	'51 min'	18.232	0.044	0.001	0.025	0.484	1.132	0.000
5/18/2012	'Baseline before 6 tests'	16.495	0.072	0.004	0.037	0.637	1.132	0.000
	'Baseline after 6 tests'	14.926	0.076	0.003	0.033	0.540	1.132	0.000
	'3 min'	36.510	0.001	-0.001	0.002	0.127	1.132	0.000
	'60 min'	26.438	0.004	0.000	0.005	0.141	1.132	0.000
	'78 min'	25.323	0.004	0.000	0.004	0.111	1.132	0.000
5/18/2012_2	'Baseline before stress relaxation'	22.188	0.107	0.002	0.038	0.952	1.099	0.000
	'Baseline before 6 tests'	23.172	0.100	0.001	0.037	0.979	1.098	0.000
	'Baseline after 6 tests'	21.630	0.088	0.001	0.030	0.742	1.099	0.000
	'3 min'	10.328	0.035	0.000	0.006	0.096	1.099	0.000
	'30 min'	17.128	0.020	0.000	0.005	0.106	1.099	0.000
	'55 min'	20.177	0.017	0.000	0.005	0.124	1.099	0.000

Table 14: Continued

Test	Filename	A	B	C	F_{max}	E_{max}	λ_{max}	Error
5/19/2012	'Baseline before 6 tests'	18.144	0.064	0.002	0.028	0.546	1.118	0.000
	'Baseline after 6 tests'	14.074	0.068	0.002	0.023	0.359	1.118	0.000
	'2 min'	23.957	0.011	0.001	0.008	0.183	1.118	0.000
	'31 min'	12.457	0.027	0.002	0.010	0.119	1.118	0.000
	'69 min'	12.387	0.030	0.001	0.009	0.128	1.118	0.000
	'84 min'	15.732	0.027	0.001	0.010	0.169	1.118	0.000
	'100 min'	15.115	0.028	0.002	0.011	0.166	1.118	0.000
5/20/2012	'Baseline before 6 tests'	24.095	0.015	0.001	0.027	0.689	1.159	0.000
	'Baseline after 6 tests'	20.752	0.019	0.001	0.023	0.513	1.159	0.000
	'3 min'	31.139	0.001	0.002	0.004	0.088	1.159	0.000
	'32 min'	9.855	0.010	0.001	0.004	0.050	1.159	0.000
	'45 min'	8.344	0.009	0.002	0.005	0.035	1.159	0.000
5/26/2012	'Baseline before 6 tests'	22.971	0.024	-0.001	0.039	0.937	1.160	0.000
	'Baseline after 6 tests'	23.440	0.018	0.000	0.031	0.786	1.160	0.000
	'3 min'	25.870	0.004	0.000	0.009	0.270	1.160	0.000
	'28 min'	37.874	0.001	0.000	0.009	0.406	1.160	0.000
	'54 min'	27.044	0.004	0.000	0.009	0.266	1.160	0.000
	'64 min'	31.423	0.002	0.001	0.010	0.307	1.160	0.000
	'84 min'	33.404	0.002	0.000	0.009	0.332	1.160	0.000
	'102 min'	25.102	0.005	0.000	0.010	0.267	1.160	0.000
5/26/2012_2	'Baseline before 6 tests'	14.772	0.039	0.000	0.026	0.421	1.162	0.000
	'Baseline after 6 tests'	17.912	0.027	0.000	0.025	0.484	1.162	0.000
	'2 min'	16.285	0.010	0.001	0.009	0.134	1.162	0.000
	'25 min'	13.925	0.015	0.000	0.009	0.144	1.162	0.000
	'50 min'	13.708	0.018	0.000	0.011	0.165	1.162	0.000
	'110 min'	11.352	0.023	0.000	0.011	0.145	1.162	0.000

Table 15: Continued

Test	Filename	A	B	C	F_{max}	E_{max}	λ_{max}	Error
6/1/2012	'Baseline'	25.252	0.051	0.001	0.048	1.306	1.129	0.000
	'2 min'	-3.132	0.038	0.001	0.004	0.027	1.103	0.000
	'34 min'	35.499	0.004	0.000	0.004	0.168	1.103	0.000
	'109 min'	18.771	0.013	0.001	0.005	0.092	1.103	0.000
	'145 min'	28.693	0.005	0.000	0.003	0.100	1.103	0.000
6/1/2012_2	'Baseline'	20.546	0.094	0.001	0.034	0.784	1.104	0.000
	'2 min'	16.987	0.088	0.002	0.026	0.512	1.104	0.000
	'26 min'	16.613	0.100	0.000	0.028	0.557	1.104	0.000
	'89 min'	21.353	0.067	0.001	0.026	0.613	1.104	0.000
	'129 min'	21.700	0.070	0.000	0.026	0.664	1.104	0.000
	'198 min'	23.063	0.066	0.001	0.029	0.723	1.104	0.000
6/1/2012_3	'Baseline'	26.192	0.441	0.013	0.038	1.142	1.036	0.000
	'2 min'	24.362	0.334	0.010	0.028	0.812	1.036	0.000
	'29 min'	27.219	0.350	0.011	0.031	0.939	1.036	0.000
	'73 min'	25.945	0.338	0.010	0.029	0.867	1.036	0.000
	'89 min'	25.707	0.326	0.009	0.027	0.827	1.036	0.000
6/2/2012	'Baseline'	23.444	0.171	0.001	0.032	0.944	1.073	0.000
	'29 min'	20.571	0.014	0.000	0.002	0.064	1.073	0.000
	'58 min'	-3.720	0.037	0.000	0.003	0.028	1.072	0.000
	'96 min'	23.294	0.017	0.000	0.003	0.093	1.073	0.000
6/14/2012	'Baseline'	23.057	0.294	0.004	0.033	0.995	1.053	0.000
	'3 min'	16.037	0.103	0.002	0.010	0.241	1.053	0.000
	'23 min'	15.388	0.128	0.002	0.012	0.290	1.053	0.000
	'43 min'	20.036	0.115	0.002	0.012	0.333	1.053	0.000
	'63 min'	20.915	0.096	0.001	0.010	0.291	1.053	0.000

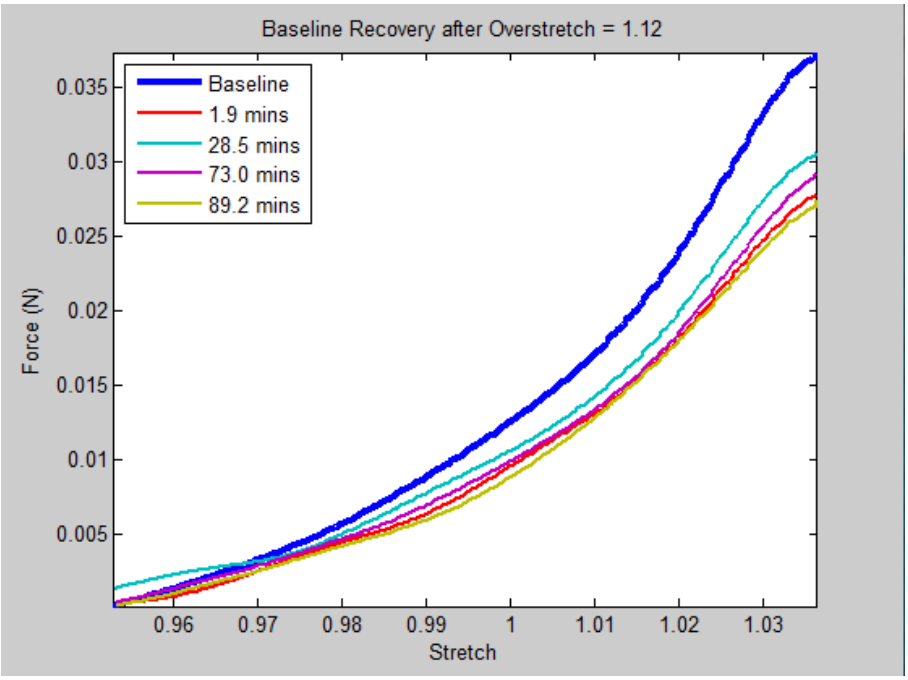

Figure 38: Recovery plot for overstretch of 1.12

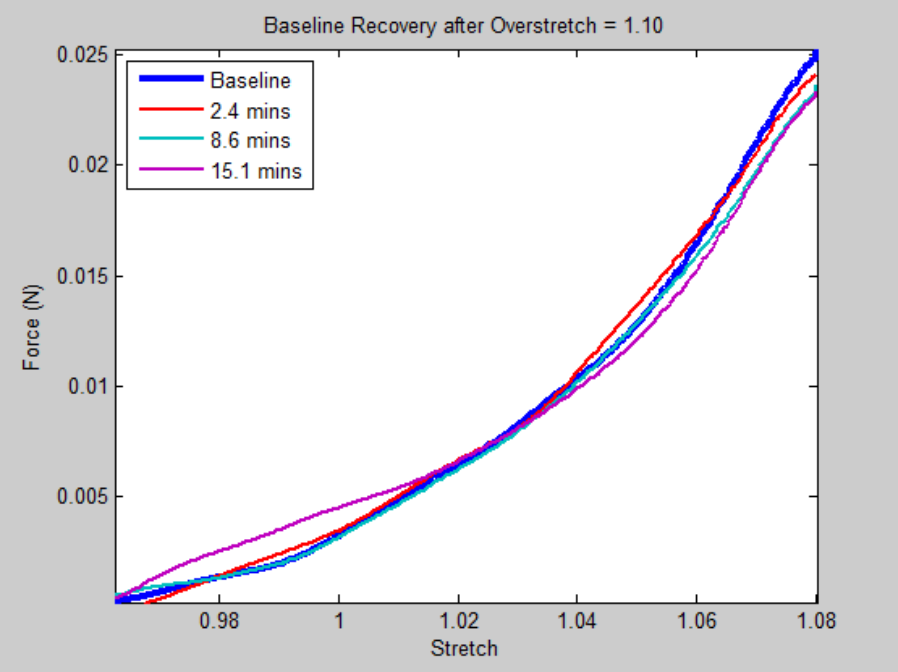

Figure 39: Recovery plot for overstretch of 1.10

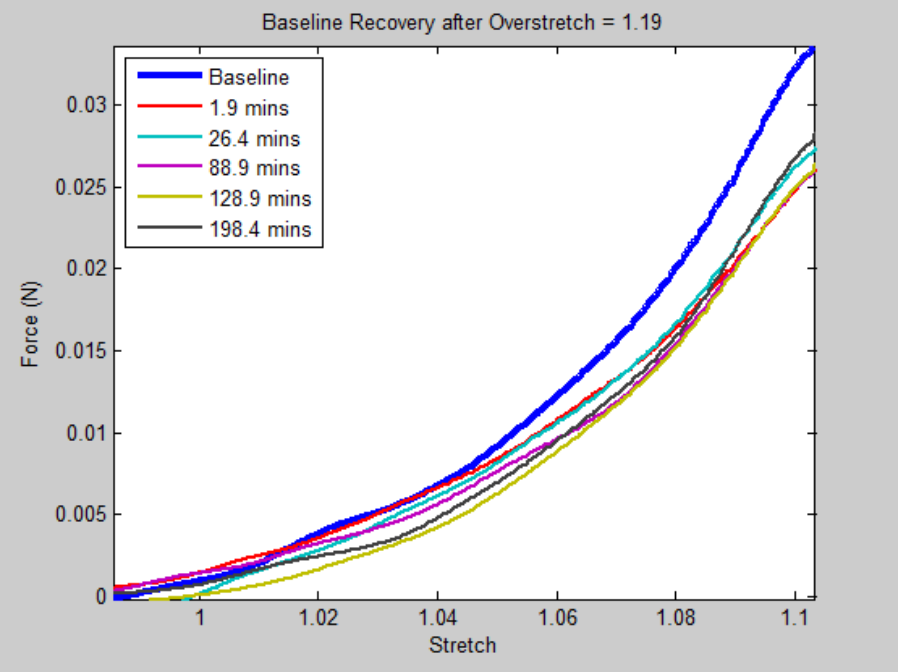

Figure 40: Recovery plot for overstretch of 1.19

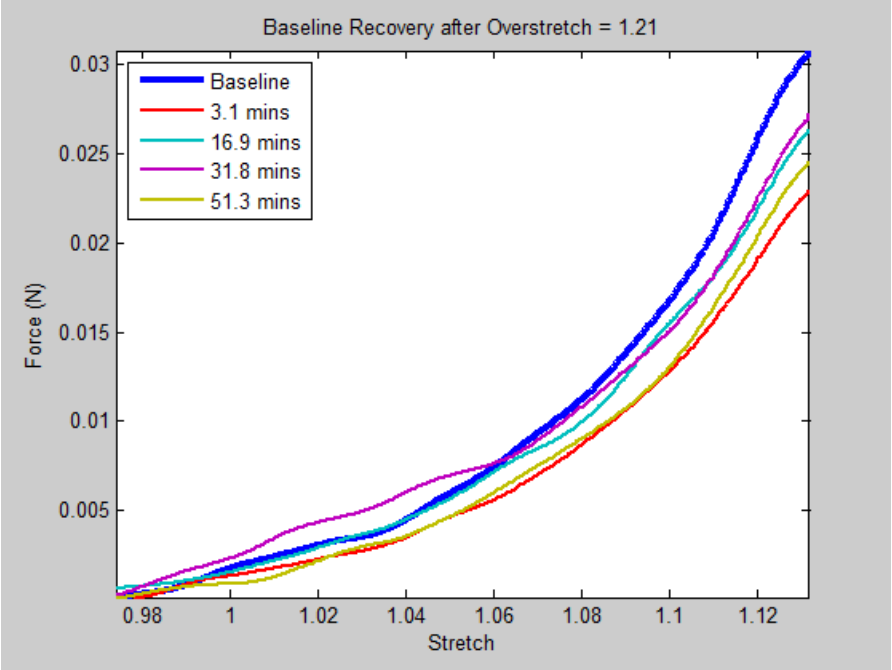

Figure 41: Recovery plot for overstretch of 1.21

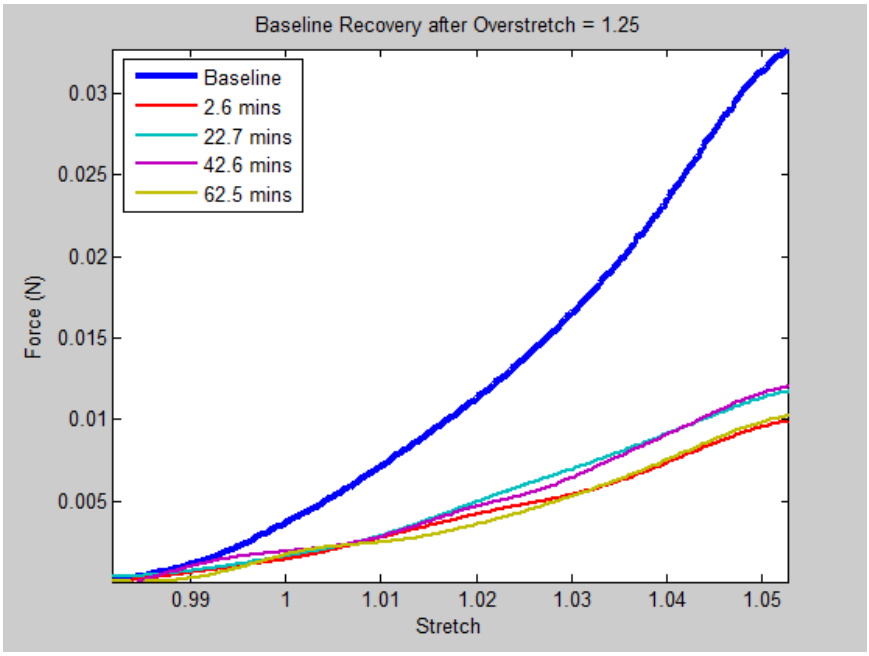

Figure 42: Recovery plot for overstretch of 1.25

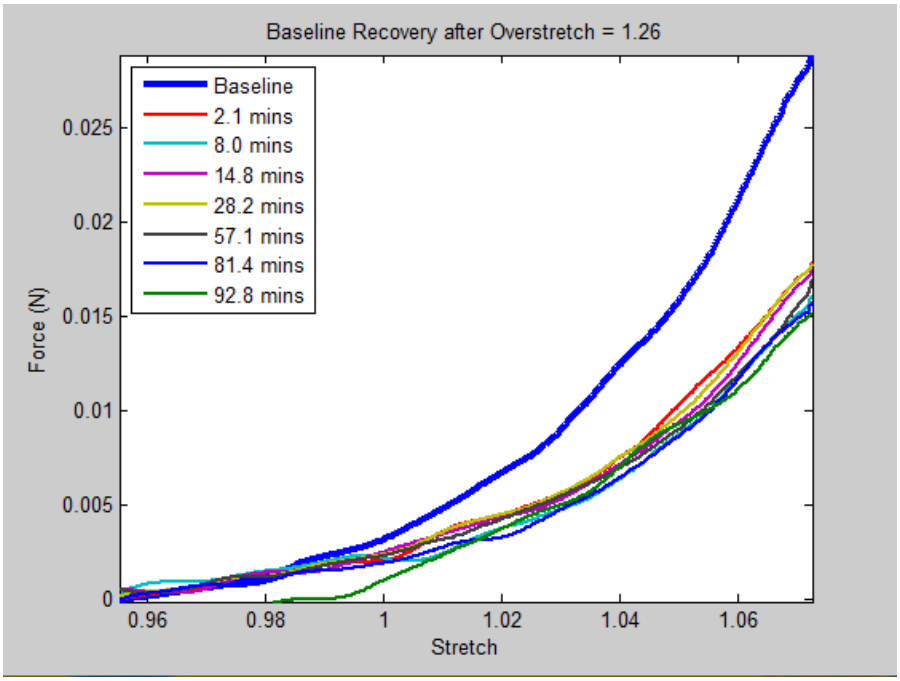

Figure 43: Recovery plot for overstretch of 1.26

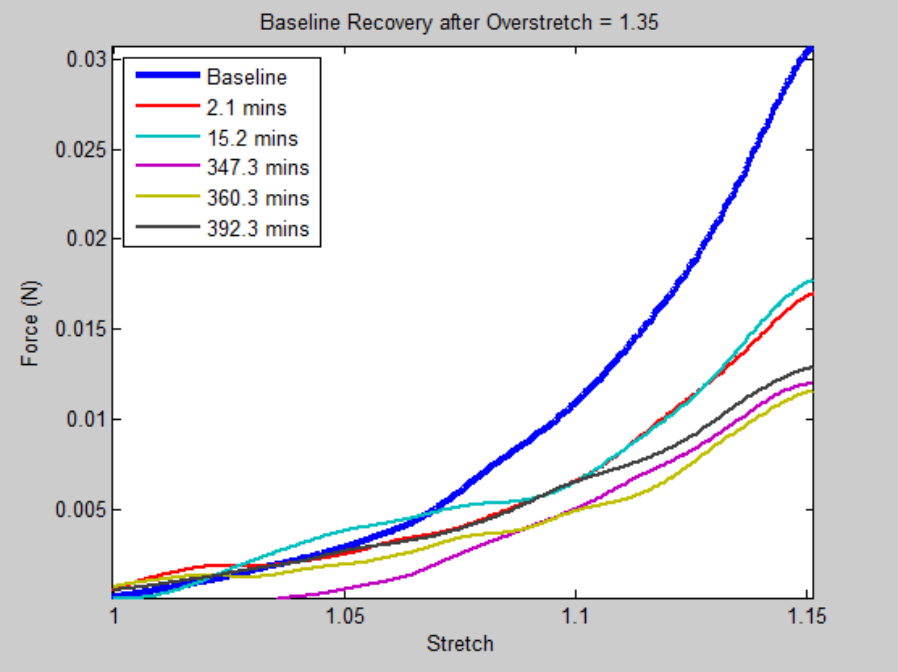

Figure 44: Recovery plot for overstretch of 1.35

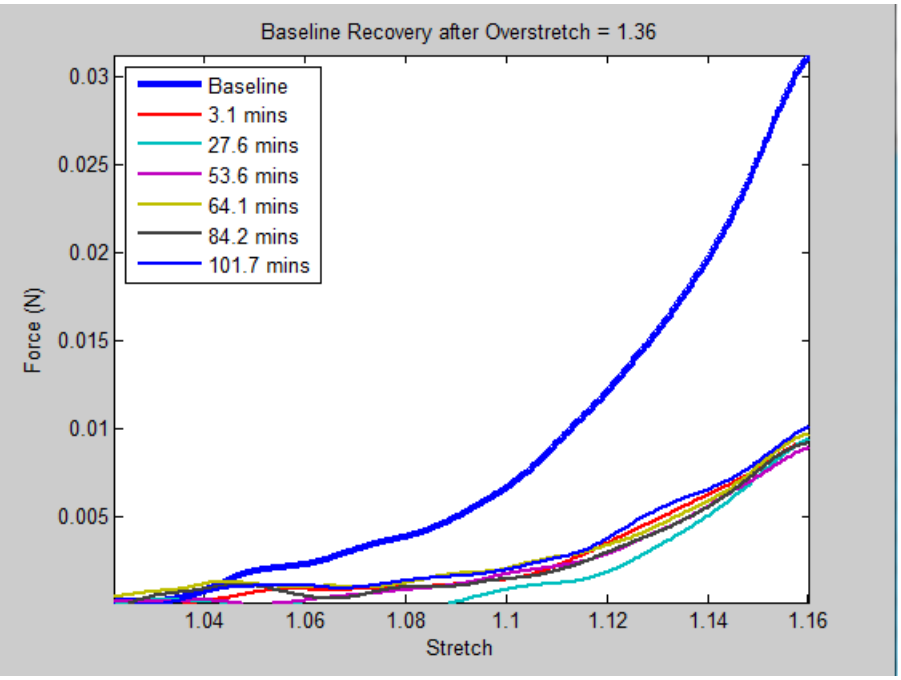

Figure 45: Recovery plot for overstretch of 1.36

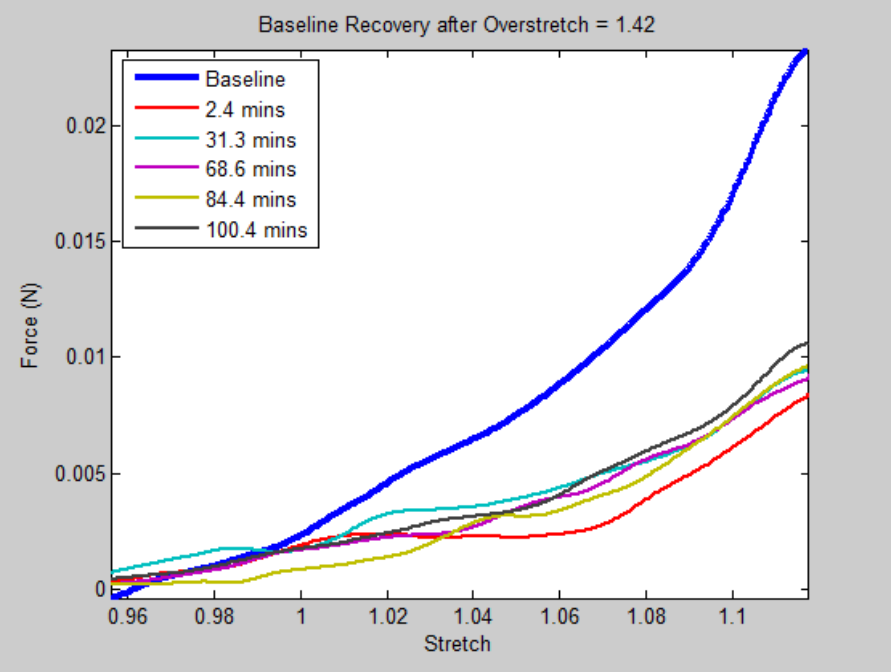

Figure 46: Recovery plot for overstretch of 1.42

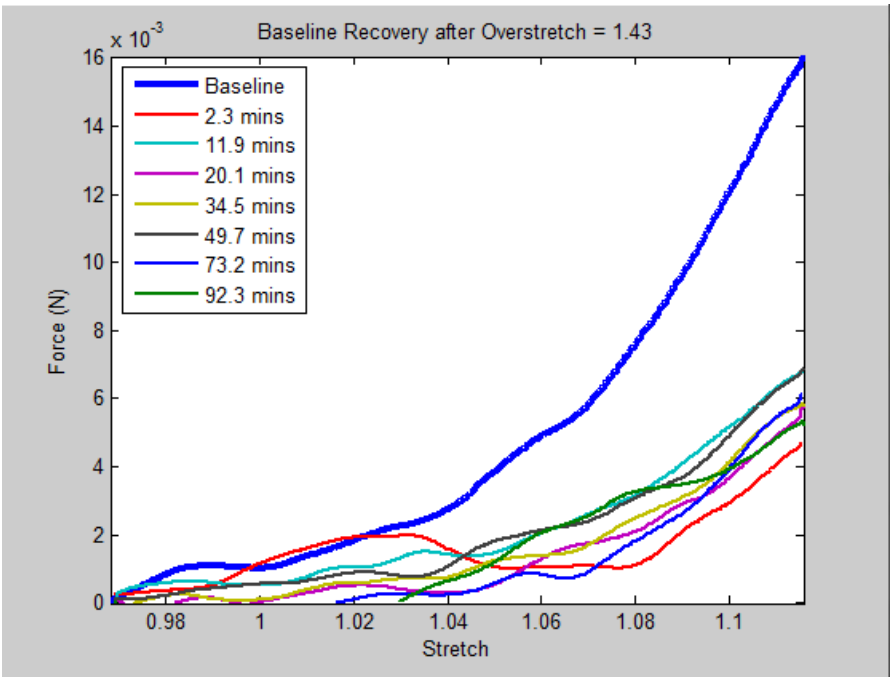

Figure 47: Recovery plot for overstretch of 1.43

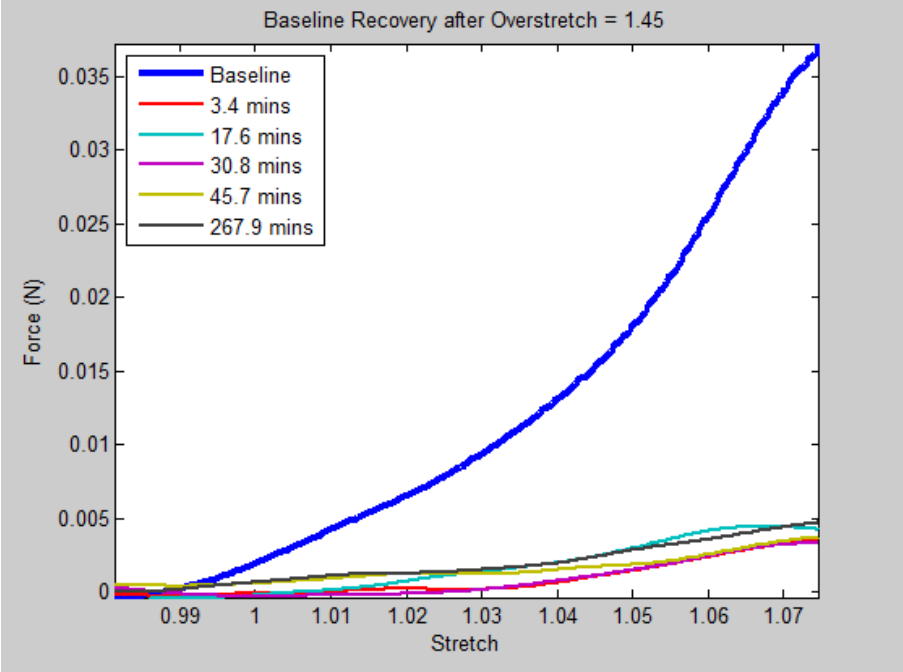

Figure 48: Recovery plot for overstretch of 1.45

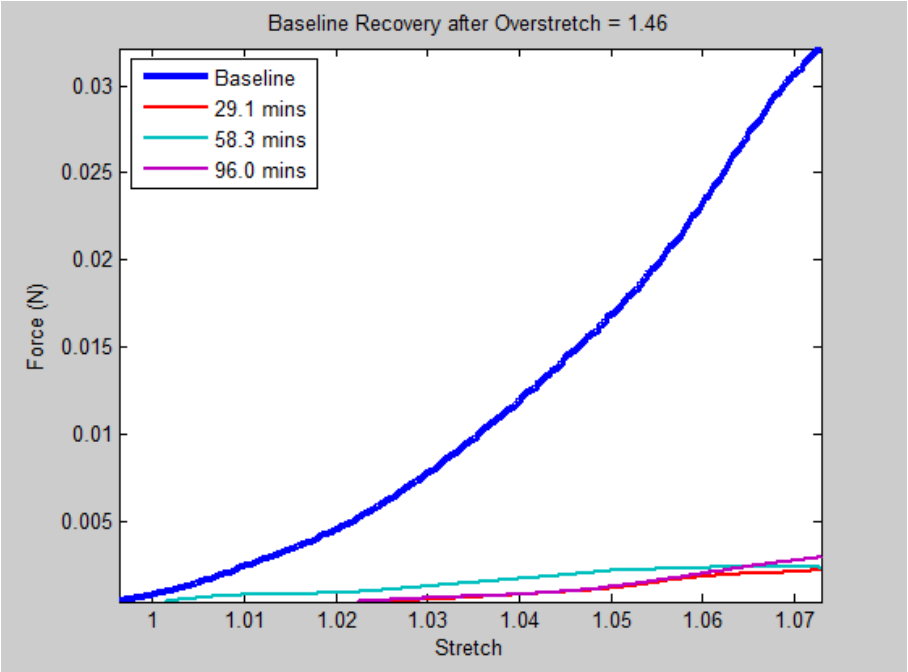

Figure 49: Recovery plot for overstretch of 1.46

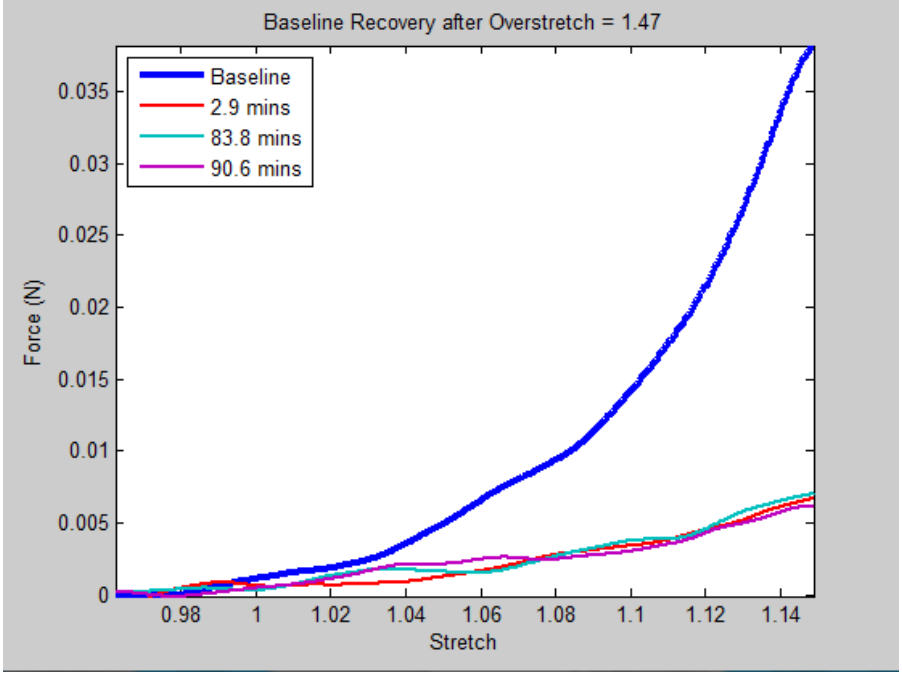

Figure 50: Recovery plot for overstretch of 1.47

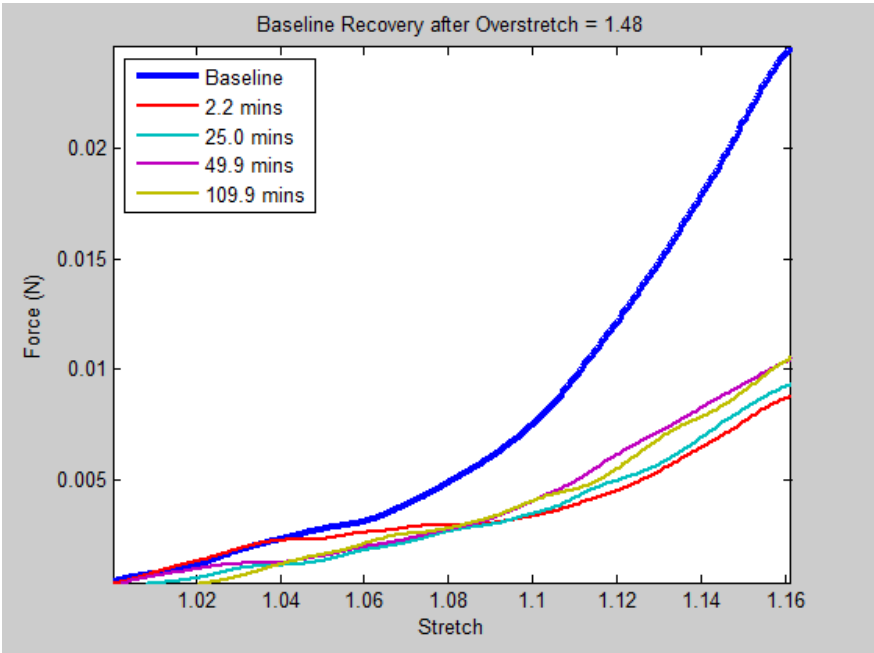

Figure 51: Recovery plot for overstretch of 1.48

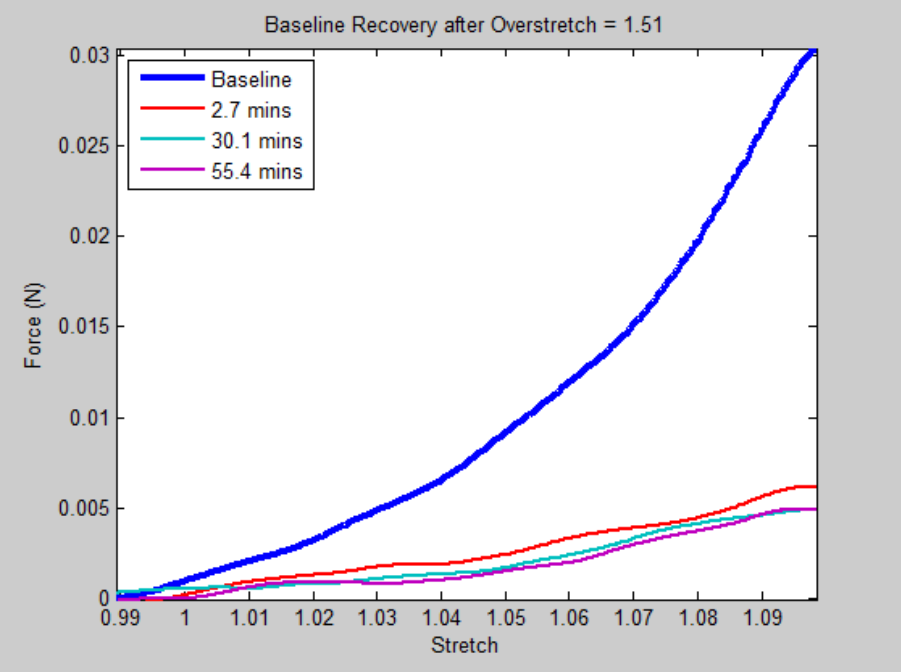

Figure 52: Recovery plot for overstretch of 1.51

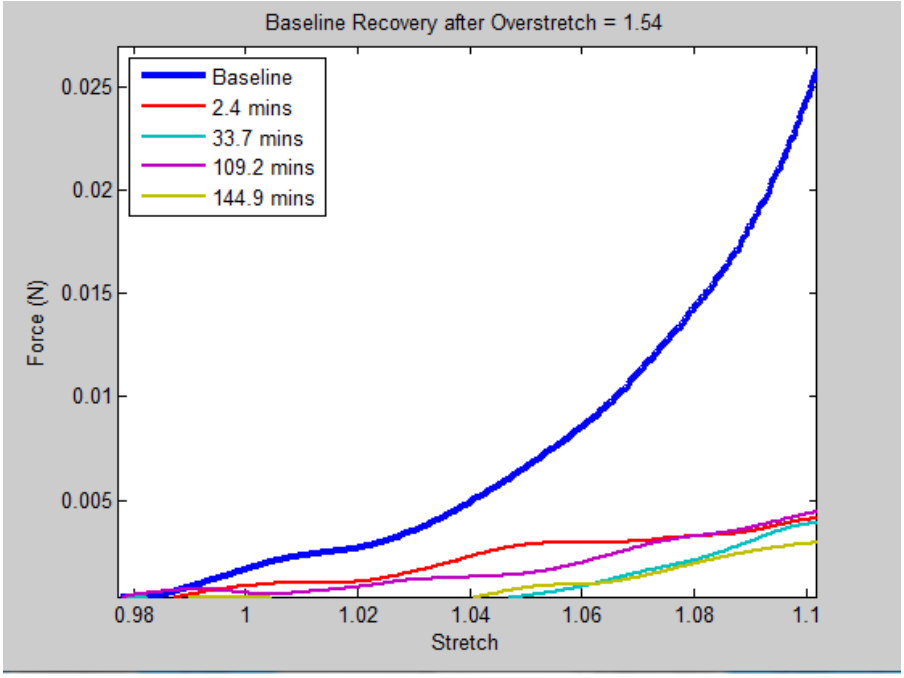

Figure 53: Recovery plot for overstretch of 1.54

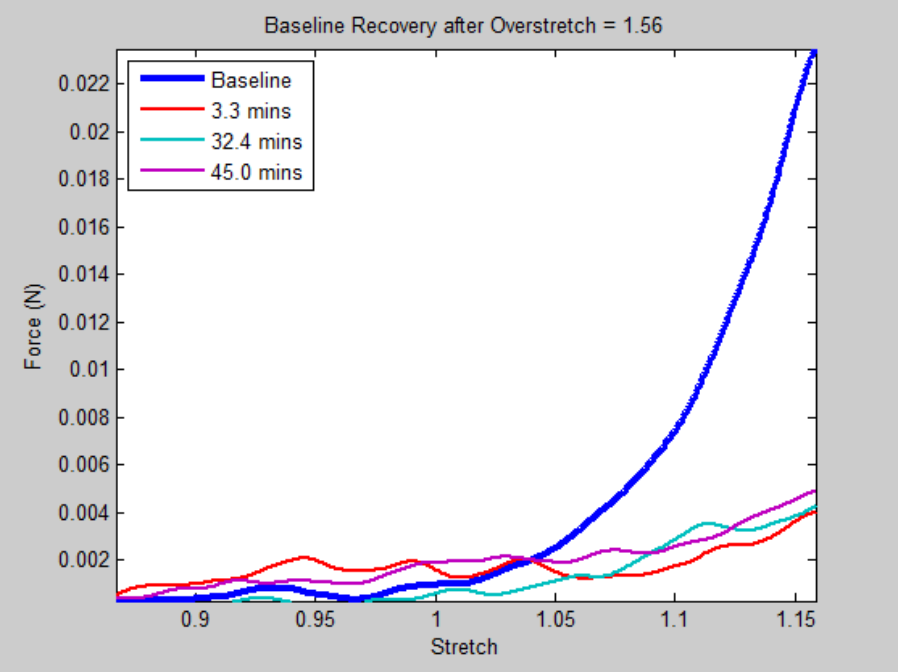

Figure 54: Recovery plot for overstretch of 1.56

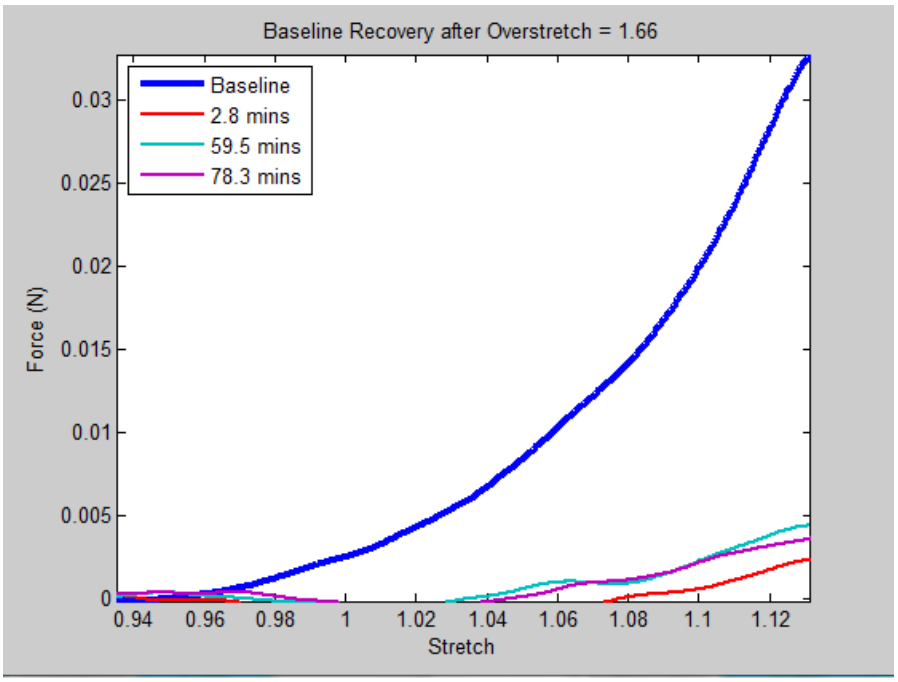

Figure 55: Recovery plot for overstretch of 1.66

Code

```
%Program Name: ZLFIND_Analysis.m
%Program author: E David Bell modified slightly by Jake Sullivan
%Date written: Jan. 25, 2012

%This program will take the data from a zlfind text file created from a
%vessel test, and perform the following:
% 1) Filter the force signal
% 2) Plot the voicecoil position vs unfiltered force signal
% 3) Plot the voicecoil position vs the filtered force signal
% 4) Automate to a degree the method of determining the zero load
length by
% calculating hte point when the filtered force signal goes above a
certain
% margian above the baseline force level.
% 5) Will also plot the filtered and unfiltered force signal on the
same
% plot for varification that the signal is not overly filtered.

clear all
clear global
clc


%% Choose File (.xls)
    [filename, pathname] = uigetfile('*.xls', 'Choose the data file');
    if isequal(filename,0)||isequal(pathname,0)
        disp('File not found')
    else
        disp(['File ', pathname, filename, ' found'])
    end
    [data,TXT,Raw] = xlsread ([pathname,filename]);

%% Set Variables
    %filenames{a} = char(filename(1:end-5)); % Create an array of the
filenames without .xlsx extension
    Orig_Time = data(:,1);
    VCpos = data(:,2);     % changed to 2 because used daedel for test
    Unfilt_Force = data(:,11); %column 12 = model 31- 250g; column 11 =
model 31 - 1000g; column 10 = MDB - 1000g
    ImageNum = data(:,13);     %Image numbers associated with each data
point

%% Plot Voice Coil Position VS. Index to identify area of interest
    L = length(VCpos);
    Index = linspace(1, L, L);

    figure(1)
    plot(Index,VCpos)

    display('   ')
```

```
    display('Please use the cursor and export function to identify the
upper ')
    display('and lower limits of the last cycle of the zlfind test.
Export the ')
    display('cursor data to the variables: "upper" and "lower"
respectively.  ')
    display('Press any button when ready to continue.  ')

    arsenal = input('Hit any button to continue ');
    close(figure(1));

    Lavg = a.Position(1,1);
    LLim = s.Position(1,1);
    ULim = d.Position(1,1);
    Uavg=LLim;

%% Plot
figure(1)
[haxes,hline1,hline2] = plotyy(Orig_Time,VCpos,Orig_Time,Unfilt_Force);
Fig1_H = gcf;
set(Fig1_H, 'Position', [67 37 560 420]);
title('Unfilted Position and Force')
axes(haxes(1));
xlabel('Time (s)'), ylabel('Actuator Position (mm)')
set(haxes(1), 'XLim', [Orig_Time(LLim) Orig_Time(ULim)]);
axes(haxes(2));
ylabel('Unfiltered Force (N)')
set(haxes(2), 'XLim', [Orig_Time(LLim) Orig_Time(ULim)]);

TimeAdj = Orig_Time((LLim - 200):(ULim + 113)) - Orig_Time(LLim - 200);
%Change 140 back to 200 for other data sets
ForceUnfilter = Unfilt_Force((LLim - 200):(ULim + 113));
%Change 140 back to 200 for other data sets
Favg=mean(Unfilt_Force(Lavg:Uavg));

% Filter the Force
    ffdata=[TimeAdj,ForceUnfilter];
    Fc=0.6;
    delT=0.01;
    adjnpts=length(TimeAdj);
    Wd=2*pi*1.246498*Fc;
    Wa=sin(Wd*delT/2)/cos(Wd*delT/2);
    T0=1.0+1.41421356*Wa+Wa*Wa;
    A0=Wa*Wa/T0;
    A1=2*A0;
    A2=A0;
    B1=-2.0*(Wa*Wa-1)/T0;
    B2=(-1.0+1.41421356*Wa-Wa*Wa)/T0;
    T1=ones(adjnpts,2);
    T2=ones(adjnpts,2);
    T1=ffdata;
    i=3;
    while i<=adjnpts
        T1(i,2)=A0*ffdata(i,2)+A1*ffdata(i-1,2)+A2*ffdata(i-
2,2)+B1*T1(i-1,2)+B2*T1(i-2,2);
        i=i+1;
```

```
    end
    T2=T1;
    i=adjnpts-3;
    while i>=2

T2(i,2)=A0*T1(i,2)+A1*T1(i+1,2)+A2*T1(i+2,2)+B1*T2(i+1,2)+B2*T2(i+2,2);
        i=i-1;
    end
    FilteredForceData=T2;   % with extra points
    Filt_Force_1=FilteredForceData(201:(length(TimeAdj)-113),2);
%change 140 back to 200 for other data sets
    Filt_Force=Filt_Force_1-Favg;  %zero out the force data

figure(2)
plot(Orig_Time, Unfilt_Force,'-k', Orig_Time(LLim:ULim), Filt_Force,'-
r','LineWidth',2)
set(gca, 'XLim', [Orig_Time(LLim) Orig_Time(ULim)]);
display('Check that the filtering of force looks ok.')
pause
close Figure 2
%Creates a short vector that will appear as a vertical line indicating
%where the zero load length has been calculated to be used for visual
%confirmation. Then the VC position, filtered force signal and this
%vertical line are all ploted in the same figure for visual
confirmation.
%The user is then given the option to reject this calculation and
change
%the portion of the data segment that is used to find the "baseline
force"
%range.  The variable seg represents a division of the segment of
interest
%that is used to define the initial noise range (seg = 2 means the
first
%half of the segment is used to find the noise range).
p=0.5;
seg = 2;
Cont2 = 0;

while Cont2 == 0
    upper_noise = max(Filt_Force(1:(length(Filt_Force)/seg)));
    lower_noise = min(Filt_Force(1:(length(Filt_Force)/seg)));
% %     upper_noise = max(Filt_Force(LLim:(LLim + round((ULim-
LLim)/seg))));
% %     lower_noise = min(Filt_Force(LLim:(LLim + round((ULim-
LLim)/seg))));
    range = upper_noise - lower_noise;


    %The zero load length is selected as the point where the force
signal goes
    %above a certain percentage above the initial noise range in the
segment of
    %interest. This percentage is 100*p, where p is a variable in the
below
    %code that can be altered by the user
    Cont3=0;
```

```
    for i = 1:1:length(Filt_Force)
        if Filt_Force(i) > (upper_noise + (p*range)) && Cont3 == 0
            ZeroLoadLength_I = LLim + i;
            Cont3 = 1;
        end
    end


    Zero_LineX = [Orig_Time(ZeroLoadLength_I),
Orig_Time(ZeroLoadLength_I)];
    Zero_LineY = [-10, 10];

    figure(3)
    [haxes,hline1,hline2] =
plotyy(Orig_Time,VCpos,Orig_Time(LLim:ULim),Filt_Force);
    Fig1_H = gcf;
    set(Fig1_H, 'Position', [67 37 560 420]);
    title('Position and Filtered Force')
    axes(haxes(1));
    xlabel('Time (s)'), ylabel('Actuator Position (mm)')
    set(haxes(1), 'XLim', [Orig_Time(LLim) Orig_Time(ULim)]);
    axes(haxes(2));
    ylabel('Filtered Force (N)')
    set(haxes(2), 'XLim', [Orig_Time(LLim) Orig_Time(ULim)]);

    figure(4)
    subplot(2,1,1)
    plot(Orig_Time,VCpos,'-k',Zero_LineX,Zero_LineY,'-b');
    set(gca, 'XLim', [Orig_Time(LLim) Orig_Time(ULim)],'YLim',[-0.2
0.4]);
    subplot(2,1,2)
    plot(Orig_Time(LLim:ULim),Filt_Force,'-r',Zero_LineX,Zero_LineY,'-
b');
    set(gca, 'XLim', [Orig_Time(LLim) Orig_Time(ULim)],'YLim', [-0.005
0.005]);
    set(gcf, 'Position', [981 39 356 652])

    display('  ')
    display('Does the vertical line represent a reasonable zero load
length? ')
    Cont2 = input('(For Yes enter "1", for No enter "0" :  ');

    if Cont2 == 0
        %gives user oppurtunity to alter the parameters used to find
zero load
        %length
        close(figure(4))
        close(figure(3))
        display('  ')
        display(['The first 1/',num2str(seg),' of the segment of
interest is '])
        display('used to determine the initial noise range (y-range of
flat portion.')
        seg = input('Enter the new denominator for fraction above to be
used:  ');
```

```
        display('  ')
        display('The current proportion above the noise range needed to
trigger ')
        display(['the selection of zero load length is ',num2str(p)])
        p = input('Enter the new proportion to be used (0 > p > point
before ZLL):  ');
    end
end
fprintf('The zero load length is %12.10g\n',VCpos(ZeroLoadLength_I))
fprintf('The zero load length image # is
%12.10g\n',ImageNum(ZeroLoadLength_I))
```

```
%Program Name: In_Vivo_Length.m
%Program author: J Sullivan with bits of code from Monson lab
%Date written: October 6, 2012

%This program will take preconditioning data (PC tests) and convert the
data into a graph that will
%allow the identification of the in-vivo length.

clear all
clear global
clc

%% Setup colors for plots
ColOrd = get(gca,'ColorOrder');
[m,n] = size(ColOrd);
close

%% Enter number of PC tests
pause on
num_tests = input('Please enter the total number of PC tests ');

%% Begin Loop
qq=1;
for qq =1:num_tests

%% Choose File (.xls)
    [filename, pathname] = uigetfile('*.xls', 'Pick the data file to
check region of interst');
    if isequal(filename,0)||isequal(pathname,0)
        disp('File not found')
    else
        disp(['File ', pathname, filename, ' found'])
    end
    [data,TXT,Raw] = xlsread ([pathname,filename]);

%% Set Variables
    filenames{qq} = char(filename(1:end-5)); % Create an array of the
filenames without .xlsx extension
    Orig_Time = data(:,1);
    VCpos = data(:,2);
    Unfilt_Force = data(:,11);
    Unfilt_Press = data(:,8);

%% Plot Voice Coil Position VS. Index to identify area of interest
    L = length(VCpos);
    Index = linspace(1, L, L);

    figure(1)
    plot(Index,VCpos)

    arsenal = input('Hit any button to continue ');
    close(figure(1));

    Lavg = a.Position(1,1);
    Uavg = s.Position(1,1);
```

```
    LLim = d.Position(1,1);
    ULim = f.Position(1,1);

%% Filter the force data
    TimeAdj = Orig_Time((LLim - 200):(ULim + 150)) - Orig_Time(LLim -
200);  %Change 140 back to 200 for other data sets
    ForceUnfilter = Unfilt_Force((LLim - 200):(ULim + 150));
%Change 140 back to 200 for other data sets
    PressUnFilt=Unfilt_Press((LLim - 200):(ULim + 150));

% Filter the Force
    ffdata=[TimeAdj,ForceUnfilter];
    Fc=0.6;
    delT=0.01;
    adjnpts=length(TimeAdj);
    Wd=2*pi*1.246498*Fc;
    Wa=sin(Wd*delT/2)/cos(Wd*delT/2);
    T0=1.0+1.41421356*Wa+Wa*Wa;
    A0=Wa*Wa/T0;
    A1=2*A0;
    A2=A0;
    B1=-2.0*(Wa*Wa-1)/T0;
    B2=(-1.0+1.41421356*Wa-Wa*Wa)/T0;
    T1=ones(adjnpts,2);
    T2=ones(adjnpts,2);
    T1=ffdata;
    i=3;
    while i<=adjnpts
        T1(i,2)=A0*ffdata(i,2)+A1*ffdata(i-1,2)+A2*ffdata(i-
2,2)+B1*T1(i-1,2)+B2*T1(i-2,2);
        i=i+1;
    end
    T2=T1;
    i=adjnpts-3;
    while i>=2

T2(i,2)=A0*T1(i,2)+A1*T1(i+1,2)+A2*T1(i+2,2)+B1*T2(i+1,2)+B2*T2(i+2,2);
        i=i-1;
    end
    FilteredForceData=T2;   % with extra points
    Filt_Force=FilteredForceData(201:(length(TimeAdj)-150),2);  %change
140 back to 200 for other data sets

    clear T2

%% Filter the Pressure
    fprdata=[TimeAdj,PressUnFilt];
    Fc=0.6;
    delT=0.01;
    adjnpts=length(TimeAdj);
    Wd=2*pi*1.246498*Fc;
    Wa=sin(Wd*delT/2)/cos(Wd*delT/2);
    T0=1.0+1.41421356*Wa+Wa*Wa;
    A0=Wa*Wa/T0;
    A1=2*A0;
    A2=A0;
```

```
    B1=-2.0*(Wa*Wa-1)/T0;
    B2=(-1.0+1.41421356*Wa-Wa*Wa)/T0;
    T1=ones(adjnpts,2);
    T2=ones(adjnpts,2);
    T1=fprdata;
    i=3;
    while i<=adjnpts
        T1(i,2)=A0*fprdata(i,2)+A1*fprdata(i-1,2)+A2*fprdata(i-
2,2)+B1*T1(i-1,2)+B2*T1(i-2,2);
        i=i+1;
    end
    T2=T1;
    i=adjnpts-3;
    while i>=2

T2(i,2)=A0*T1(i,2)+A1*T1(i+1,2)+A2*T1(i+2,2)+B1*T2(i+1,2)+B2*T2(i+2,2);
        i=i-1;
    end
    FilteredPressData=T2;   % with extra points
    Filt_Press=FilteredPressData(201:(length(TimeAdj)-150),2);

%% Save all data and make sure all columns have the same amount of rows
in
    time = Orig_Time(LLim:ULim);
    t = (0:1:length(time)-1)/100; % divide by 100 for seconds
    VCpos_aoi = VCpos(LLim:ULim);

%% Plot Postion and Filtered Force VS. Time
    ColRow = rem(qq+1,m);
    if ColRow == 0
        ColRow = m;
    end
    Col = ColOrd(ColRow,:);

    figure(2)
    if qq ==1;
        plot(Filt_Press, Filt_Force,'LineWidth',2)
        title('Force vs. Pressure')
        xlabel('Pressure (kPa)')
        ylabel('Force (N)')
        axis([min(Filt_Press) max(Filt_Press) 0 .1])

        hold on
    else
        plot(Filt_Press, Filt_Force,'Color',Col,'LineWidth',2)

    end

    qq=qq+1;
    clear a
    clear s
    clear d
    clear f
end
legend(filenames)
```

```
%Program Name: overstretch.m
%Program author: J Sullivan with bits of code from Monson lab
%Date written: October 10, 2012

%This program will tell you the maximum overstretch ratio, the image
%associated with it and the time of overstretch.

clear all
clear global
clc

%% Enter data for variables
ref_length = 4.262;
ZL = 4.377;

%% Choose File (.xls)
    [filename, pathname] = uigetfile('*.xls', 'Choose the data file');
    if isequal(filename,0)||isequal(pathname,0)
        disp('File not found')
    else
        disp(['File ', pathname, filename, ' found'])
    end
    [data,TXT,Raw] = xlsread ([pathname,filename]);

%% Set Variables
    filenames = char(filename(1:end-5)); % Create an array of the
filenames without .xlsx extension
    Orig_Time = data(:,1);
    VCpos = data(:,2);     % changed to 2 because used daedel for test
    Unfilt_Force = data(:,11);
    imagenum = data(:,13);

%% Plot Voice Coil Position VS. Index to identify area of interest
    L = length(VCpos);
    Index = linspace(1, L, L);

    figure(1)
    plot(Index,VCpos)

    arsenal = input('Hit any button to continue ');
    close(figure(1));

    Lavg = a.Position(1,1);
    LLim = s.Position(1,1);
    ULim = d.Position(1,1);
    Uavg=LLim;

%% Print Overstretch Info
Ldmg=(ref_length+VCpos(ULim))/ZL;
Image_dmg=imagenum(ULim);
time = Orig_Time(LLim:ULim);
fprintf('\nThe overstretch value is %6.3f\nThe max stretch image is
%6i\nThe time of overstretch is %6.3f\n', Ldmg,Image_dmg,time(end));
```

```
%Program Name: force_disp.m
%Program author: J Sullivan with bits of code from Monson lab
%Date written: December 2012

%This program will create recovery plots, relating the pre-injury
baseline
%with post-injury baselines

clear all
clear global
clc

%% Setup colors for plots
ColOrd = get(gca,'ColorOrder');
[m,n] = size(ColOrd);
close

%% Enter Variables
ref_length = 4.262;
ZL = 4.377;
zero_time = 1337164703; %Unix standard time
overstretch = '1.21'; %Enter as string for plotting title

%% Enter number of baseline tests
pause on
num_tests = input('Please enter the total number of baseline tests
(including original) ');

%% Begin Loop
j=1;
for j =1:num_tests

%% Choose File (.xls)
    [filename, pathname] = uigetfile('*.xls', 'Pick the data file to
check region of interst');
    if isequal(filename,0)||isequal(pathname,0)
        disp('File not found');
    else
        disp(['File ', pathname, filename, ' found']);
    end
    [data,TXT,Raw] = xlsread ([pathname,filename]);

%% Set Variables
    filenames{j} = char(filename(1:end-5)); % Create an array of the
filenames without .xlsx extension
    Orig_Time = data(:,1);
    VCpos = data(:,2);
    Unfilt_Force = data(:,11);

%% Plot Voice Coil Position VS. Index to identify area of interest
    L = length(VCpos);
    Index = linspace(1, L, L);

    figure(1)
    plot(Index,VCpos)
```

```
    arsenal = input('Hit any button to continue ');
    close(figure(1));

%     Uavg = ua.Position(1,1);
    Lavg = a.Position(1,1);
    LLim = s.Position(1,1);
    ULim = d.Position(1,1);
    Uavg=LLim;

%% Filter the force data
    TimeAdj = Orig_Time((LLim - 198):(ULim + 65)) - Orig_Time(LLim -
198);  %Change 140 back to 200 for other data sets
    ForceUnfilter = Unfilt_Force((LLim - 198):(ULim + 65));
%Change 140 back to 200 for other data sets
    Favg=mean(Unfilt_Force(Lavg:Uavg));

% Filter the Force
    ffdata=[TimeAdj,ForceUnfilter];
    Fc=0.6;
    delT=0.01;
    adjnpts=length(TimeAdj);
    Wd=2*pi*1.246498*Fc;
    Wa=sin(Wd*delT/2)/cos(Wd*delT/2);
    T0=1.0+1.41421356*Wa+Wa*Wa;
    A0=Wa*Wa/T0;
    A1=2*A0;
    A2=A0;
    B1=-2.0*(Wa*Wa-1)/T0;
    B2=(-1.0+1.41421356*Wa-Wa*Wa)/T0;
    T1=ones(adjnpts,2);
    T2=ones(adjnpts,2);
    T1=ffdata;
    i=3;
    while i<=adjnpts
        T1(i,2)=A0*ffdata(i,2)+A1*ffdata(i-1,2)+A2*ffdata(i-
2,2)+B1*T1(i-1,2)+B2*T1(i-2,2);
        i=i+1;
    end
    T2=T1;
    i=adjnpts-3;
    while i>=2

T2(i,2)=A0*T1(i,2)+A1*T1(i+1,2)+A2*T1(i+2,2)+B1*T2(i+1,2)+B2*T2(i+2,2);
        i=i-1;
    end
    FilteredForceData=T2;   % with extra points
    Filt_Force=FilteredForceData(199:(length(TimeAdj)-65),2);  %change
140 back to 200 for other data sets

%% Save all data and make sure all columns have the same amount of rows
in
    force=Filt_Force-Favg;
    disp = VCpos(LLim:ULim);
    stretch = (disp+ref_length)/ZL;
    current_time = Orig_Time(LLim);
```

```
%% Plot Postion and Filtered Force VS. Time
    ColRow = rem(j+1,m);
    if ColRow == 0
        ColRow = m;
    end
    Col = ColOrd(ColRow,:);

    figure(2)
    if j ==1;
        h1= plot(stretch,force);
        set(h1, 'LineWidth',3);
        title(['Baseline Recovery after Overstretch = ',overstretch])
        xlabel('Stretch')
        ylabel('Force (N)')
        axis([min(stretch) max(stretch) min(force) max(force)])
        hold on
        time_pass(j) = (current_time-zero_time)/60; %mins
    else
        hold on
        plot(stretch, force,'Color',Col,'LineWidth',1.5)
        time_passed(j) = (current_time-zero_time)/60; %mins
    end

    clear a
%     clear ua
    clear s
    clear d
    fprintf('File: %s successful\n',filenames{j});
    j=j+1;
end

%% Create a legend that specifies the time that has passed between
tests
legendCell{1}='Baseline';
for zz=2:j-1
    tp = sprintf('%.1f',time_passed(zz));
    legendCell(zz)=strcat(strtrim(cellstr(tp)),' mins');
end
legend(legendCell,'Location','NorthWest')
```

```
%Program Name: failurestretch.m
%Program author: J Sullivan with bits of code from Monson lab
%Date written: February 2012

%This program was tailored to plot my failure data on one graph. Alot
was
%hardcoded so that it would be easy to repeat and I wouldn't have to
input
%so much data each time. This code also spits out paramaters for each
%trace.

clear all
clear global
clc

%% Setup colors for plots
ColOrd = get(gca,'ColorOrder');
[m,n] = size(ColOrd);
close


%% Enter number of baseline tests
pause on
%num_tests = input('Please enter the total number of baseline tests
(including original) ');
num_tests =11;
%% Begin Loop
j=1;
for j =1:num_tests

%% Choose File (.xls)
    [filename, pathname] = uigetfile('*.xls', 'Pick the data file to
check region of interst');
    if isequal(filename,0)||isequal(pathname,0)
        disp('File not found');
    else
        disp(['File ', pathname, filename, ' found']);
    end
    [data,TXT,Raw] = xlsread ([pathname,filename]);
%% Failure data
    machine =[2 2 2 2 2 1 1 1 1 1 1];
    d=[6650 12500 5000 9900 2600 5200 5500 3800 5300 4820 5250];
    ref_length =[3.776 7.198 4.795 4.292 2.726 3.921 4.109 4.149 3.307
4.5 3.53];
    ZL =[4.164 7.527 4.747 4.349 2.74 3.921 4.2685 4.227 3.535 4.901
3.654];
    CS =[.478 .661 .43 .43 .481 .306 .325 .307 .486 .529 .612];
    name ={'Biaxial 1' 'Biaxial 2' 'Biaxial 3' 'Biaxial 4' 'Biaxial 5'
'Overstretch of 1.2' 'Overstretch of 1.3' 'Overstretch of 1.4'
'Overstretch of 1.5' 'Incremental stretch 1' 'Incremental stretch 2'};
%% Set Variables
    filenames{j} = char(filename(1:end-5)); % Create an array of the
filenames without .xlsx extension
    Orig_Time = data(:,1);
    if machine(j) ==1
        VCpos = data(:,2);
```

```
    end
    if machine(j) ==2
        VCpos=data(:,3);
    end
    Unfilt_Force = data(:,11);


%% Plot Voice Coil Position VS. Index to identify area of interest
    L = length(VCpos);
    Index = linspace(1, L, L);

    figure(1)
    plot(Index,VCpos)

    arsenal = input('Hit any button to continue ');
    close(figure(1));

%     Uavg = ua.Position(1,1);
    Lavg = a.Position(1,1);
    LLim = s.Position(1,1);
    %ULim = d.Position(1,1);
    ULim = d(j);
    Uavg=LLim;

%% Filter the force data
    TimeAdj = Orig_Time((LLim - 198):(ULim + 65)) - Orig_Time(LLim -
198);  %Change 140 back to 200 for other data sets
    ForceUnfilter = Unfilt_Force((LLim - 198):(ULim + 65));
%Change 140 back to 200 for other data sets
    Favg=mean(Unfilt_Force(Lavg:Uavg));

% Filter the Force
    ffdata=[TimeAdj,ForceUnfilter];
    Fc=0.6;
    delT=0.01;
    adjnpts=length(TimeAdj);
    Wd=2*pi*1.246498*Fc;
    Wa=sin(Wd*delT/2)/cos(Wd*delT/2);
    T0=1.0+1.41421356*Wa+Wa*Wa;
    A0=Wa*Wa/T0;
    A1=2*A0;
    A2=A0;
    B1=-2.0*(Wa*Wa-1)/T0;
    B2=(-1.0+1.41421356*Wa-Wa*Wa)/T0;
    T1=ones(adjnpts,2);
    T2=ones(adjnpts,2);
    T1=ffdata;
    i=3;
    while i<=adjnpts
        T1(i,2)=A0*ffdata(i,2)+A1*ffdata(i-1,2)+A2*ffdata(i-
2,2)+B1*T1(i-1,2)+B2*T1(i-2,2);
        i=i+1;
    end
    T2=T1;
    i=adjnpts-3;
```

```
    while i>=2

T2(i,2)=A0*T1(i,2)+A1*T1(i+1,2)+A2*T1(i+2,2)+B1*T2(i+1,2)+B2*T2(i+2,2);
        i=i-1;
    end
    FilteredForceData=T2;   % with extra points
    Filt_Force=FilteredForceData(199:(length(TimeAdj)-65),2);  %change
140 back to 200 for other data sets

%% Save all data and make sure all columns have the same amount of rows
in
    force=Filt_Force-Favg;
    disp = VCpos(LLim:ULim);
    stretch = (disp+ref_length(j))/ZL(j);
    current_time = Orig_Time(LLim);
    stress=force/CS(j);

%% Get Toe Region data
figure(5)
L2 = length(stress);
Index2 = linspace(1, L2, L2);
plot(Index2,stress)

display('   ')
display('Please use the cursor and export function to identify upper ')
display('limit of the toe region. ')

arsenal2 = input('Hit any button to continue ');
close(figure(5));

uppertoe = u.Position(1,1);

stretch_toe = stretch(1:uppertoe);
stress_toe =stress(1:uppertoe);

%% Plot Data
figure(3)
clf
plot(stretch_toe,stress_toe,'ko','MarkerFaceColor','k');
%h1=plot(lambda,FF,'k.');
hold on
xlabel('Stretch Ratio');
ylabel('Stress (MPa)');
%% Initialize p structure with 2 free variables and make a plot
clear p
p.A = 15;
p.B = .08;
gg=1.5;

if j<6
    gg=1.35;
end
if j>5 && j<10
    gg=1.55;
end
```

```
if j>9
    gg=1.85;
end

lambdaPlot = linspace(.9,gg,100);
[tmp,pred] = predRecoveryErr2(p,lambdaPlot);
plot(lambdaPlot,pred,'g-');
err = predRecoveryErr2(p,stretch_toe,stress_toe);

%% best fit parameters
bestP = fit('predRecoveryErr2',p,{'A','B'},stretch_toe,stress_toe);
[bestErr,bestPred] = predRecoveryErr2(bestP,lambdaPlot); %not able to
insert Stress because lambdaPlot has more points for smooth plot
bestErr = predRecoveryErr2(bestP,stretch_toe,stress_toe); %insert
stress to calculate best error
plot(lambdaPlot,bestPred,'r-');

sigmax = max(stress);
%% Find slope at each point

% slopes = movingslope(stress,5,1,.0001);
% slopemax=max(slopes);
ms=diff(stress)./diff(stretch);
maxslope=0;
for k=1:length(ms)
    if ms(k)~=Inf;
        if ms(k)>maxslope
            maxslope=ms(k);
        end
    end
end

count1=0;
for i=1:length(stress)
    count1=count1+1;
    if stress(i)==max(stress)
        lambdamax=stretch(i);
        index1=count1;
    end
end

count2=0;
for i=1:length(ms)
    count2=count2+1;
    if ms(i)==maxslope
        lambdaslope=stretch(i);
        index2=count2;
    end
 end

params(j,:)={name(j) bestP.A bestP.B bestErr sigmax lambdamax
maxslope};
%% Plot Postion and Filtered Force VS. Time
    ColRow = rem(j+1,m);
    if ColRow == 0
```

```
        ColRow = m;
    end
    Col = ColOrd(ColRow,:);

    figure(2)
        if j<6
            h(j)=plot(stretch,stress,'--','Color',Col,'LineWidth',1.5);
        end
        if j>5 && j<10
            h(j)=plot(stretch,stress,'Color',Col,'LineWidth',1.5);
        end
        if j>9
            h(j)=plot(stretch,stress,'-.','Color',Col,'LineWidth',1.5);
        end
        title('Effect of subfailure damage on failure point')
        %title('Effect of 12 Min Stress Relaxation on Baseline')
        xlabel('Stretch')
        ylabel('Stress (MPa)')
        if j==1
            ministretch=min(stretch);
            maxistretch=max(stretch);
            ministress=min(stress);
            maxistress=max(stress);
        end
        if j~=1
            if min(stretch)<ministretch
                ministretch=min(stretch);
            end
            if max(stretch)>maxistretch
                maxistretch=max(stretch);
            end
            if min(stress)<ministress
                ministress=min(stress);
            end
            if max(stress)>maxistress
                maxistress=max(stress);
            end
        end
       axis([ministretch maxistretch 0 maxistress])
        hold on
        plot(stretch(index1),stress(index1),'^')
        plot(stretch(index2),stress(index2),'o')
    clear a
    clear s
    clear d
    clear u
    fprintf('File: %s successful\n',filenames{j});
    j=j+1;
end
legend(h,name)
```

```
%Program Name: baseline_params2.m
%Program author: J Sullivan with bits of code from Monson lab
%Date written: January 2013

%This program fits a model to the toe region of each baseline and spits
out
%the important parameters.

clear all
clear global
clc

%% Enter test data
ref_length = 4.262; %[mm]
ZL = 4.377; %[mm]

%% Choose File (.xls)
    [filename, pathname] = uigetfile('*.xls', 'Choose the data file');
    if isequal(filename,0)||isequal(pathname,0)
        disp('File not found')
    else
        disp(['File ', pathname, filename, ' found'])
    end
    [data,TXT,Raw] = xlsread ([pathname,filename]);

%% Set Variables
    filenames = char(filename(1:end-5)); % Create an array of the
filenames without .xlsx extension
    Orig_Time = data(:,1); %[s]
    VCpos = data(:,2);     %[mm] changed to 2 because used daedel for
test
    Unfilt_Force = data(:,11); %[N]
    Unfilt_Press = data(:,8); %[kPa]
    imagenum = data(:,13);

%% Plot Voice Coil Position VS. Index to identify area of interest
    L = length(VCpos);
    Index = linspace(1, L, L);

    figure(1)
    plot(Index,VCpos)

    arsenal = input('Hit any button to continue ');
    close(figure(1));

    Lavg = a.Position(1,1);
    LLim = s.Position(1,1);
    ULim = d.Position(1,1);
    Uavg=LLim;

%% Filter the force data                        $$$
    TimeAdj = Orig_Time((LLim - 198):(ULim + 50)) - Orig_Time(LLim -
198);  %Change 140 back to 200 for other data sets
    ForceUnfilter = Unfilt_Force((LLim - 198):(ULim + 50));
%Change 140 back to 200 for other data sets
```

```
    Favg=mean(Unfilt_Force(Lavg:Uavg));
    PressUnFilt=Unfilt_Press((LLim - 198):(ULim + 50));
%                                                       $$$
% Filter the Force
    ffdata=[TimeAdj,ForceUnfilter];
    Fc=0.6;
    delT=0.01;
    adjnpts=length(TimeAdj);
    Wd=2*pi*1.246498*Fc;
    Wa=sin(Wd*delT/2)/cos(Wd*delT/2);
    T0=1.0+1.41421356*Wa+Wa*Wa;
    A0=Wa*Wa/T0;
    A1=2*A0;
    A2=A0;
    B1=-2.0*(Wa*Wa-1)/T0;
    B2=(-1.0+1.41421356*Wa-Wa*Wa)/T0;
    T1=ones(adjnpts,2);
    T2=ones(adjnpts,2);
    T1=ffdata;
    i=3;
    while i<=adjnpts
        T1(i,2)=A0*ffdata(i,2)+A1*ffdata(i-1,2)+A2*ffdata(i-
2,2)+B1*T1(i-1,2)+B2*T1(i-2,2);
        i=i+1;
    end
    T2=T1;
    i=adjnpts-3;
    while i>=2

T2(i,2)=A0*T1(i,2)+A1*T1(i+1,2)+A2*T1(i+2,2)+B1*T2(i+1,2)+B2*T2(i+2,2);
        i=i-1;
    end
    FilteredForceData=T2;   % with extra points        $$$
    FF1 =FilteredForceData(199:(length(TimeAdj)-50),2);  %change 140
back to 200 for other data sets

%% Filter the Pressure
    fprdata=[TimeAdj,PressUnFilt];
    Fc=0.6;
    delT=0.01;
    adjnpts=length(TimeAdj);
    Wd=2*pi*1.246498*Fc;
    Wa=sin(Wd*delT/2)/cos(Wd*delT/2);
    T0=1.0+1.41421356*Wa+Wa*Wa;
    A0=Wa*Wa/T0;
    A1=2*A0;
    A2=A0;
    B1=-2.0*(Wa*Wa-1)/T0;
    B2=(-1.0+1.41421356*Wa-Wa*Wa)/T0;
    T1=ones(adjnpts,2);
    T2=ones(adjnpts,2);
    T1=fprdata;
    i=3;
    while i<=adjnpts
        T1(i,2)=A0*fprdata(i,2)+A1*fprdata(i-1,2)+A2*fprdata(i-
2,2)+B1*T1(i-1,2)+B2*T1(i-2,2);
        i=i+1;
```

```
    end
    T2=T1;
    i=adjnpts-3;
    while i>=2

T2(i,2)=A0*T1(i,2)+A1*T1(i+1,2)+A2*T1(i+2,2)+B1*T2(i+1,2)+B2*T2(i+2,2);
        i=i-1;
    end
    FilteredPressData=T2;   % with extra points
    Filt_Press=FilteredPressData(199:(length(TimeAdj)-150),2);


%% Calculate other variables
FF=FF1-Favg;  %[N] zero out the force using avg of unfiltered force
data from when vc was at zero
L=VCpos(s.Position(1,1):d.Position(1,1))+ref_length; %[mm]
lambda=L/ZL;
time = Orig_Time(LLim:ULim); %unix time
t = (0:1:length(time)-1)/100; % each tic of unix time is 1/100 of a
second

%% Plot Data
figure(1)
clf
%h1=plot(lambda,Stress,'ko','MarkerFaceColor','k');
h1=plot(lambda,FF,'k.');
hold on
xlabel('Stretch Ratio (lambda)');
ylabel('Force (N)');

%% Initialize p structure with 2 free variables and make a plot
clear p
p.A = 15;
p.B = .08;
p.C=.03;

lambdaPlot = linspace(.9,1.5,100);
[tmp,pred] = predRecoveryErr2(p,lambdaPlot);
h2=plot(lambdaPlot,pred,'g-');
err = predRecoveryErr2(p,lambda,FF);

%% best fit parameters
bestP = fit('predRecoveryErr2',p,{'A','B','C'},lambda,FF);
[bestErr,bestPred] = predRecoveryErr2(bestP,lambdaPlot); %not able to
insert Stress because lambdaPlot has more points for smooth plot
bestErr = predRecoveryErr2(bestP,lambda,FF); %insert stress to
calculate best error
h3=plot(lambdaPlot,bestPred,'r-');

Fmax = max(FF);
Lambdamax = max(lambda);

%% Second method for calculating max slope
%It appears that the Fung equation for the toe region is a good fit.
The
```

```
%max slope can be calculated by taking the derivative of the equation
and
%evaluating it at the highest lambda.

%The derivative of the equation is B*e^(A*(L-1)).

maxslope = bestP.B*exp(bestP.A*(Lambdamax-1));

legend([h1,h2,h3],{'Data','Initial Guess','Best
Fit'},'Location','SouthEast');
axis([min(lambda) max(lambda) min(FF) max(FF)])
textbp(sprintf('A = %6.4f \nB = %6.4f\nC =  %6.4f\nSSE = %6.5f\nFmax =
%6.4f\nLambdamax = %6.4f\nMax Slope = %6.4f',bestP.A,bestP.B,
bestP.C,bestErr,Fmax,Lambdamax,maxslope));
title([filenames,' Toe Region Data vs. Model'])
fprintf('\nThe A value is %6.3f.\nThe B value is %6.3f.\nThe C value is
%6.3f.\nThe sum of squared error is %6.4f.\n', bestP.A, bestP.B,
bestP.C,bestErr)
%% Write to Excel
params={filenames bestP.A bestP.B bestP.C bestErr Fmax Lambdamax
maxslope};
%xlswrite('Parameters.xlsx',params,'Sheet1','A1:H1');


%%%%%%%%%%%%%%%%%%%%%%%%%%%%%%%%%%%%%%%%%%%%%%%%%%%%%%%%%%%%%%%%%%%%%%%%
%% This is the end of the code that I wrote. All following code was %%
%% written by other authors. I found most of it through matlab forums%
%%%%%%%%%%%%%%%%%%%%%%%%%%%%%%%%%%%%%%%%%%%%%%%%%%%%%%%%%%%%%%%%%%%%%%%%
```

```
%Program Name: colorcheck.m
%Program author: Unknown

%This program allows me to generate a different color for each trace on
my
%plot.

clear all
clc

ColOrd = get(gca,'ColorOrder');
[m,n] = size(ColOrd);
x=1:1:25;

for a=1:10
    ColRow = rem(a,m);
    if ColRow == 0
        ColRow = m;
    end
    Col = ColOrd(ColRow,:);
    y=a*10+x.^2;
    plot(x,y,'Color',Col);
    hold on
end

function [params,err] = fit(funName,params,freeList,varargin)
%[params,err] = fit(funName,params,freeList,var1,var2,var3,...)
%
%Helpful interface to matlab's 'fminsearch' function.
%
%INPUTS
% 'funName':  function to be optimized.  Must have form err =
<funName>(params,var1,var2,...)
% params   :  structure of parameter values for fitted function
%     params.options :  options for fminsearch program (see OPTIMSET)
% freeList :  Cell array containing list of parameter names (strings)
to be free in fi
% var<n>   :  extra variables to be sent into fitted function
%
%OUTPUTS
% params   :  structure for best fitting parameters
% err      :  error value at minimum
%
%See 'FitDemo.m' for an example.
%
%Written by Geoffrey M. Boynton, Summer of '00

%turn free parameters in to 'var'
if isfield(params,'options')
  options = params.options;
else
  options = [];
end

if isempty(freeList)
  freeList = fieldnames(params);
```

```
end
vars = params2var(params,freeList);
if ~isfield(params,'shutup')
  disp(sprintf('Fitting "%s" with %d free
parameters.',funName,length(vars)));
end
vars =
fminsearch('fitFunction',vars,options,funName,params,freeList,varargin)
;
% vars =
fminsearch(funName,vars,options,funName,params,freeList,varargin);

%get final parameters
params=  var2params(vars,params,freeList);

%evaluate the function

evalStr = sprintf('err = %s(params',funName);
for i=1:length(varargin)
  evalStr= [evalStr,',varargin{',num2str(i),'}'];
end
evalStr = [evalStr,');'];
eval(evalStr);


function err = fitFunction(var,funName,params,freeList,origVarargin)
%err = fitFunction(var,funName,params,freeList,origVarargin)
%
%Support function for 'fit.m'
%Written by G.M Boynton


%stick values of var into params

params = var2params(var,params,freeList);

%evaluate the function

evalStr = sprintf('err = %s(params',funName);
for i=1:length(origVarargin)
  evalStr= [evalStr,',origVarargin{',num2str(i),'}'];
end
evalStr = [evalStr,');'];
eval(evalStr);

function var = params2var(params,freeList)
%var = params2var(params,freeList)
%
%Support function for 'fit.m'
%Written by G.M Boynton, Summer of '00

var = [];
for i=1:length(freeList)
  evalStr = sprintf('tmp = params.%s;',freeList{i});
```

```
  eval(evalStr);
  var = [var,tmp(:)'];
end
function params = var2params(var,params,freeList)
%params = var2params(var,params,freeList)
%
%Support function for 'fit.m'
%Written by G.M Boynton, Summer of '00

count = 1;
for i=1:length(freeList)
  evalStr = sprintf('len = length(params.%s);',char(freeList(i)));
  eval(evalStr);
  evalStr = sprintf('params.%s =
var([%d:%d]);',char(freeList(i)),count,count+len-1);
  eval(evalStr);
  count = count+len;
end

function [err,pred] = predRecoveryErr2(p,lambda2,Pzz)

%model goes here.
pred = p.B/p.A*(exp(p.A*(lambda2-1))-1)+p.C;

%SSE calculation goes here.
if exist('Pzz','var')
    if ~exist('s','var')
       s = ones(size(Pzz));
    end

    err = sum( (pred(:)-Pzz(:)).^2./s.^2);
else
    err = NaN;
end

function ht = textbp(string,varargin)
% TEXTBP  implements 'best' location for text, a la legend
%    TEXTBP uses a modified LSCAN algorithm from the old MATLAB
%    LEGEND command to place text such that it minimizes the
%    obscuration of data points.
%
%    TEXTBP(STRING) is the simplest use of this function.  Any text
%    properties can be passed in by the same methods implemented in
%    the MATLAB TEXT builtin function. ie, following the STRING
%    with (PropertyName,PropertyValue) pairs.
%
%    HT = TEXTBP(STRING) returns the handle to the text object
%    Author: Unknown

TOL = 5; % Max # of data points we are allowed to obscure

% first get the size of the text in plot-normalized units
h_temp = text(0,0,string,'units','normalized',varargin{:});
extent = get(h_temp,'Extent');
width = extent(3);
```

```
height = extent(4);
delete(h_temp);

% do the hard work
pos = tscan(gca,width,height,TOL);
% if everything went fine, then put the text onto the plot
if (pos ~= -1)
  ht_local = text(pos(1),pos(2),string,'units','normalized',...
          'Vert','bottom',varargin{:});
end
% export the text object handle, if requested.
if nargout > 0,
  ht = ht_local;
end
```

REFERENCES

1. Wagenseil, J. E.; Ciliberto, C. H.; Knutsen, R. H.; Levy, M. A.; Kovacs, A.; Mecham, R. P., Reduced Vessel Elasticity Alters Cardiovascular Structure and Function in Newborn Mice. *Circulation Research* **2009,** *104* (10), 1217-24.

2. Liu, S. Q.; Fung, Y. C., Influence of STZ-induced Diabetes on Zero-stress States of Rat Pulmonary and Systemic Arteries. *Diabetes* **1992,** *41* (2), 136-46.

3. He, X.-J.; Yu, M.-H.; Li, W.-C.; Wang, H.-Q.; Li, J.; Peng, X.-C.; Tang, J.; Feng, N.; Huang, T.-Z., Morphological and Biomechanical Remodelling of the Hepatic Artery in a Swine Model of Portal Hypertension. *Hepatol International.* **2012,** *6* (3), 631-638.

4. Safar, M. E.; Blacher, J.; Mourad, J. J.; London, G. M., Stiffness of Carotid Artery Wall Material and Blood Pressure in Humans: Application to Antihypertensive Therapy and Stroke Prevention. *Stroke* **2000,** *31* (3), 782-790.

5. Bund, S. J.; Lee, R. M., Arterial Structural Changes in Hypertension: A Consideration of Methodology, Terminology and Functional Consequence. *Journal of Vascular Research* **2003,** *40* (6), 547-57.

6. Koniari, I.; Mavrilas, D.; Papadaki, H.; Karanikolas, M.; Mandellou, M.; Papalois, A.; Koletsis, E.; Dougenis, D.; Apostolakis, E., Structural and Biomechanical Alterations in Rabbit Thoracic Aortas Are Associated With the Progression of Atherosclerosis. *Lipids in Health and Disease* **2011,** *10*, 125.

7. Consigny, P. M.; Tulenko, T. N.; Nicosia, R. F., Immediate and Long-term Effects of Angioplasty-balloon Dilation on Normal Rabbit Iliac Artery. *Arteriosclerosis, Thrombosis, and Vascular Biology* **1986,** *6* (3), 265-276.

8. Bell, E. D.; Kunjir, R. S.; Monson, K. L., Biaxial and Failure Properties of Passive Rat Middle Cerebral Arteries. *Journal of Biomechanics* **2013,** *46* (1), 91-6.

9. Golding, E. M., Sequelae Following Traumatic Brain Injury: The Cerebrovascular Perspective. *Brain Research Reviews* **2002,** *38* (3), 377-88.

10. DeWitt, D. S.; Prough, D. S., Traumatic Cerebral Vascular Injury: The Effects of Concussive Brain Injury on the Cerebral Vasculature. *Journal of Neurotrauma* **2003,** *20* (9), 795-825.

11. Faul, M.; L, X.; MM, W., *Traumatic Brain Injury in the United States: Emergency Department Visits, Hospitalizations, and Deaths 2002-2006.* Centers for Disease Control and Prevention, National Center for Injury Prevention and Control Atlanta, GA, 2010.

12. Lloyd-Jones, D.; Adams, R. J.; Brown, T. M.; Carnethon, M.; Dai, S.; De Simone, G.; Ferguson, T. B.; Ford, E.; Furie, K.; Gillespie, C.; Go, A.; Greenlund, K.; Haase, N.; Hailpern, S.; Ho, P. M.; Howard, V.; Kissela, B.; Kittner, S.; Lackland, D.; Lisabeth, L.; Marelli, A.; McDermott, M. M.; Meigs, J.; Mozaffarian, D.; Mussolino, M.; Nichol, G.; Roger, V. L.; Rosamond, W.; Sacco, R.; Sorlie, P.; Thom, T.; Wasserthiel-Smoller, S.; Wong, N. D.; Wylie-Rosett, J., Heart Disease and Stroke Statistics--2010 Update: A Report from the American Heart Association. *Circulation* **2010,** *121* (7), e46-e215.

13. Rosamond, W.; Flegal, K.; Furie, K.; Go, A.; Greenlund, K.; Haase, N.; Hailpern, S. M.; Ho, M.; Howard, V.; Kissela, B.; Kittner, S.; Lloyd-Jones, D.; McDermott, M.; Meigs, J.; Moy, C.; Nichol, G.; O'Donnell, C.; Roger, V.; Sorlie, P.; Steinberger, J.; Thom, T.; Wilson, M.; Hong, Y., Heart Disease and Stroke Statistics--2008 Update: A Report from the American Heart Association Statistics Committee and Stroke Statistics Subcommittee. *Circulation* **2008,** *117* (4), e25-146.

14. Langfitt, T. W.; Obrist, W. D.; Gennarelli, T. A.; O'Connor, M. J.; Weeme, C. A., Correlation of Cerebral Blood Flow With Outcome in Head Injured Patients. *Annals of Surgery* **1977,** *186* (4), 411-4.

15. Armstead, W. M., Cerebral Hemodynamics After Traumatic Brain Injury of Immature Brain. *Experimental and Toxicologic Pathology* **1999,** *51* (2), 137-142.

16. Eucker, S. A.; Smith, C.; Ralston, J.; Friess, S. H.; Margulies, S. S., Physiological and Histopathological Responses Following Closed Rotational Head Injury Depend on Direction of Head Motion. *Experimental Neurology* **2011,** *227* (1), 79-88.

17. Orlando Regional Healthcare Education Web Page. http://www.orlandoregional.org/pdf%20folder/overview%20adult%20brain%20injury.pdf (accessed Feb 10, 2013).

18. Harper, S. L.; Bohlen, H. G.; Rubin, M. J., Arterial and Microvascular Contributions to Cerebral Cortical Autoregulation in Rats. *American Journal of Physiology* **1984,** *246* (1 Pt 2), H17-24.

19. Martinez-Lemus, L. A.; Hill, M. A.; Meininger, G. A., The Plastic Nature of the Vascular Wall: A Continuum of Remodeling Events Contributing to Control of Arteriolar Diameter and Structure. *Physiology (Bethesda)* **2009,** *24*, 45-57.

20. Nakamura, M.; Yock, P. G.; Kataoka, T.; Bonneau, H. N.; Suzuki, T.; Yamaguchi, T.; Honda, Y.; Fitzgerald, P. J., Impact of Deep Vessel Wall Injury on Acute

Response and Remodeling of Coronary Artery Segments After Cutting Balloon Angioplasty. *The American Journal of Cardiology* **2003,** *91* (1), 6-11.

21. Van den Akker, J.; Schoorl, M. J.; Bakker, E. N.; Vanbavel, E., Small Artery Remodeling: Current Concepts and Questions. *Journal of Vascular Research* **2010,** *47* (3), 183-202.

22. VanBavel, E.; Siersma, P.; Spaan, J. A., Elasticity of Passive Blood Vessels: A New Concept. *American Journal of Physiology - Heart and Circulatory Physiology* **2003,** *285* (5), H1986-2000.

23. Goyal, R.; Henderson, D. A.; Chu, N.; Longo, L. D., Ovine Middle Cerebral Artery Characterization and Quantification of Ultrastructure and Other Features: Changes with Development. *American Journal of Physiology - Regulatory, Integrative and Comparative Physiology* **2012,** *302* (4), R433-45.

24. Holzapfel, G.; Gasser, T.; Ogden, R., A New Constitutive Framework for Arterial Wall Mechanics and a Comparative Study of Material Models. *Journal of Elasticity* **2000,** *61* (1-3), 1-48.

25. Dobrin, P. B., Vascular Mechanics. *Comprehensive Physiology*, **2011,** 65-102.

26. Finlay, H. M.; McCullough, L.; Canham, P. B., Three-dimensional Collagen Organization of Human Brain Arteries at Different Transmural Pressures. *Journal of Vascular Research* **1995,** *32* (5), 301-12.

27. Findley WN, S. Y. J., Onaran Kasif, *Creep and Relaxation of Nonlinear Viscoelastic Materials*; Courier Dover Publications: 1976; p 371.

28. Scoliosis Research Society Biomechanics Glossary Web Page. http://www.srs.org/professionals/glossary/SRS_biomechanics_glossary.htm (accessed Feb 12, 2013).

29. Zhang, W.; Liu, Y.; Kassab, G. S., Viscoelasticity Reduces the Dynamic Stresses and Strains in the Vessel Wall: Implications for Vessel Fatigue. *American Journal of Physiology - Heart and Circulatory Physiology* **2007,** *293* (4), H2355-60.

30. Stemper, B. D.; Yoganandan, N.; Pintar, F. A., Mechanics of Arterial Subfailure with Increasing Loading Rate. *Journal of Biomechanics* **2007,** *40* (8), 1806-12.

31. Chalupnik, J. D.; Daly, C. H.; Merchant, H. C., *Material Properties of Cerebral Blood Vessels*. Department of Mechanical Engineering, University of Washington: 1971.

32. Monson, K. L.; Goldsmith, W.; Barbaro, N. M.; Manley, G. T., Axial Mechanical Properties of Fresh Human Cerebral Blood Vessels. *Journal of Biomechanical Engineering* **2003,** *125* (2), 288.

33. Dorfmann, A.; Pancheri, F. Q., A Constitutive Model for the Mullins Effect with Changes in Material Symmetry. *International Journal of Non-Linear Mechanics* **2012,** *47* (8), 874-887.

34. Hayashi, K., Experimental Approaches on Measuring the Mechanical Properties and Constitutive Laws of Arterial Walls. *Journal of Biomechanical Engineering* **1993,** *115* (4B), 481-8.

35. Roach, M. R.; Burton, A. C., The Reason for the Shape of the Distensibility Curves of Arteries. *Canadian Journal of Biochemistry and Physiology* **1957,** *35* (8), 681-90.

36. Panjabi, M. M.; Moy, P.; Oxland, T. R.; Cholewicki, J., Subfailure Injury Affects the Relaxation Behavior of Rabbit ACL. *Clinical Biomechanics* **1999,** *14* (1), 24-31.

37. Provenzano, P. P.; Heisey, D.; Hayashi, K.; Lakes, R.; Vanderby, R., Jr., Subfailure Damage in Ligament: A Structural and Cellular Evaluation. *Journal of Applied Physiology* **2002,** *92* (1), 362-71.

38. Monson, K. L.; Barbaro, N. M.; Manley, G. T., Biaxial Response of Passive Human Cerebral Arteries. *Annals of Biomedical Engineering* **2008,** *36* (12), 2028-41.

39. Gleason, R. L.; Wilson, E.; Humphrey, J. D., Biaxial Biomechanical Adaptations of Mouse Carotid Arteries Cultured at Altered Axial Extension. *Journal of Biomechanics* **2007,** *40* (4), 766-76.

40. Monson, K. Mechanical and Failure Properties of Human Cerebral Blood Vessels. Ph.D. Dissertation, University of California, Berkeley, Fall 2001.

41. Donovan, D. L.; Schmidt, S. P.; Townshend, S. P.; Njus, G. O.; Sharp, W. V., Material and Structural Characterization of Human Saphenous Vein. *Journal of Vascular Surgery* **1990,** *12* (5), 531-537.

42. Fung, Y. C.; Liu, S. Q., Determination of the Mechanical Properties of the Different Layers of Blood Vessels In Vivo. *Proceedings of the National Academy of Sciences of the United States of America* **1995,** *92* (6), 2169-73.

43. Burton, A. C., On the Physical Equilibrium of Small Blood Vessels. *American Journal of Physiology* **1951,** *164* (2), 319-29.

44. Van Loon, P., Length-force and Volume-pressure Relationships of Arteries. *Biorheology* **1977,** *14* (4), 181-201.

45. Weizsacker, H. W.; Pinto, J. G., Isotropy and Anisotropy of the Arterial Wall. *Journal of biomechanics* **1988,** *21* (6), 477-87.

46. Fung, Y. C., Elasticity of Soft Tissues in Simple Elongation. *American Journal of Physioogyl* **1967,** *213* (6), 1532-44.

47. Mathworks Matlab Central File Exchange Web Page. http://www.mathworks.com/matlabcentral/fileexchange/8468-fminsearch-interface (accessed Oct 15, 2012).

48. Guo, H.; Humphrey, J. D.; Davis, M. J., Effects of Biaxial Stretch on Arteriolar Function In Vitro. *American Journal of Physiology - Heart and Circulatory Physiology* **2007,** *292* (5), H2378-86.

49. Hilgers, R. H.; Bergaya, S.; Schiffers, P. M.; Meneton, P.; Boulanger, C. M.; Henrion, D.; Levy, B. I.; De Mey, J. G., Uterine Artery Structural and Functional Changes During Pregnancy in Tissue Kallikrein-deficient Mice. *Arteriosclerosis, Thrombosis, and Vascular Biology* **2003,** *23* (10), 1826-32.

50. Cipolla, M. J., Cerebrovascular Function in Pregnancy and Eclampsia. *Hypertension* **2007,** *50* (1), 14-24.

51. Duckles, S. P.; Krause, D. N., Cerebrovascular Effects of Oestrogen: Multiplicity of Action. *Clinical and Experimental Pharmacology & Physiology* **2007,** *34* (8), 801-8.

52. Jovanovic, S.; Jovanovic, A., Pregnancy is Associated with Hypotrophy of Carotid Artery Endothelial and Smooth Muscle Cells. *European Society for Human Reproduction and Embryology* **1998,** *13* (4), 1074-1078.

53. Griendling, K. K.; Fuller, E. O.; Cox, R. H., Pregnancy-induced Changes in Sheep Uterine and Carotid Arteries. *American Journal of Physiology* **1985,** *248* (5), H658-H665.

54. Hu, J. J.; Fossum, T. W.; Miller, M. W.; Xu, H.; Liu, J. C.; Humphrey, J. D., Biomechanics of the Porcine Basilar Artery in Hypertension. *Annals of Biomedical Engineering* **2007,** *35* (1), 19-29.

55. Fung, Y. C., Biorheology of Soft Tissues. *Biorheology* **1973,** *10* (2), 139-55.